

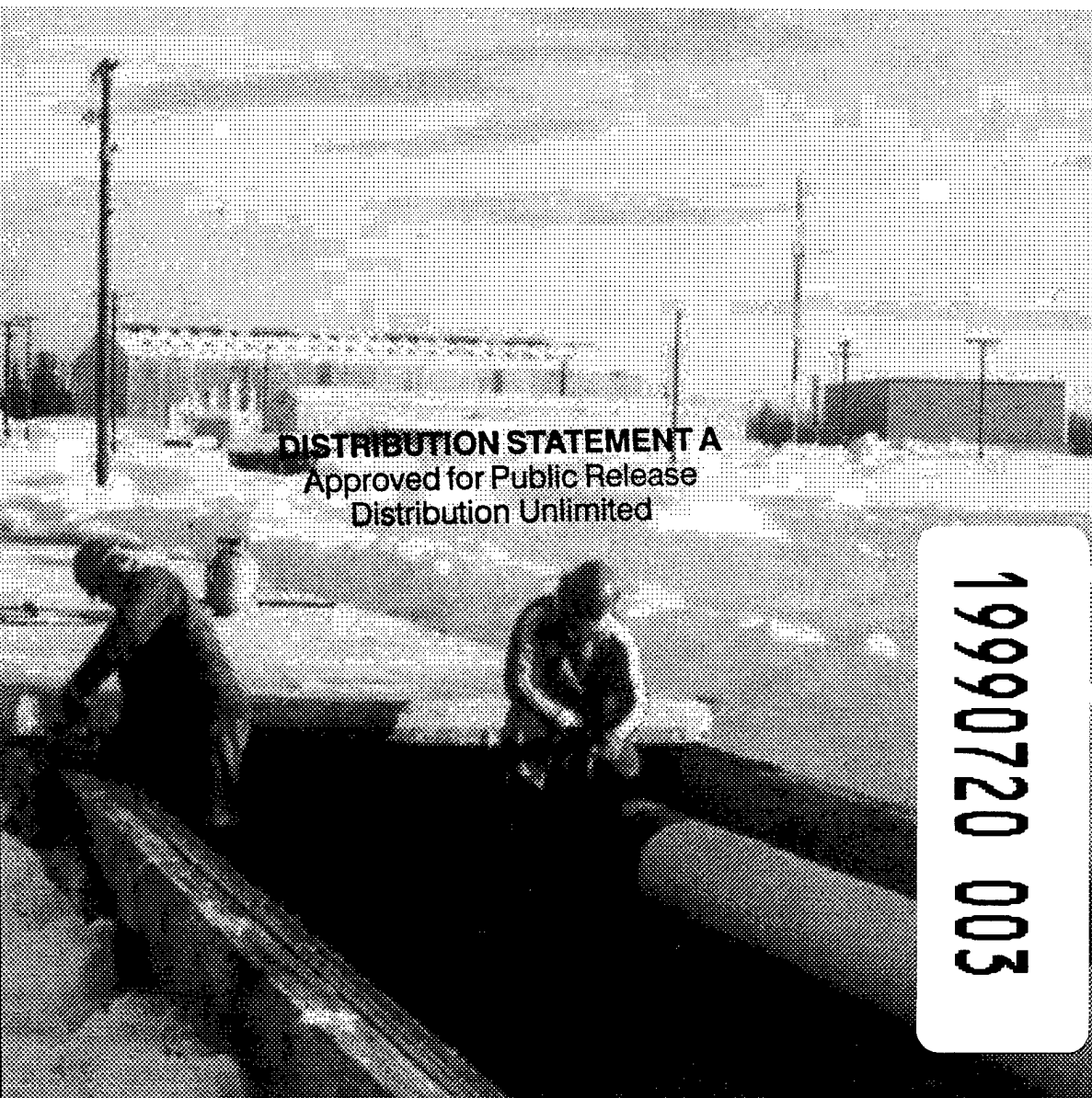
**US Army Corps  
of Engineers®**

Cold Regions Research &  
Cold Regions Research &  
Engineering Laboratory  
Engineering Laboratory

# Two-Dimensional Analysis of Natural Convection and Radiation in Utilidors

Paul W. Richmond

June 1999



**DISTRIBUTION STATEMENT A**  
Approved for Public Release  
Distribution Unlimited

19990720 003

# REPORT DOCUMENTATION PAGE

Form Approved  
OMB No. 0704-0188

Public reporting burden for this collection of information is estimated to average 1 hour per response, including the time for reviewing instructions, searching existing data sources, gathering and maintaining the data needed, and completing and reviewing the collection of information. Send comments regarding this burden estimate or any other aspect of this collection of information, including suggestion for reducing this burden, to Washington Headquarters Services, Directorate for Information Operations and Reports, 1215 Jefferson Davis Highway, Suite 1204, Arlington, VA 22202-4302, and to the Office of Management and Budget, Paperwork Reduction Project (0704-0188), Washington, DC 20503.

1. AGENCY USE ONLY (Leave blank)	2. REPORT DATE	3. REPORT TYPE AND DATES COVERED	
June 1999			
4. TITLE AND SUBTITLE  Two-Dimensional Analysis of Natural Convection and Radiation in Utilidors			5. FUNDING NUMBERS  PE: 4A762784AT42 PR: 6.27.84A TA: M WU: 07
6. AUTHORS  Paul W. Richmond			
7. PERFORMING ORGANIZATION NAME(S) AND ADDRESS(ES)  U.S. Army Cold Regions Research and Engineering Laboratory 72 Lyme Road Hanover, New Hampshire 03755-1290			8. PERFORMING ORGANIZATION REPORT NUMBER  CRREL Report 99-7
9. SPONSORING/MONITORING AGENCY NAME(S) AND ADDRESS(ES)  Office of the Chief of Engineers Washington, DC 20314-1000			10. SPONSORING/MONITORING AGENCY REPORT NUMBER  DoD HPC Center Arctic Region Supercomputing Center
11. SUPPLEMENTARY NOTES  For conversion of SI units to non-SI units of measurement, consult ASTM Standard E380-93, <i>Standard Practice for Use of the International System of Units</i> , published by the American Society for Testing and Materials, 1916 Race St., Philadelphia, Pa. 19103.			
12a. DISTRIBUTION/AVAILABILITY STATEMENT  Approved for public release; distribution is unlimited.  Available from NTIS, Springfield, Virginia 22161		12b. DISTRIBUTION CODE	
A13. ABSTRACT (Maximum 200 words)  Central heating plants are often used on large building complexes such as university campuses or military bases. Utilidors can be used to contain heat distribution lines and other utilities between a utility station and serviced buildings. Traditional thermal analysis of utilidors is one-dimensional, with heat transfer correlations used to estimate the effects of convection, radiation, and two-dimensional geometric effects. The expanding capabilities of computers and numerical methods suggest that more detailed analysis and possibly more energy-efficient designs could be obtained. This work examines current methods of estimating the convection and radiation that occur across an air space in square and rectangular enclosures and compares them with numerical and experimental data.			
14. SUBJECT TERMS Central heat distribution Effective conductivity Enclosures Numerical heat transfer		Radiation and convection Utilidors Utilities	15. NUMBER OF PAGES 78
			16. PRICE CODE
17. SECURITY CLASSIFICATION OF REPORT  UNCLASSIFIED	18. SECURITY CLASSIFICATION OF THIS PAGE  UNCLASSIFIED	19. SECURITY CLASSIFICATION OF ABSTRACT  UNCLASSIFIED	20. LIMITATION OF ABSTRACT  UL

NSN 7540-01-280-5500 [Go to Contents](#)

Standard Form 298 (Rev. 2-89)  
Prescribed by ANSI Std. Z39-18  
298-102

**Abstract:** Central heating plants are often used on large building complexes such as university campuses or military bases. Utilidors can be used to contain heat distribution lines and other utilities between a utility station and serviced buildings. Traditional thermal analysis of utilidors is one-dimensional, with heat transfer correlations used to estimate the effects of convection, radiation, and two-dimensional geometric effects. The

expanding capabilities of computers and numerical methods suggest that more detailed analysis and possibly more energy-efficient designs could be obtained. This work examines current methods of estimating the convection and radiation that occur across an air space in square and rectangular enclosures and compares them with numerical and experimental data.

**Cover:** Construction of a utilidor at Eielson AFB, Alaska. (Photo courtesy of Dr. Gary Phetteplace.)

**How to get copies of CRREL technical publications:**

Department of Defense personnel and contractors may order reports through the Defense Technical Information Center:

DTIC-BR SUITE 0944  
8725 JOHN J KINGMAN RD  
FT BELVOIR VA 22060-6218  
Telephone 1 800 225 3842  
E-mail help@dtic.mil  
msorders@dtic.mil  
WWW <http://www.dtic.mil/>

All others may order reports through the National Technical Information Service:

NTIS  
5285 PORT ROYAL RD  
SPRINGFIELD VA 22161  
Telephone 1 800 553 6847 or 1 703 605 6000  
1 703 487 4639 (TDD for the hearing-impaired)  
E-mail orders@ntis.fedworld.gov  
WWW <http://www.ntis.gov>

A complete list of all CRREL technical publications is available from  
USACRREL (CEERD-IM-HL)

72 LYME RD  
HANOVER NH 03755-1290  
Telephone 1 603 646 4338  
E-mail techpubs@crrel.usace.army.mil

**For information on all aspects of the Cold Regions Research and Engineering Laboratory, visit our World Wide Web site:**  
<http://www.crrel.usace.army.mil>

## Two-Dimensional Analysis of Natural Convection and Radiation in Utilidors

Paul W. Richmond

June 1999

Prepared for  
OFFICE OF THE CHIEF OF ENGINEERS

Approved for public release; distribution is unlimited.

[Back to Contents](#)

## PREFACE

This report was prepared by Dr. Paul W. Richmond, Mechanical Engineer, Applied Research Division, U.S. Army Cold Regions Research and Engineering Laboratory (CRREL), Hanover, New Hampshire. Funding for this effort was provided by DA Project 4A762784AT42, *Cold Regions Engineering Technology*, Work Unit MO7, *Heat Transfer from Buried Utility Lines*. The work was also supported in part by a grant of HPC time from the Department of Defense HPC Center, Arctic Region Supercomputing Center (denali.edu).

The author expresses his appreciation to the people at CRREL who assisted in this project. Special thanks go to Ronald Farr, who constructed the experimental apparatuses. The author particularly thanks Dr. Ronald Liston for his continued encouragement and support. This report was reviewed by Dr. John P. Zarling, Dr. Thomas Kinney, Dr. Debendra K. Das, and Dr. Gary Gislason.

The contents of this report are not to be used for advertising or promotional purposes. Citation of brand names does not constitute an official endorsement or approval of the use of such commercial products.

## CONTENTS

	Page
<u>Preface</u> .....	ii
<u>Nomenclature and abbreviations</u> .....	vi
<u>Introduction</u> .....	1
<u>Background</u> .....	3
<u>Numerical model</u> .....	13
Interpolation functions .....	16
Solution procedure .....	17
Radiation .....	20
Model verification .....	21
<u>Experimental procedure</u> .....	24
Experimental apparatuses .....	24
Data acquisition system .....	26
Procedure .....	29
<u>Results</u> .....	30
General information .....	30
Experimental data .....	32
Numerical data .....	35
<u>Analysis</u> .....	39
<u>Summary</u> .....	49
<u>Conclusions and recommendations</u> .....	49
<u>Literature cited</u> .....	50
<u>Appendix A: Experimental results</u> .....	53
<u>Appendix B: Numerical results</u> .....	57
<u>Abstract</u> .....	68

## ILLUSTRATIONS

### Figure

1. Cross sections of two utilidors constructed in the Arctic .....	2
2. Heat transfer correlations for vertical enclosures .....	5
3. Cross section of a concentric pipe conduit .....	7
4. Rectangular enclosure configuration of Ghaddar .....	8
5. Experimental configuration of Stewart and Verhulst .....	9
6. Experimental apparatus of Babus'Haq et al. .....	10
7. Heat transfer equations for pipes in enclosures .....	10

Figure	Page
8. Generic utilidors for current utilidor thermal analysis procedure.....	11
9. Curved isoparametric quadrilateral element.....	16
10. Viewfactor analysis of $F_{1-6}$ .....	20
11. Two-dimensional conduction problem .....	22
12. FECOME results for a vertical square enclosure at Rayleigh number $10^5$ .....	23
13. Grid used for comparing viewfactors and radiation heat flux calculations .....	23
14. 1-ft $\times$ 1-ft experimental apparatus without lid .....	24
15. Thermal conductivity of expanded polystyrene .....	25
16. Schematic cross section of the 1-ft $\times$ 1-ft apparatus .....	25
17. Thermal conductivity of fiberglass pipe insulation .....	26
18. 2-ft $\times$ 4-ft enclosure with 4-in. and 8-in. insulated pipes .....	27
19. Schematic diagram of the 2-ft $\times$ 4-ft enclosure .....	27
20. Data acquisition system for use with the 1-ft $\times$ 1-ft enclosure .....	29
21. Nusselt and Rayleigh number plot for the 4-in. pipe in the 1-ft $\times$ 1-ft enclosure (experimental data) .....	33
22. Nusselt and Rayleigh number plot for the insulated 4-in. pipe in the 1-ft $\times$ 1-ft enclosure (experimental data) .....	33
23. Nusselt and Rayleigh number plot for the 2-in. pipe in the 1-ft $\times$ 1-ft enclosure (experimental data) .....	34
24. Nusselt and Rayleigh number plot for the 2-in. insulated pipe in the 1-ft $\times$ 1-ft enclosure (experimental data) .....	34
25. Nusselt and Rayleigh number plot for the 2-ft $\times$ 4-ft enclosure (experimental data) .....	35
26. Mesh for the 1-ft $\times$ 1-ft enclosure with a 4-in. pipe .....	35
27. Mesh for the 2-ft $\times$ 2-ft enclosure with a 2-in. insulated pipe .....	36
28. Mesh for the 2-ft $\times$ 4-ft enclosure, 4-in. and 8-in. insulated pipes .....	36
29. Mesh for the 2-ft $\times$ 2-ft enclosure with two 2-in. pipes .....	36
30. Nusselt and Rayleigh number plot for the 4-in. pipe in the 1-ft $\times$ 1-ft enclosure (numerical data) .....	37
31. Nusselt and Rayleigh number plot for the insulated 4-in. pipe in the 1-ft $\times$ 1-ft enclosure (numerical data) .....	37
32. Nusselt and Rayleigh number plot for the 2-in. pipe in the 1-ft $\times$ 1-ft enclosure (numerical data) .....	38
33. Nusselt and Rayleigh number plot for the insulated 2-in. pipe in the 1-ft $\times$ 1-ft enclosure (numerical data) .....	38
34. Nusselt and Rayleigh number plot for the 1.27-ft $\times$ 1.27-ft and 2-ft $\times$ 2-ft enclosures (numerical data) .....	38
35. Heat flux from the 4-in. pipe through the 1-ft $\times$ 1-ft enclosure .....	39
36. Heat flux from the 2-in. pipe through the 1-ft $\times$ 1-ft enclosure .....	40
37. Heat flux from the 4-in. insulated pipe through the 1-ft $\times$ 1-ft enclosure .....	40
38. Heat flux from the 2-in. insulated pipe through the 1-ft $\times$ 1-ft enclosure .....	40
39. Ratio of effective conductivity to the conductivity of air vs. the average interior temperature (4-in. pipe) .....	41

Figure	Page
40. Ratio of effective conductivity to the conductivity of air vs. the average interior temperature (2-in. pipe) .....	41
41. Ratio of effective conductivity to the conductivity of air vs. the average interior temperature (4-in. insulated pipe) .....	42
42. Ratio of effective conductivity to the conductivity of air vs. the average interior temperature (2-in. insulated pipe) .....	42
43. Effective conductivity correlations .....	43
44. Correlation of pipe radius with intercepts .....	43
45. Temperature contours for sq4ib65a .....	45
46. Inside surface temperatures for sq4ib65a .....	45
47. Temperature contours for sq2d35c .....	45
48. Inside surface temperatures for sq2d35c .....	46
49. Temperature contours for sq2ic65a .....	46
50. Inside surface temperatures for sq2ic65a .....	46
51. Ratio of effective conductivity to the conductivity of air vs. the average interior temperature .....	47
52. Polynomial curve fits to experimental boundary data .....	48
53. Finite element mesh used for conduction solution of the 2-ft $\times$ 4-ft enclosure .....	48
54. Comparison of experimental and numerical inside insulation surface temperatures .....	48

## TABLES

### Table

1. Methods of determining the effective thermal conductivity of an air gap .....	12
2. Comparison of published velocity predictions with FECOME for a vertical enclosure .....	22
3. Comparison of viewfactor calculations .....	24
4. Comparison of radiation heat fluxes .....	24
5. Test apparatus configurations .....	26
6. Locations of thermocouples in the 1-ft $\times$ 1-ft enclosure .....	28
7. Locations of thermocouples in the 2-ft $\times$ 4-ft enclosure .....	29
8. Enclosure dimensions and effective gap widths .....	32
9. Configurations for the numerical experiments .....	32
10. Coefficients for eq 133 .....	43
11. Comparison of effective conductivity correlations .....	44
12. Conditions for comparisons between numerical conduction and convection solutions .....	44

## NOMENCLATURE AND ABBREVIATIONS

<i>A</i>	A heat transfer correlation coefficient
<i>a</i>	Area
<i>B</i>	A heat transfer correlation coefficient
<i>C</i>	A heat transfer correlation coefficient
$C_p$	Specific heat at constant pressure
$C_v$	Volumetric specific heat, ( $C_p\rho$ )
CRREL	Cold Regions Research and Engineering Laboratory
<i>D</i>	Diameter
d.o.f.	Degrees of freedom
<i>E</i>	Eccentricity (eq 50)
<i>F</i>	Radiation viewfactor
FE	Finite element
FECOME	Finite Element Combined Equations (computer code)
FERF	Frost Effects Research Facility
FEVIEW	Computer code using FE to determine radiation view factors
<i>G</i>	Vertical gap width (eq 48)
<i>g</i>	Acceleration due to gravity
<i>Gr</i>	Grashof number
<i>H</i>	Inside height of an enclosure
<i>h</i>	Convective heat transfer conductance
<i>k</i>	Thermal conductivity
<i>L</i>	Arc length of an element side
$L_e$	Hypothetical gap width ( $R-r$ ), or characteristic length
<i>N</i>	Interpolation functions
<i>n</i>	number of nodes
<i>Nu</i>	Nusselt number
<i>P</i>	Perimeter
<i>p</i>	Pressure
<i>Pr</i>	Prandtl number
<i>Q</i>	Internal heat generation
<i>q</i>	Heat flux
$Q_j$	Radiation heat flux through surface <i>j</i>
<i>R</i>	Hypothetical radius of a circle with the same parameter as the enclosure
<i>r</i>	Radius of a cylinder
<i>Ra</i>	Rayleigh number
$R_{xxx}$	Thermal resistance of <i>xxx</i>
<i>s</i>	Boundary surface
<i>T</i>	Temperature
<i>t</i>	Thickness
<i>u</i>	<i>x</i> -direction velocity
<i>v</i>	<i>y</i> -direction velocity
<i>W</i>	Inside width of an enclosure
<i>x</i>	<i>x</i> -coordinate location
<i>Y</i>	Inside height of enclosure
<i>y</i>	<i>y</i> -coordinate location
<i>z</i>	<i>z</i> -coordinate location
$\alpha$	Thermal diffusivity
$\beta$	Coefficient of thermal expansion

$\delta_{kj}$	Dirac delta function, equal to 1 if $k=j$ and equal to 0 if $k \neq j$ .
$\epsilon_j$	Emissivity of surface $j$
$\phi$	Heat flux across a boundary $s$ , or dimensionless temperature (eq 30)
$\nu$	Kinematic viscosity
$\mu$	Dynamic viscosity
$\rho$	Density
$\xi$	Shape function parameter (vertical direction)
$\eta$	Shape function parameter (horizontal direction)
$\sigma$	Boltzmann's constant

#### Subscripts

air	Of air
b	Boundary layer or distance traveled by the boundary layer on cylinder ( $\pi r$ )
c	Convection
ci	Inner radius of conduit
cond	Conduction
conv	Convection
D	Diameter
E	Exterior casing
eff	Effective
eq	Equivalent
i	Indices for pipe number, directions, inside (pipe diameter or radius), etc.
j	Indices for pipe number, directions, etc.
k	Indices for pipe number, directions, etc.
L	Characteristic length, or perimeter lining
o	Outside (diameter or radius)
p	Pipe
r	Radiation
ref	Reference for the coefficient of thermal expansion
s	Sphere
$\infty$	Reference for convective heat transfer

#### Superscripts

a	Area
B	Heat transfer correlation coefficient
e	Element
m	Indices for iteration numbers
p	Pressure
s	A boundary (general)

BLANK

## Two-Dimensional Analysis of Natural Convection and Radiation in Utilidors

PAUL W. RICHMOND

### INTRODUCTION

Many large building complexes, such as military facilities and university campuses, are served by central heat distribution systems. Utilidors are often used to contain the heat distribution lines and other utilities between utility stations and the serviced buildings. These enclosures are generally constructed of concrete and are usually installed below ground level. Other materials, such as wood and sheet metal, are also used. Figure 1 shows cross sections of two utilidors constructed in Arctic regions.

In the southern United States, utilidors are referred to as utility trenches and often have their upper side (lid) at ground level. Because utilidors are used to distribute heat (steam or hot water), it is important to know what the heat loss from the utilidor is in order to estimate losses in the heat distribution system and to design for efficient use of insulation. Additionally, the presence of unheated lines (e.g., domestic water, fire protection, or sewer lines) requires that the air temperature within the utilidor remain above freezing. Because of the complexity of the geometry, the heat transfer analysis must be done using approximate or numerical procedures.

Recently, numerical methods (finite difference, finite element) have been used to evaluate utilidor performance. Modeling of conductive heat transfer around utilidors and building foundations has been done successfully (Zarling and Braley 1984, Phetteplace et al. 1986, Kennedy et al. 1988). Modeling of heat transfer within utilidors is generally done using conductive approximations (Smith et al. 1979). Convection and radiation can have a significant effect on the total heat transfer, and accurate models are necessary. Once available, numerical models and correlations of heat transfer within utilidors can be used in the design process of new utilidors. A second application is in the thermal evaluation of existing utilidors for rehabilitation or renovation, replacing current approximation methods.

Researchers of numerical methods have demonstrated that convection and radiation can be modeled using finite element, finite difference, or other numerical techniques (Gebhart et al. 1988, Arpacı and Bayazitoglu 1990). However, these efforts have not been applied to utilidors, and in general have been limited to simple geometries. Additionally, the two modes of heat transfer are not often evaluated in tandem.

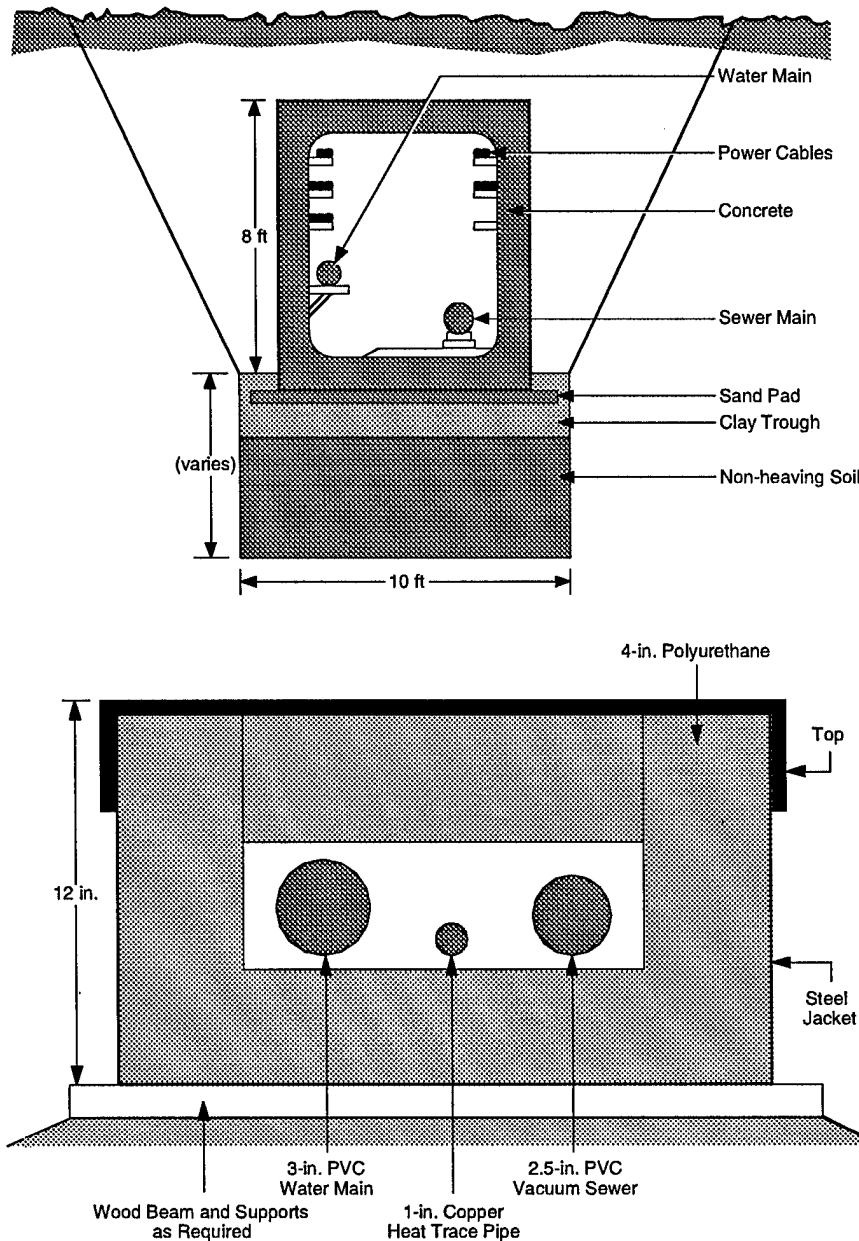


Figure 1. Cross sections of two utilidors constructed in the Arctic. (After U.S. Army 1987.)

Utilidor sizes and shapes are determined by considering the number and sizes of the pipes they will contain, their location relative to the ground surface, and the ease of access desired for maintenance or repairs. Phetteplace et al. (1981) presented the utilidor and pipe sizes for all the utilidors located on Fort Wainwright, Alaska. They reported approximately 200 different configurations; utilidor sizes ranged from 1 ft  $\times$  1 ft to 7 ft  $\times$  9 ft, and pipe sizes varied from 1 in. to 24 in. in diameter. Clearly, it is not possible to conduct physical experiments using every combination of utilidor size and pipe combination.

The objective of this work was to investigate convection and radiation in enclosures, specifically rectangular utilidors containing one or more heated pipes. The work presented considers the steady-state, two-dimensional problem of convec-

tion and radiation within an enclosure. Results of numerical and experimental investigations are combined to obtain a methodology for the two-dimensional thermal analysis of utilidors.

## BACKGROUND

The governing equations for incompressible Newtonian fluid flow in an enclosure are the Navier-Stokes (momentum) equations, the energy equation, and the continuity equation. The steady state, laminar flow momentum equations are

$$\left( u \frac{\partial u}{\partial x} + v \frac{\partial u}{\partial y} \right) + \frac{1}{\rho} \frac{\partial p}{\partial x} - v \left( \frac{\partial^2 u}{\partial y^2} + \frac{\partial^2 u}{\partial x^2} \right) = 0 \quad (1)$$

$$\left( v \frac{\partial v}{\partial y} + u \frac{\partial v}{\partial x} \right) - g\beta(T - T_{ref}) + \frac{1}{\rho} \frac{\partial p}{\partial y} - v \left( \frac{\partial^2 v}{\partial x^2} + \frac{\partial^2 v}{\partial y^2} \right) = 0 \quad (2)$$

for a two-dimensional flow field, where  $y$  is the vertical direction and  $x$  is the horizontal direction. The continuity equation is

$$\frac{\partial u}{\partial x} + \frac{\partial v}{\partial y} = 0 \quad (3)$$

and the energy equation (neglecting viscous dissipation) is

$$C_v \left( v \frac{\partial T}{\partial y} + u \frac{\partial T}{\partial x} \right) - k \left( \frac{\partial^2 T}{\partial x^2} + \frac{\partial^2 T}{\partial y^2} \right) - Q = 0 \quad (4)$$

The energy equation reduces to

$$-k \left( \frac{\partial^2 T}{\partial x^2} + \frac{\partial^2 T}{\partial y^2} \right) - Q = 0 \quad (5)$$

for solid regions with homogeneous, isotropic materials, and constant thermal conductivity ( $k$ ). These equations are coupled and result in four equations and four unknowns: pressure, temperature, and the  $x$  and  $y$  components of velocity ( $p, T, u$ , and  $v$ ). For complex geometries, these equations cannot be simplified and solved directly.

Heat transfer correlations for convective heat flow in enclosures are generally expressed in terms of the Nusselt number ( $Nu$ ) and the Rayleigh number ( $Ra$ ). These dimensionless parameters are defined as

$$Nu = \frac{h_c L}{k} \quad (6)$$

$$Gr = \frac{g\beta\rho^2\Delta T L^3}{\mu^2} \quad (7)$$

$$Pr = \frac{\nu}{\alpha} \quad (8)$$

$$Ra = PrGr = \frac{g\beta\rho^2\Delta T L^3}{\mu^2} \frac{\nu}{\alpha} \quad (9)$$

where  $g$  is the acceleration due to gravity,  $\beta$  is the thermal coefficient of expansion,  $\mu$  is dynamic fluid viscosity,  $\nu$  is the kinematic fluid viscosity,  $h_c$  is the heat transfer conductance,  $\alpha$  is the thermal diffusivity, and  $k$  is the thermal conductivity of the fluid.  $Pr$  is the Prandtl number and  $Gr$  is the Grashof number. The two remaining undefined terms,  $\Delta T$  and  $L$ , are dependent on the boundary conditions and geometry of the problem. In the simplest case,  $\Delta T$  will be the temperature difference between a warm surface and a cold surface. The variable  $L$  is a characteristic length of the geometry. For concentric cylinders the difference in radii or gap width is often used; other examples are discussed below. Correlations for  $Nu$  are found in the form of

$$Nu = ARa^B \quad (10)$$

when a specific material, such as air, is specified, or

$$Nu = AGr^B \quad (11)$$

for the general case of natural convection in fluids or gases.

Heat transfer by radiation between two surfaces can have a large effect on the heat transfer correlations. Experiments and analytical or numerical analysis can include these effects or they can be removed. Radiation is primarily reflected in the heat transfer conductance  $h$ . Generally,  $h$  should be considered to be the sum of two components,  $h_r$  and  $h_c$ , i.e., the conductances due to radiation and to convection. It is not always clear when examining heat transfer correlations if this is the case, or if  $h$  represents merely  $h_c$ .

A vertical rectangular cavity (enclosure) is defined as an enclosure bounded by two vertical surfaces held at different temperatures. The other two parallel surfaces, top and bottom, are taken as insulated (Gebhart et al. 1988). Heat transfer occurs only at the vertical surfaces. The characteristic length  $L$  for this geometry is the distance between the hot and cold walls, and the characteristic temperature  $\Delta T$  is the difference between the vertical wall temperatures. For an air-filled square enclosure, Ostrach (1972) summarized the following numerical results for the average Nusselt number in the form of eq 11.

Reference	A	B	eq
Newell and Schmidt (1969)	0.0547	0.397	(12)
Han (1967)	0.0782	0.3594	(13)
Elder (1965)	0.231	0.25	(14)

He reported tolerable agreement between these correlations and experiments.

Recently, de Vahl Davis and Jones (1983) presented a numerical benchmark solution for air in a square vertical enclosure at  $Ra$  values from  $10^3$  to  $10^6$ . Fitting an equation to their Nusselt number data at the cold surface yields

$$Nu = 0.14162Gr^{0.2996} \quad (15)$$

Equations 12–15 are drawn on Figure 2.

Correlations have also been developed for vertical enclosures with aspect ratios (height/width) other than one. Gebhart et al. (1988) present several correlations of the form

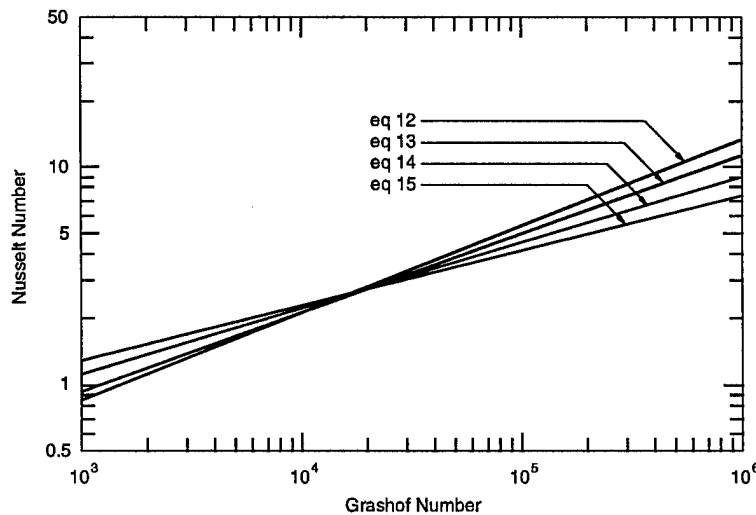


Figure 2. Heat transfer correlations for vertical enclosures.

$$Nu = A Gr^B \left( \frac{Y}{W} \right)^C \quad (16)$$

where  $Y/W$  is the height/width ratio, and  $A$ ,  $B$ , and  $C$  are the constants for air (see table below).

Reference	$A$	$B$	$C$	eq
Newell and Schmidt (1969)	0.155	0.315	-0.265	(17)
Eckert and Carlson (1961)	0.119	0.3	-0.1	(18)
Jakob (1949)	0.18	0.25	-0.111	(19)
MacGregor and Emery (1969)	0.25	0.25	-0.25	(20)

Horizontal rectangular enclosures are described as cavities in which the lower horizontal surface is heated while the upper surface is cooled; the sides are insulated. The correlations obtained by several researchers can be presented in the form of eq 10, when the Prandtl number for air is taken as 0.72. The characteristic length  $L$  in the  $Re$  number is the height of the enclosure. The constants for several correlations are shown in the following table (Gebhart et al. 1988).

Reference	$A$	$B$	eq
Dropkin and Somerscales (1965)	0.0673	0.3333	(21)
Silveston (1958)	0.0877	0.31	(22)
Kraichnan (1962)	0.1524	0.3333	(23)

Probably the most investigated enclosure containing an interior heat source is a concentric pipe system. Gebhart et al. (1988) reviewed the significant number of experimental and numerical investigations of this geometry, noting that different nondimensional systems have been used in most studies. For correlations based on mean heat transfer rates, gap width (outer radius-inner radius) is often used as the characteristic length ( $L$ ). An example of this is the following equation by Grigull and Hauf (1966):

$$Nu_L = \left[ 0.2 + 0.145 \left( \frac{L}{D_i} \right) \right] Gr^{0.25e^{-0.02}} \quad (24)$$

for  $30,000 \leq Gr_L \leq 716,000$

and  $0.55 \leq \frac{L}{D_i} \leq 2.65$

where  $D_i$  is the diameter of the internal cylinder. Gap width, however, does not provide all the heat transfer information that may be desired, i.e., the conductances for the two surfaces are not obtained individually, but are lumped together. The results of many studies are presented using an equivalent conductivity ( $k_{eq}$ ), which is defined as the ratio of actual heat flow to that due to conduction alone across the region. For concentric cylinders, the equivalent conductivities based on the inside and outside surface areas are

$$(k_{eq})_i = \frac{Nu_i}{Nu_{cond}} = \frac{h_i D_i}{2k} \ln \left( \frac{D_o}{D_i} \right) \quad (25)$$

$$(k_{eq})_o = \frac{Nu_o}{Nu_{cond}} = \frac{h_o D_o}{2k} \ln \left( \frac{D_o}{D_i} \right) \quad (26)$$

where

$$Nu_{cond} = \frac{2}{\ln(D_o/D_i)}. \quad (27)$$

The total energy lost by one cylinder equals that gained by the other (i.e., eq 25 equals eq 26). The subscript  $i$  refers to the inner cylinder and  $o$  to the outer one, and  $Nu_{cond}$  is the Nusselt number for pure conduction between concentric cylinders (Gebhart et al. 1988).

Kuehn and Goldstein (1978) combined a large amount of data and obtained the following correlations for  $Pr = 0.7$  (air):

$$Nu_i = \frac{2}{\ln \left\{ 1 + 2 \left/ \left[ \left( 0.5 Ra_{D_i}^{1/4} \right)^{15} + \left( 0.12 Ra_{D_i}^{1/3} \right)^{15} \right]^{1/15} \right\} \right.} \quad (28)$$

$$Nu_o = \frac{-2}{\ln \left\{ 1 - 2 \left/ \left[ \left( Ra_{D_o}^{1/4} \right)^{15} + \left( 0.12 Ra_{D_o}^{1/3} \right)^{15} \right]^{1/15} \right\} \right.} \quad (29)$$

$$\phi_b = \frac{Nu_i}{Nu_i + Nu_o} = \frac{(\bar{T}_b - T_o)}{(T_i - T_o)} \quad (30)$$

$$Nu_{conv} = \left( \frac{1}{Nu_i} + \frac{1}{Nu_o} \right)^{-1} \quad (31)$$

$$Nu_{cond} = \frac{2}{\ln(D_o/D_i)} \quad (32)$$

$$Nu = \left[ (Nu_{cond})^{15} + (Nu_{conv})^{15} \right]^{1/15} \quad (33)$$

$$k_{\text{eq}} = \frac{Nu}{Nu_{\text{cond}}} \quad (34)$$

where the Nusselt numbers are averaged values for the overall heat transfer around the cylindrical surfaces, and are based on  $D_o$ .  $Ra_{D_i}$  is the Rayleigh number based on  $D_i$  and  $Ra_{D_o}$  is that based on  $D_o$ . The temperature difference in  $Ra$  is the difference between the inner ( $T_i$ ) or outer ( $T_o$ ) surface temperatures and the average fluid temperature ( $T_b$ ) between the inner and outer cylinder boundary layers.  $T_b$  can be determined from  $\phi_b$ , the average dimensionless fluid temperature between boundary layers. An iterative solution to the correlation will be required to obtain the Nusselt numbers. What is significant about this correlation is that the conductances for both surfaces can be obtained along with the mean fluid temperature.

Lunardini (1990) conducted experiments using a conduit system used at many government installations (Fig. 3). He identified four ways to evaluate the thermal resistance of the air gap  $R_a$  given by

$$R_a = \frac{1}{2\pi r_i h} \quad (35)$$

from the Federal Guide Specification (1981), where the convective coefficient ( $h$ ) assumes a constant value of 3 Btu/hr ft<sup>2</sup>°F, or

$$R_a = \frac{\ln\left(\frac{r_{ci}}{r_i}\right)}{2\pi k_{\text{eff}}} \quad (36)$$

where

$$k_{\text{eff}} = 0.11 Ra_L^{0.29} k_{\text{air}} \quad (37)$$

obtained from Grober et al. (1961), or from his own data

$$k_{\text{eff}} = 1.463 Ra_L^{0.123} k_{\text{air}}, \quad (38)$$

which includes radiation effects, or

$$k_{\text{eff}} = 0.68 Ra_L^{0.157} k_{\text{air}}, \quad (39)$$

which has had the effect of radiation removed.  $k_{\text{eff}}$  is the effective conductivity of air,  $k_{\text{air}}$  is the conductivity of air,  $r_{ci}$  is the inner radius of the outer conduit, and  $r_i$  is the outer radius of the insulation. The air gap thickness is used as the characteristic length in the Rayleigh number.

Boyd (1981) combined data from concentric circular cylinders with data from

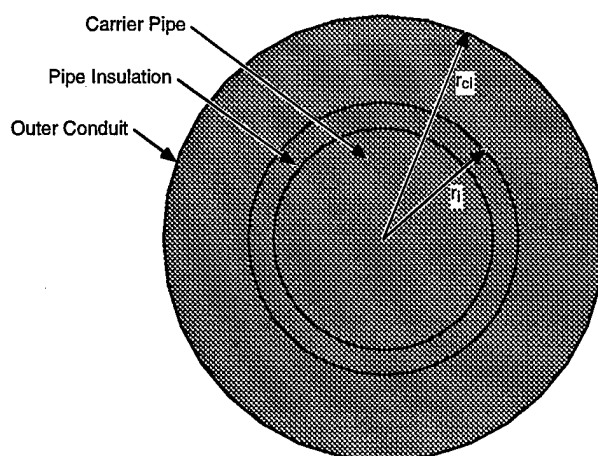


Figure 3. Cross section of a concentric pipe conduit.

hexagonal cylinders inside a circular cylinder. He found that the  $Nu$  should be based on gap width while  $Ra$  should be based on the radius of the internal cylinder. This approach indirectly includes the aspect ratio used by other investigators (e.g., eq 24).

Powe and Warrington (1983) and Warrington and Powe (1985) investigated cylinders and spheres mounted in spherical or cubical enclosures. Although their experimental correlations are probably not appropriate to this study, some of their observations are of interest. They used parameter  $L/r_s$  as a multiplier to the  $Ra$  number in correlations similar to those above, where  $L$  is the gap width and  $r_s$  is the hypothetical spherical radius based on volume. This parameter is used to account for the observation that, as the interior body becomes smaller, the natural convection phenomena can be divided into three regimes. These regimes are (1) infinite atmosphere solution for large  $L/r_s$ , (2) enclosure solutions for moderate  $L/r_s$ , and (3) conduction solutions for small  $L/r_s$ . Additionally, Warrington and Powe (1985) determined that for nonisothermal internal bodies, analyses using the average body temperature compared well with results from isothermal internal bodies.

Ghaddar (1992) conducted a numerical study of a uniformly heated (constant heat flux) cylinder in an enclosure as shown in Figure 4. Note that the pipe is not centered vertically, but is in the lower portion of the enclosure. She used a constant wall temperature of 59°F, and varied the heat flux into the cylinder; a mean cylinder temperature was used to calculate the Rayleigh and Nusselt numbers. Her numerical model did not include radiation. The heat transfer correlations developed were

$$Nu_L = 1.81 \left[ Ra_L \left( \frac{L}{r_p} \right) \right]^{0.207} \quad (40)$$

$$Nu_b = 0.604 Ra_b^{0.2083} \quad (41)$$

where  $L$  is the hypothetical gap width,  $r_p$  is the pipe radius, and  $b$  is the distance traveled by the boundary layer on the pipe (half the pipe circumference). The hypothetical gap width is defined as the difference between the effective radius of a cylinder that has a circumference equal to the perimeter of the noncircular enclosure and the radius of the interior pipe. Equation 40 becomes eq 42 after inserting Ghaddar's test conditions into the  $L/r_p$  term:

$$Nu_L = 3.756 Ra_L^{0.207} \quad (42)$$

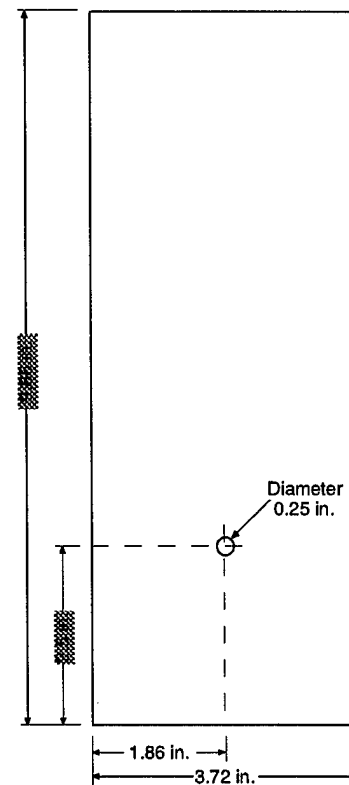


Figure 4. Rectangular enclosure configuration of Ghaddar (1992).

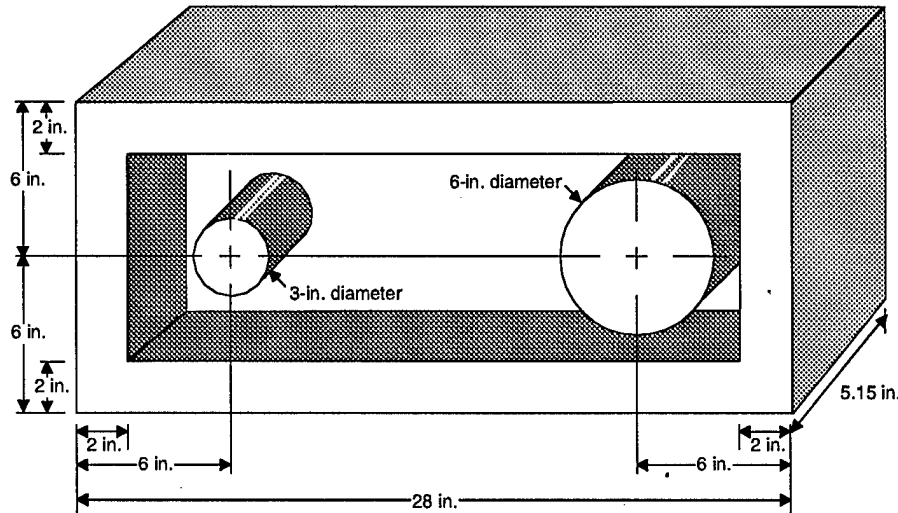


Figure 5. Experimental configuration of Stewart and Verhulst (1985)

Stewart and Verhulst (1985) presented the results of experiments in which two heated cylinders were in a cooled rectangular enclosure. Figure 5 shows their apparatus, which was filled with distilled water; measurements were made with both cylinders heated and when heated individually. They investigated a number of different characteristic lengths and found that the best correlation (least deviation from the data) occurred when the hypothetical gap width  $L$  was used. (When more than one pipe was used to calculate  $L$ , an effective radius that included both interior pipes was used.)

For both cylinders heated

$$Nu_L = 0.420 Ra_L^{0.219} \quad (L \text{ includes both cylinders}) \quad (43)$$

$$Nu_L = 1.534 Ra_L^{0.169} \quad (L \text{ using large cylinder only}) \quad (44)$$

$$Nu_L = 0.231 Ra_L^{0.243} \quad (L \text{ using small cylinder only}). \quad (45)$$

For only one cylinder heated

$$Nu_L = 0.256 Ra_L^{0.266} \quad (\text{large cylinder heated, } L \text{ using large cylinder only}) \quad (46)$$

$$Nu_L = 0.027 Ra_L^{0.371} \quad (\text{small cylinder heated, } L \text{ using small cylinder only}). \quad (47)$$

Babus'Haq et al. (1986) used interferometric flow visualization to determine the optimized location of a single warm pipe in a cool square enclosure with the anticipated application being district heating distribution lines, i.e., utilidors. Figure 6 is a diagram of their experimental apparatus. Although Babus'Haq et al. did not develop any heat transfer correlations per se, their data for heat loss from a centered pipe to the enclosure walls can be represented by

$$Nu_G = 0.34 Gr_D^{0.25} \quad (48)$$

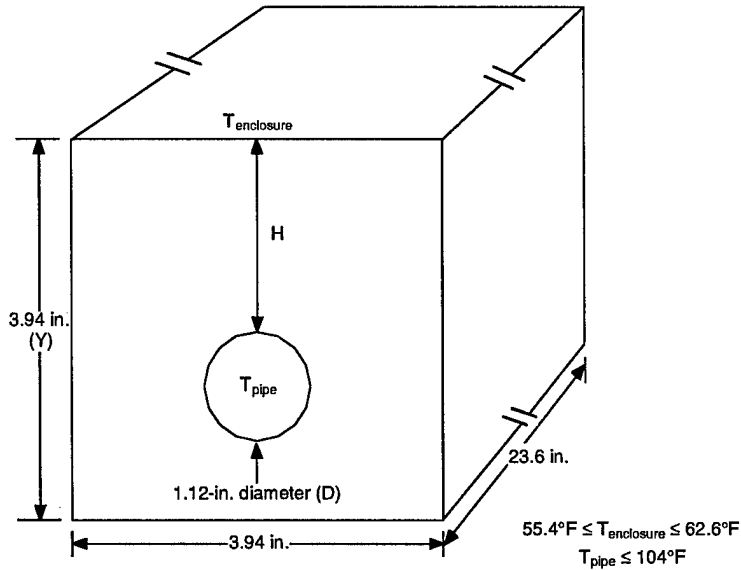


Figure 6. Experimental apparatus of Babus'Haq et al. (1986).

where the characteristic lengths  $G$  and  $D$  are the average vertical gap width,  $(Y-D)/2$ , and the pipe diameter, respectively. This equation can be converted to the following form using their test conditions:

$$Nu_L = 0.4048 Ra_L^{0.25} \quad (49)$$

Additionally, they found that the optimal location for a heated pipe in a cooled square enclosure is in the upper part of the enclosure, specifically at  $E = -0.73$ , where  $E$  is the eccentricity given by

$$E = \left[ \frac{2H}{Y-D} \right] - 1 \quad (50)$$

and  $H$  is the distance from the top of the pipe to the inside of the enclosure lid.  $Y$  is the interior vertical dimension and  $D$  is the pipe diameter. Figure 7 compares the

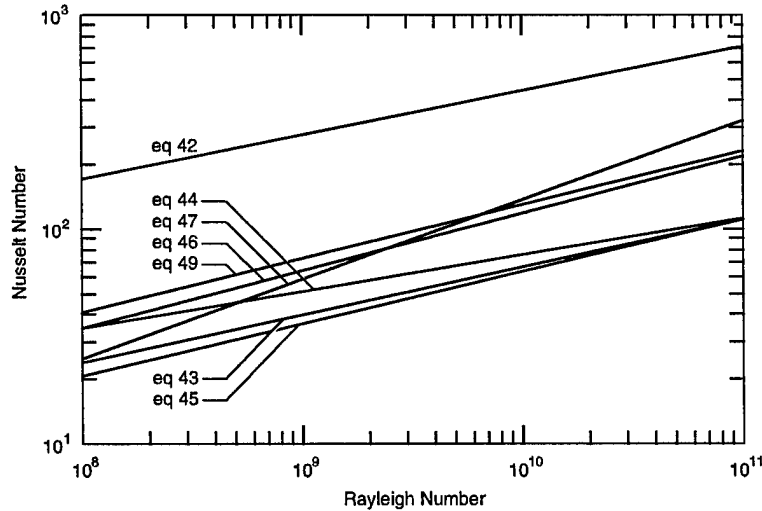


Figure 7. Heat transfer equations for pipes in enclosures.

heat transfer correlations based on the hypothetical gap width  $L$ . All of the equations yield Nusselt numbers within 20% of each other with the exception of Ghaddar's (eq 42), which is about 260% higher than the mean value of the other equations at a Rayleigh number of  $10^8$ . This could be due to the pipe location ( $E = 0.52$  using eq 50), which agrees with the findings of Babus'Haq et al. (1986) that more heat transfer occurs from hot pipes when placed lower in the enclosure (positive values of  $E$ ).

Currently accepted practice by Federal agencies, for the thermal analysis of the utilidors shown generically in Figure 8, is presented by Smith et al. (1979) and by the U.S. Army (1987). Two assumptions are made: (1) the air temperature inside the utilidor is uniform and (2) interior air film resistance can be ignored. The procedure consists of determining the thermal resistances by assuming that the rectangular enclosures can be treated as circular by using a radius calculated from the mean perimeters ( $P_L$  and  $P_E$  in Fig. 8). If the interior pipes are insulated, the conduction resistance of the air gap is neglected. If the interior pipes are uninsulated, then the resistance may be based on both the air film and pipe material. For multiple pipes with differing temperatures, all of the resistances and pipe temperatures are included to obtain an interior air temperature.

It is also possible to determine an effective conductivity of the air that includes all the film resistances, radiation, and natural convection effects. These procedures depend upon estimates of rectangular enclosures as circular and neglecting any effects of eccentricity of the pipe location. These approaches are illustrated as follows: Using the square enclosure in Figure 8, the heat loss per unit length is

$$Q = \frac{\Delta T}{\sum R} \quad (51)$$

where  $\Delta T$  is the difference between  $T_0$  and  $T_3$ , and  $\sum R$  is the sum of the resistances. With the assumption that the square enclosure can be treated as a cylinder of equal perimeter, the resistances are determined as

$$R_{\text{pipe}} = \frac{t_{\text{pipe}}}{k_{\text{pipe}} P_{\text{pipe}} \cdot 1} \quad (52)$$

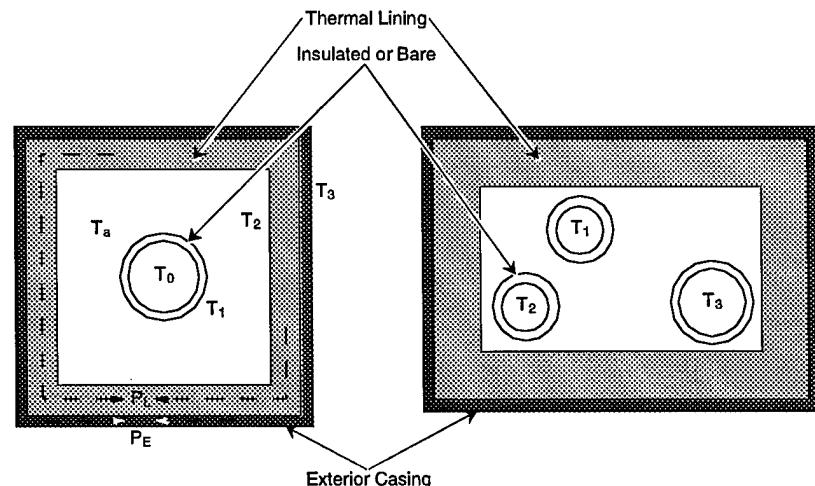


Figure 8. Generic utilidors for current utilidor thermal analysis procedure.  
(After U.S. Army 1987.)

$$R_{\text{pipe insulation}} = \frac{t_{\text{insulation}}}{k_{\text{insulation}} P_{\text{insulation}} \cdot 1} \quad (53)$$

$$R_{\text{air gap}} = \frac{\ln \frac{D_o}{D_i}}{2\pi k_{\text{eff}} \cdot 1}, \text{ or } R_{\text{air gap}} = \frac{\ln \frac{D_o}{D_i}}{2\pi k_{\text{eff}} + A_2 h_r \ln \frac{D_o}{D_i}} \quad (54)$$

where

$$h_r = \frac{\sigma (T_1^2 + T_2^2)(T_1 + T_2)}{\left[ \frac{1}{\epsilon_2} + \frac{A_1}{A_2} \left( \frac{1}{\epsilon_1} - 1 \right) \right]} \quad (55)$$

$$R_{\text{thermal lining}} = \frac{t_{\text{lining}}}{k_{\text{lining}} P_L \cdot 1} \quad (56)$$

$$R_{\text{exterior casing}} = \frac{t_{\text{casing}}}{k_{\text{casing}} P_E \cdot 1} \quad (57)$$

where  $k$  is the conductivity,  $P$  is the mean perimeter,  $D_o$  is the outside diameter,  $D_i$  is the inside diameter (of the air gap), and  $t$  is the thickness of the casing or lining.

**Table 1. Methods of determining the effective thermal conductivity of an air gap.**

Number	$k_{\text{eff}}$	Source	Comments
1	$0.11 Ra_L^{0.29} k_{\text{air}}$	eq 37	Based on cylinder, radiation included*
2	$1.463 Ra_L^{0.153} k_{\text{air}}$	eq 38	Based on cylinder, radiation included†
3	$0.34 G_r^{0.25} k_{\text{air}} \frac{D_o \ln \frac{D_o}{D_i}}{(y - D_i)}$	eq 48	Based on rectangular enclosure, $y$ is enclosure height, includes radiation.**
4	$0.40 Ra_L^{0.2} k_{\text{air}}$	Holman (1976)	Based on cylinder, radiation not included.
5	$0.68 Ra_L^{0.157} k_{\text{air}}$	eq 39	Based on cylinder, radiation not included.
6	$k_{\text{eq}} k_{\text{air}}$	eq 28-34	Based on cylinder, radiation not included.
7	$1.81 \left( Ra_L \frac{L}{r_p} \right)^{0.207} k_{\text{air}} \frac{D_o - D_i}{D_o \ln \left( \frac{D_o}{D_i} \right)}$	eq 40	Based on rectangular enclosure, radiation not included.
8	$0.23 \left( \frac{T_0 - T_a}{r_p} \right)^{0.25} \frac{1}{\ln \left( \frac{D_o}{D_i} \right)}$	Smith et al. (1979)	Based on cylinder, pipe is uninsulated, $T_a$ is the air temperature, radiation included††. $k_{\text{eff}}$ is zero if the pipes are insulated.

\* Emissivities unknown; the correlation is based on work reported in German, circa 1930.

† Emissivities were assumed to be 0.5 and 0.9 for the insulated pipe surface (two test conditions), 0.9 for the enclosure.

\*\* Materials were copper pipe and polymerized methyl methacrylate for the enclosure; no surface treatment or level of copper pipe oxidation was reported.

†† This is another "older" correlation; the underlying references were not given, but may be attributed to McAdams (see Grober et al. 1961, pp. 320-321).

The effective thermal conductivity,  $k_{\text{eff}}$ , can be determined using any of the relationships in Table 1. In most cases an iterative solution will be required to determine the air temperature upon which to base thermal properties, if unknown, and the temperature of surface 2. In general, the air properties can be evaluated at the average interior surface temperatures. If the effective conductivity relation includes radiation, then  $h_r$  is zero in eq 54. For those correlations that do not include radiation, appropriate emissivities can be selected for use in eq 55; for those that do, information on the emissivities values used to develop the correlations is limited; the available data are noted in Table 1.

A number of investigators (Zirjacks and Hwang 1983, Phetteplace et al. 1986, Kennedy et al. 1988) measured temperatures and heat flows in and around utilidors. These measurements were generally extensions of modeling efforts and analysis was limited to confirmation of the conduction models used to predict soil temperatures around the utilidors.

## NUMERICAL MODEL

A numerical model using a finite-element approach was developed to solve the momentum, energy, and continuity equations in two dimensions for the steady-state case. The following assumptions were made:

- The fluid (air) is Newtonian and incompressible within the Boussinesq approximation. (Fluid properties are constant, except for density, which is a function of temperature and affects only the buoyancy term.)
- Fluid flow is laminar.
- Thermal conductivity is constant for each fluid/material.

Following Gartling (1977) and Jaluria and Torrance (1986), the momentum equations are, as stated earlier,

$$\left( u \frac{\partial u}{\partial x} + v \frac{\partial u}{\partial y} \right) + \frac{1}{\rho} \frac{\partial p}{\partial x} - \nu \left( \frac{\partial^2 u}{\partial x^2} + \frac{\partial^2 u}{\partial y^2} \right) = 0 \quad (58)$$

$$\left( v \frac{\partial v}{\partial y} + u \frac{\partial v}{\partial x} \right) - g\beta(T - T_{\text{ref}}) + \frac{1}{\rho} \frac{\partial p}{\partial y} - \nu \left( \frac{\partial^2 v}{\partial x^2} + \frac{\partial^2 v}{\partial y^2} \right) = 0 \quad (59)$$

where  $y$  is in the vertical direction and  $x$  is in the horizontal direction. The continuity equation is

$$\frac{\partial u}{\partial x} + \frac{\partial v}{\partial y} = 0 \quad (60)$$

and the energy equation is

$$C_v \left( v \frac{\partial T}{\partial y} + u \frac{\partial T}{\partial x} \right) - k \left( \frac{\partial^2 T}{\partial x^2} + \frac{\partial^2 T}{\partial y^2} \right) - Q = 0, \quad (61)$$

which becomes for a solid region without convection

$$-k \left( \frac{\partial^2 T}{\partial x^2} + \frac{\partial^2 T}{\partial y^2} \right) - Q = 0. \quad (62)$$

The dependent variables  $p$ ,  $T$ ,  $u$ , and  $v$  for the general finite element  $e$  are approximated by

$$u^e = \sum_{i=1}^n N_i(x, y) u_i \quad (63)$$

$$v^e = \sum_{i=1}^n N_i(x, y) v_i \quad (64)$$

$$p^e = \sum_{i=1}^n N_i^p(x, y) p_i \quad (65)$$

$$T^e = \sum_{i=1}^n N_i(x, y) T_i. \quad (66)$$

Applying the Galerkin criterion to element  $e$  of an  $m+1^{th}$  iterate of the governing equations, the continuity equation becomes (using eq 63 and 64 and  $dV = 1 dx dy$ )

$$\int_{A^e} N_j^p \frac{\partial N_i}{\partial x} dx dy u_i + \int_{A^e} N_j^p \frac{\partial N_i}{\partial y} dx dy v_i = 0 \quad (67)$$

where  $N_j^p$  is the transpose of  $N_i$ . By letting the notation  $\langle a, b \rangle$  represent the area integral of  $ab$ , eq 67 becomes

$$\left\langle N_j^p, \frac{\partial N_i}{\partial x} \right\rangle u_i + \left\langle N_j^p, \frac{\partial N_i}{\partial y} \right\rangle v_i = 0. \quad (68)$$

A simplification is made at this point in that there are no boundaries with pressure differences. Using integration by parts on  $\partial^2$  terms in eq 58, 59, and 61 yields

$$\begin{aligned} & \left[ \left\langle u_i^m, N_j \frac{\partial N_i}{\partial x} \right\rangle + 2v \left\langle \frac{\partial N_i}{\partial x}, \frac{\partial N_j}{\partial x} \right\rangle + v \left\langle \frac{\partial N_i}{\partial y}, \frac{\partial N_j}{\partial y} \right\rangle + \left\langle v_i^m, N_j \frac{\partial N_i}{\partial y} \right\rangle \right] u_i \\ & + v \left\langle \frac{\partial N_i}{\partial x}, \frac{\partial N_j}{\partial y} \right\rangle + \frac{1}{\rho} \left\langle \frac{\partial N_i}{\partial x}, N_j^p \right\rangle p_i - v \int_s N_i \nabla u^e \bullet \bar{n} ds = 0 \end{aligned} \quad (69)$$

$$\begin{aligned} & \left[ \left\langle u_i^m, N_j \frac{\partial N_i}{\partial x} \right\rangle + 2v \left\langle \frac{\partial N_i}{\partial x}, \frac{\partial N_j}{\partial x} \right\rangle + v \left\langle \frac{\partial N_i}{\partial y}, \frac{\partial N_j}{\partial y} \right\rangle + \left\langle v_i^m, N_j \frac{\partial N_i}{\partial y} \right\rangle \right] v_i \\ & + v \left\langle \frac{\partial N_i}{\partial y}, \frac{\partial N_j}{\partial x} \right\rangle u_i + \frac{1}{\rho} \left\langle \frac{\partial N_i}{\partial y}, N_j^p \right\rangle p_i - v \int_s N_i \nabla v^e \bullet \bar{n} ds \\ & - g\beta \left\langle N_i, N_j \right\rangle T_i + g\beta T_{ref} \left\langle N_i \right\rangle = 0 \end{aligned} \quad (70)$$

$$\begin{aligned} & \left[ C_v \left\langle v_i^m, N_j \frac{\partial N_i}{\partial y} \right\rangle + C_v \left\langle u_i^m, N_j \frac{\partial N_i}{\partial x} \right\rangle + k \left\langle \frac{\partial N_j}{\partial x}, \frac{\partial N_i}{\partial x} \right\rangle \right. \\ & \left. + k \left\langle \frac{\partial N_j}{\partial y}, \frac{\partial N_i}{\partial y} \right\rangle \right] T_i - \left\langle N_j Q \right\rangle - \int_s N_i k \bar{n} \bullet \nabla T^e ds = 0. \end{aligned} \quad (71)$$

Because there will be no forced convection, the velocity at the boundary surface  $s$  in eq 69 and 70 will be zero, thus these two terms drop out. In the global formulation, the equations representing velocity boundary nodes will be set to zero and no other velocity boundary condition will be allowed.

The buoyancy  $\beta$  is defined by

$$\beta = \frac{1}{\rho} \left( \frac{\rho_{\text{ref}} - \rho}{T - T_{\text{ref}}} \right) \quad (72)$$

where  $T_{\text{ref}}$  is a reference temperature at which buoyancy has no effect. Gebhart et al. (1988) suggested using the minimum boundary surface temperature for the reference temperature, and that suggestion was followed.

The  $\langle N_j, Q \rangle$  and the  $\int_s N_i k \bar{n} \bullet \nabla T^e ds$  terms of eq 71 represent heat generated within an element and the thermal boundary conditions. For this application it is assumed that there is no heat generated within an element, thus this term is eliminated. Expanding the remaining term to account for specified heat flux and convective boundaries yields

$$\int_s N_i k \bar{n} \bullet \nabla T^e ds = \int_s h N_j T_\infty ds - \int_s h N_j N_i T_i ds - \int_s \phi N_j ds \quad (73)$$

where  $h$  and  $T_\infty$  are the convective heat transfer coefficient and associated temperature and  $\phi$  is the heat flux for the boundaries  $s$ .

Summarizing the integrals required for eq 68, 69, 70, 71, and 73, the following list is obtained:

$$\left\langle N_j^p, \frac{\partial N_i}{\partial x} \right\rangle \quad (74)$$

$$\left\langle N_j^p, \frac{\partial N_i}{\partial y} \right\rangle \quad (75)$$

$$\left\langle \frac{\partial N_i}{\partial x}, N_j^p \right\rangle \quad (76)$$

$$\left\langle \frac{\partial N_i}{\partial y}, N_j^p \right\rangle \quad (77)$$

$$\left\langle u_i^m, N_j, \frac{\partial N_i}{\partial x} \right\rangle \quad (78)$$

$$\left\langle v_i^m, N_j, \frac{\partial N_i}{\partial y} \right\rangle \quad (79)$$

$$\left\langle \frac{\partial N_j}{\partial y}, \frac{\partial N_i}{\partial y} \right\rangle \quad (80)$$

$$\left\langle \frac{\partial N_j}{\partial x}, \frac{\partial N_i}{\partial x} \right\rangle \quad (81)$$

$$\left\langle \frac{\partial N_i}{\partial x}, \frac{\partial N_j}{\partial y} \right\rangle \quad (82)$$

$$\left\langle \frac{\partial N_i}{\partial y}, \frac{\partial N_j}{\partial x} \right\rangle \quad (83)$$

$$\langle N_i, N_j \rangle \quad (84)$$

$$\langle N_i \rangle \quad (85)$$

$$\int_s N_i ds \quad (86)$$

$$\int_s N_i N_j ds. \quad (87)$$

### Interpolation functions

In the above equations, the matrix  $N$  represents interpolation functions for an arbitrary element.  $N'$  are the interpolation functions one order lower than  $N$ . Any two-dimensional shape element can be used for this set of equations so long as  $C^0$  continuity is maintained (Huebner and Thornton 1982). Considering that most of the utilidor components are rectangular in shape (walls and insulation), it would be convenient to use rectangular elements. However, the presence of pipes requires, at a minimum, triangular elements to model these curved surfaces. Many triangular elements will be required to model the pipes and meld the curved areas to rectangular areas. By using a rectangular element, which can have curved sides, fewer elements will be required.

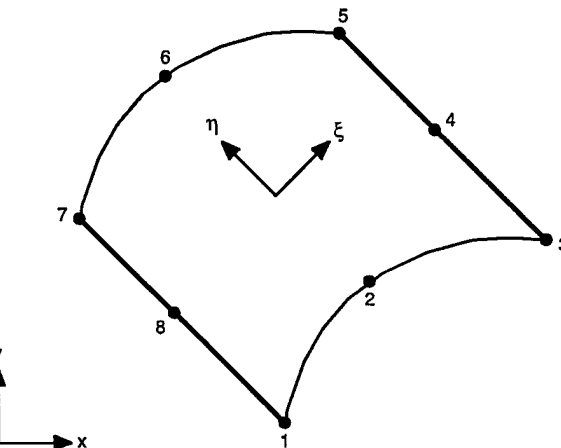


Figure 9. Curved isoparametric quadrilateral element.

Ergatoudis et al. (1968) presented the interpolation functions for curved isoparametric, quadrilateral elements. An element of this shape is shown in Figure 9; the element is defined by eight nodes, three on each side. The interpolation functions are

for nodes 1, 3, 5, and 7

$$N_i(\xi, \eta) = \frac{1}{4}(1 + \xi \xi_i)(1 + \eta \eta_i)(\xi \xi_i + \eta \eta_i - 1) \quad \xi = \pm 1, \eta = \pm 1 \quad (88)$$

for nodes 4 and 8

$$N_i(\xi, \eta) = \frac{1}{2}(1 + \xi^2)(1 + \eta \eta_i) \quad \xi = 0, \eta = \pm 1 \quad (89)$$

and for nodes 2 and 6

$$N_i(\xi, \eta) = \frac{1}{2}(1 + \xi \xi_i)(1 - \eta^2) \quad \xi = \pm 1, \eta = 0. \quad (90)$$

The variables  $\xi$  and  $\eta$  are local variables; for an individual element they are related to the global  $x_i$  and  $y_i$  coordinates by

$$x = \sum_{i=1}^8 N_i(\xi, \eta) x_i \quad (91)$$

$$y = \sum_{i=1}^8 N_i(\xi, \eta) y_i. \quad (92)$$

The derivatives  $\partial N / \partial \xi$  and  $\partial N / \partial \eta$  can be found directly; however, these derivatives must be related to  $\xi$  and  $\eta$  in order to integrate eq 74 through 87. This is done using the chain rule of differentiation and the Jacobian matrix  $J$ ; the following relationship is obtained (Huebner and Thornton 1982):

$$\begin{bmatrix} \frac{\partial N_i}{\partial x} & \frac{\partial N_i}{\partial \xi} \\ \frac{\partial N_i}{\partial y} & \frac{\partial N_i}{\partial \eta} \end{bmatrix} = [J]^{-1}, \quad i = 1, 2, \dots, 8. \quad (93)$$

Using the relationship  $dx dy = \det J d\xi d\eta$ , the above area integrals can all be written in terms of  $\xi$  and  $\eta$  and integrated from  $-1$  to  $1$  using Gaussian quadrature.

The interpolation functions ( $N^p$ ) must be linear (one order lower than  $N$ ). The same element as in Figure 9 is used; however, the sides are assumed to be straight and the element is defined only by nodes 1, 3, 5, and 7. The interpolation functions are

$$N_i^p = \frac{1}{4}(1 + \xi \xi_i)(1 + \eta \eta_i) \quad (94)$$

where  $\xi$  and  $\eta$  take on their nodal values (Fig. 9 and eq 88–90). The evaluation of the derivatives and integrals follows the same procedure as above.

The surface integral, eq 86, must also be expressed in terms of the parametric variables  $\xi_i$  and  $\eta_i$ , and the integration carried out over the boundary specified. In order to simplify programming it is assumed here that the boundary  $s$  is made up of at least one full side of an element; thus from Figure 9, side 1 is described by nodes 1, 2, and 3; side two is nodes 3, 4, 5; side three is nodes 5, 6, 7; and side 4 is nodes 7, 8, and 1. In this development no other combinations are allowed; however, more than one side per element can be specified as a boundary segment. For each side either  $\xi$  and  $\eta$  will be a constant and  $ds$  is

$$ds = \frac{1}{2} L_e d\eta \quad \text{or} \quad ds = \frac{1}{2} L_e d\xi \quad (95)$$

where  $L_e$  is the length of the side. The integral is now evaluated from  $-1$  to  $1$ , using Gaussian quadrature. The integration of eq 87 is carried out similarly, except that the term  $N_i N_j$  is a two-dimensional matrix.

### Solution procedure

The computer model FECOME (Finite Element COMBined Equations, Richmond 1995) solves eq 68–71 simultaneously for  $u$ ,  $v$ ,  $T$ , and  $p$  and uses either direct substitution or the Newton-Raphson iteration procedure. The solution procedure requires the use of a previous solution (the *old solution*) or an initial estimate, which is then used to obtain a *new solution*. Between iterations, both the direct substitu-

tion and the Newton-Raphson method can utilize a relaxation procedure, which consists of determining the weighted average of the old and new solutions. The equation is

$$\text{new solution} = \theta(\text{old solution}) + (1 - \theta) \text{ new solution} \quad (96)$$

where the weighting or relaxation factor ( $\theta$ ) varies between 0.005 and 0.25 depending on the maximum amount of change from the previous solution and the solution method. This range was determined by trial and error in an effort to improve the convergence rate. No formal optimization approach was attempted, and these values are not necessarily the best values. High values caused oscillations in the direct substitution solutions to high Rayleigh number problems (greater than  $10^5$ ) for the vertical enclosure problem, and once large oscillations begin, the procedure will not converge to a solution.

The procedure was considered to have converged to the steady-state solution when the largest change in each variable between successive solutions was less than 0.01%. Changes this small or smaller were found to produce no significant difference in the heat flux calculations through the enclosure sides.

The global matrix is  $3n+p$  by  $3n+p$  for the fluid elements plus  $n$  by  $n$  for the elements that are a solid material, where  $n$  is the number of nodes and  $p$  is the number of nodes associated with the pressure formulation (four per element). This calculation of matrix size is reduced by the number of solid-fluid boundary nodes (which were counted twice in the above analysis). There are 28 degrees of freedom for each element specified as a fluid and 8 degrees of freedom for those specified as a solid.

The global matrix for the direct substitution method has the form

$$\begin{bmatrix} AA & 0 & 0 & 0 \\ 0 & A3 & A8 & A4 \\ A1 & A9 & A7 & A5 \\ 0 & A4^T & A5^T & 0 \end{bmatrix} \begin{bmatrix} T \\ u \\ v \\ p \end{bmatrix} = \begin{bmatrix} R2 \\ 0 \\ R1 \\ 0 \end{bmatrix} \quad (97)$$

where

$$AA = k \left[ \left\langle \frac{\partial N_i}{\partial x}, \frac{\partial N_j}{\partial x} \right\rangle + \left\langle \frac{\partial N_i}{\partial y}, \frac{\partial N_j}{\partial y} \right\rangle \right] \quad (98)$$

$$+ C_v \left[ \left\langle u_i^m, N_j, \frac{\partial N_i}{\partial x} \right\rangle + \left\langle v_i^m, N_j, \frac{\partial N_i}{\partial y} \right\rangle \right] + h \int_s N_i N_j ds$$

$$A3 = \left\langle u_i^m, N_j, \frac{\partial N_i}{\partial x} \right\rangle + 2v \left\langle \frac{\partial N_i}{\partial x}, \frac{\partial N_j}{\partial x} \right\rangle + v \left\langle \frac{\partial N_i}{\partial y}, \frac{\partial N_j}{\partial y} \right\rangle \quad (99)$$

$$+ \left\langle v_i^m, N_j, \frac{\partial N_i}{\partial y} \right\rangle$$

$$A7 = \left\langle u_i^m, N_j, \frac{\partial N_i}{\partial x} \right\rangle + v \left\langle \frac{\partial N_i}{\partial x}, \frac{\partial N_j}{\partial x} \right\rangle + 2v \left\langle \frac{\partial N_i}{\partial y}, \frac{\partial N_j}{\partial y} \right\rangle \quad (100)$$

$$+ \left\langle v_i^m, N_j, \frac{\partial N_i}{\partial y} \right\rangle$$

$$A4 = -\frac{1}{\rho} \left\langle \frac{\partial N_i}{\partial x}, N_j^p \right\rangle \quad (101)$$

$$A5 = -\frac{1}{\rho} \left\langle \frac{\partial N_i}{\partial y}, N_j^p \right\rangle \quad (102)$$

$$A4^T = -\frac{1}{\rho} \left\langle N_j^p, \frac{\partial N_i}{\partial x} \right\rangle \quad (103)$$

$$A5^T = -\frac{1}{\rho} \left\langle N_j^p, \frac{\partial N_i}{\partial y} \right\rangle \quad (104)$$

$$A8 = v \left\langle \frac{\partial N_i}{\partial y}, \frac{\partial N_j}{\partial x} \right\rangle \quad (105)$$

$$A9 = v \left\langle \frac{\partial N_i}{\partial x}, \frac{\partial N_j}{\partial y} \right\rangle \quad (106)$$

$$R1 = g\beta T_{\text{ref}} \langle N_i \rangle \quad (107)$$

$$A1 = g\beta \langle N_i, N_j \rangle \quad (108)$$

$$R2 = \int_s h N_j T_\infty ds - \int_s \phi N_j ds. \quad (109)$$

The Newton-Raphson method, in its general one-dimensional form, is

$$\omega = \omega_0 - \frac{f(\omega_0)}{f'(\omega_0)} \quad (110)$$

where  $\omega$  is the root of the function  $f$  (Hornbeck 1975). In multidimensional form, following Gartling (1987),

$$\text{new solution} = \text{old solution} - J^{-1}(\text{old solution})R(\text{old solution}) \quad (111)$$

where  $J^{-1}$  is the inverse of the Jacobian matrix of eq 68–71 and  $R$  is the vector of the residuals obtained by substituting the old solution into eq 68–71. The Jacobian matrix is

$$J = \begin{bmatrix} \frac{\partial R_T}{\partial T} & \frac{\partial R_T}{\partial u} & \frac{\partial R_T}{\partial v} & 0 \\ 0 & \frac{\partial R_u}{\partial u} & \frac{\partial R_u}{\partial v} & \frac{\partial R_u}{\partial p} \\ \frac{\partial R_v}{\partial T} & \frac{\partial R_v}{\partial u} & \frac{\partial R_v}{\partial v} & \frac{\partial R_v}{\partial p} \\ 0 & \frac{\partial R_p}{\partial u} & \frac{\partial R_p}{\partial v} & 0 \end{bmatrix} \quad (112)$$

where  $R_T$ ,  $R_u$ ,  $R_v$ , and  $R_p$  are eq 68–71, respectively.

The material properties of the fluid (air) can be held constant or reevaluated between iterations using an average temperature obtained using a number of schemes. FECOME averages the temperatures of the zero velocity nodes (the inside surfaces of the enclosure) and calculates new air properties based on this average temperature between each iteration.

### Radiation

Large temperature differences can sometimes exist between utilidor steam lines and the utilidor walls. Temperature differences between surfaces cause heat flow via radiation in addition to natural convection. The heat flow due to radiation (radiosity) between surfaces is described by this equation:

$$\sum_{j=1}^n \left( \frac{\delta_{kj}}{\epsilon_j} - F_{k-j} \frac{1-\epsilon_j}{\epsilon_j} \right) Q_j = \sum_{j=1}^n F_{k-j} \sigma (T_k^4 - T_j^4) \quad (113)$$

where  $\sigma$  = Boltzmann's constant,

$T$  = absolute temperature of surface  $k$  or  $j$ ,

$F_{k-j}$  = viewfactor of surface  $k$  to  $j$ ,

$Q_j$  = radiation heat flux into or out of surface  $j$ ,

$a_j$  = area of surface  $j$ ,

$\epsilon_j$  = emissivity of surface  $j$ ,

$\delta_{kj} = 1$  if  $k = j$ , and = 0 if  $k \neq j$ .

The calculation of the radiation heat flux requires the calculation of the radiation viewfactors between each radiation surface. There are a number of procedures to make these calculations (Siegel and Howell 1992). Emery et al. (1991) made accuracy comparisons between several numerical approaches. However, none of the procedures are trivial for complex geometries. For the two-dimensional analysis of utilidors, the surfaces should be considered infinite in depth. By using the finite element boundaries as the edges of infinite strips, a special case of two-dimensional geometry is obtained.

A relatively simple method can be used to obtain the viewfactors for the case of infinite strips; known as Hottel's crossed-string method (Siegel and Howell 1992), the procedure is developed as follows. To obtain the viewfactor between surfaces 1 and 6 in Figure 10, first form the triangle  $abc$  with the infinite strips 1, 2, and 3. The viewfactors between these three surfaces can be written as

$$F_{1-2} + F_{1-3} = 1 \quad (114)$$

$$F_{2-1} + F_{2-3} = 1 \quad (115)$$

$$F_{3-1} + F_{3-2} = 1. \quad (116)$$

Multiply each equation by the area of its surface:

$$a_1 F_{1-2} + a_1 F_{1-3} = a_1 \quad (117)$$

$$a_2 F_{2-1} + a_2 F_{2-3} = a_2 \quad (118)$$

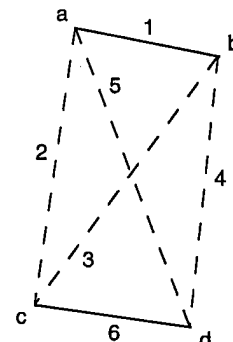


Figure 10. Viewfactor analysis of  $F_{1-6}$ .

$$a_3 F_{3-1} + a_3 F_{3-2} = a_3. \quad (119)$$

Substituting the reciprocity relations,

$$a_2 F_{2-1} = a_1 F_{1-2} \quad (120)$$

$$a_3 F_{3-1} = a_1 F_{1-3} \quad (121)$$

and solving the three equations for  $F_{1-2}$  yields

$$F_{1-2} = \frac{a_1 + a_2 - a_3}{2a_1}. \quad (122)$$

Similarly for the triangle  $adb$

$$F_{1-4} = \frac{a_1 + a_4 - a_5}{2a_1}. \quad (123)$$

Noting that

$$F_{1-2} + F_{1-4} + F_{1-6} = 1 \quad (124)$$

and solving eq 122-124 for  $F_{1-6}$  yields

$$F_{1-6} = \frac{a_2 + a_5 - a_3 - a_4}{2a_1}. \quad (125)$$

This procedure is implemented in the program FEVIEW (Richmond 1995); also included is a routine to check for the shadowing of surfaces. A surface is considered shadowed if a line connecting the midpoints of two surfaces is intersected by another radiation surface. No effort is made to distinguish partially shadowed elements, and as long as the midpoints can be connected without interference, the viewfactor is calculated using Hottel's method. The viewfactors are obtained prior to running FECOME and appended to the FECOME grid data file. A FECOME subroutine uses eq 113, nodal temperatures and the viewfactors, to obtain the radiation heat flux into or out of each of the radiation surfaces.

The radiation heat fluxes are recalculated at each iteration in FECOME using the average nodal temperatures for each surface specified as a radiation boundary. In the global formulation, the radiation flux is handled in the same manner as a boundary heat flux ( $\phi$ ) in eq 73.

### Model verification

Verification of the model consisted of comparing the model output to known (analytical) or benchmark numerical solutions. Three types of verifications were done to confirm that the model was producing accurate results; these are described in the following paragraphs.

Several computer runs were made to verify the energy equation alone and the implementation of the thermal boundary conditions. These runs also served to test the matrix assembly and inversion routines. First, a square grid was constructed in which all the elements were specified as a solid material and two opposite sides were set at different temperatures, with the other two sides having unspecified boundary conditions (this corresponds to a zero heat flux boundary). An exact solution to this simple one-dimensional problem was obtained. A second test in this phase was a two-dimensional conduction problem; here two adjacent sides were

set at a constant temperature boundary and as a thermal convection boundary, with the remaining sides having a zero heat flux. The results of this test, compared with the analytical solution given by Özisik (1980), are shown in Figure 11; good agreement was achieved. A third set of tests was run to confirm the correct implementation of the heat flux boundary condition. This was done by modeling a square solid material with one side at a constant temperature, the opposite side with a specified heat flux, and the remaining sides unspecified (zero heat flux). This configuration was repeated so that all four directions were tested with both positive (out of an element) and negative (into an element) heat flows.

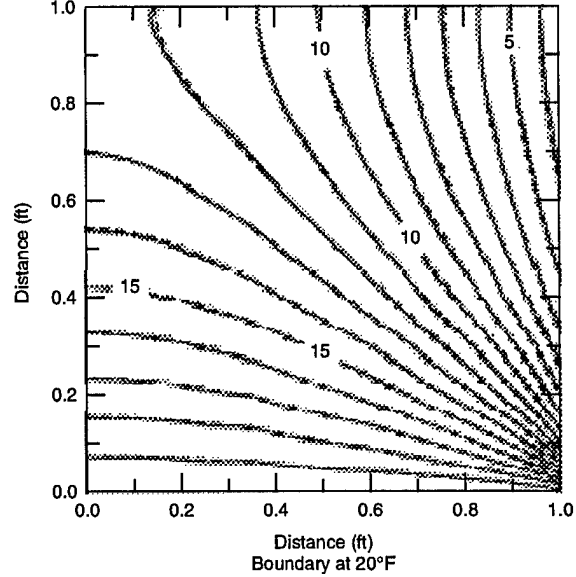


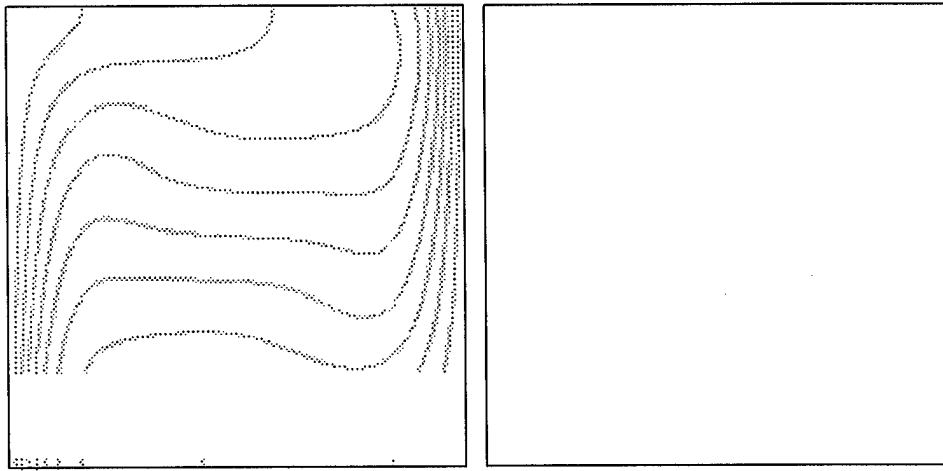
Figure 11. Two-dimensional conduction problem. Dashed lines represent the analytical solution, solid lines represent the numerical solution.

In order to test the solution of the momentum equations and the continuity equation, and their interaction with the energy equation, a comparison with a well-documented benchmark numerical solution was done. As mentioned earlier, de Vahl Davis and Jones (1983) presented benchmark solutions for natural convection in a vertical enclosure and compared their results with other investigators. A vertical enclosure is a closed cavity in which the horizontal surfaces are insulated (zero heat flux boundaries) and the vertical sides are held at two different temperatures. His solutions were for air at Rayleigh numbers of  $10^3$ ,  $10^4$ ,  $10^5$ , and  $10^6$ . Table 2 compares the velocity maximums along the  $x = 0.5$  and  $y = 0.5$  locations. Good agreement is observed, with percent differences less than 1%. Also

Table 2. Comparison of published velocity predictions with FECOME for a vertical enclosure.

Source	Maximum velocity @ $x = 0.5$		Maximum velocity @ $y = 0.5$	
	y coordinate	x velocity	x coordinate	y velocity
Benchmark* $Ra=10^3$	0.813	3.649	0.178	3.697
Gartling*	0.824	3.696	0.176	3.696
FECOME	0.825	3.640	0.175	3.697
Benchmark $Ra = 10^4$	0.823	16.178	0.119	19.617
Gartling	0.824	16.186	0.119	19.630
FECOME	0.825	16.185	0.125	19.601
Benchmark $Ra = 10^5$	0.855	34.73	0.066	68.59
Gartling	0.854	34.74	0.068	68.63
FECOME	0.850	34.71	0.067	68.63
Benchmark $Ra = 10^6$	0.850	64.63	0.038	219.36
Gartling	0.854	64.37	0.043	218.43
FECOME	0.850	64.76	0.033	218.58

\* From de Vahl Davis and Jones 1983.



a. Temperature contours.

b. Stream lines.

Figure 12. FECOME results for a vertical square enclosure at Rayleigh number  $10^5$ .

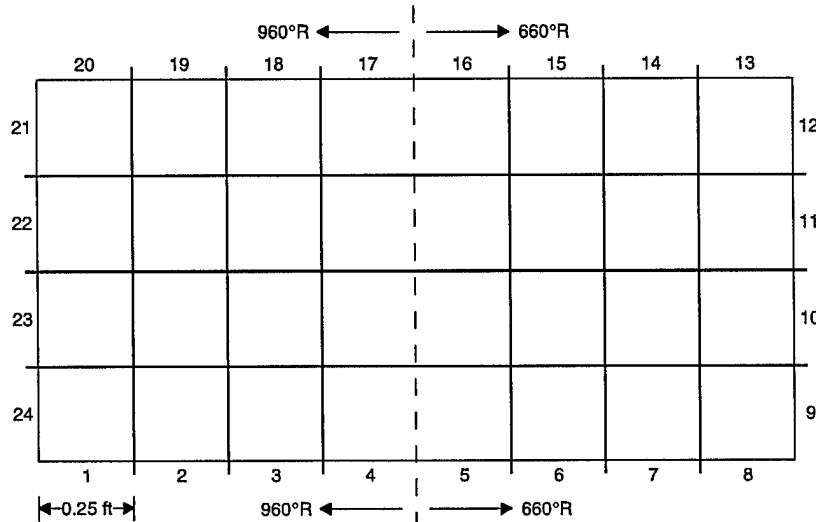


Figure 13. Grid used for comparing viewfactors and radiation heat flux calculations.

shown are the values submitted by Gartling (to de Vahl Davis and Jones). Gartling used a model similar to FECOME, but with a different mesh. Figure 12 shows the isotherms and streamlines for a Rayleigh number of  $10^5$ ; these agree well with those presented by de Vahl Davis and Jones (1983).

Radiation viewfactor calculations obtained using the computer program FEVIEW were checked by constructing a relatively simple mesh (Fig. 13) and using viewfactor algebra and tables of viewfactor equations (Siegel and Howell 1992) to determine the viewfactors both manually and using FEVIEW. Results of this analysis are shown in Table 3. Good agreement was obtained.

Implementation of the radiation heat flux boundaries was checked by solving eq 113 for the heat fluxes through each of the surfaces in Figure 13. A shell around the FECOME subroutine RADIATE was used for the input/output requirements. The manual solution (the solution of the simultaneous equations was obtained using a spreadsheet) is compared with the computer solution in Table 4; good agreement can be seen.

**Table 3. Comparison of view-factor calculations.**

Surface 1 to surface:	FEVIEW	Algebraic
1	0.000000	0.000000
2	0.000000	0.000000
3	0.000000	0.000000
4	0.000000	0.000000
5	0.000000	0.000000
6	0.000000	0.000000
7	0.000000	0.000000
8	0.000000	0.000000
9	0.004405	0.004404
10	0.012544	0.012548
11	0.018935	0.018936
12	0.023108	0.023104
13	0.015429	0.015427
14	0.021588	0.021589
15	0.030854	0.030855
16	0.044708	0.044707
17	0.064495	0.064496
18	0.089417	0.089417
19	0.112962	0.112962
20	0.123106	0.123106
21	0.019586	0.019586
22	0.036895	0.036893
23	0.089073	0.089075
24	0.292893	0.292893
Sum	0.999998	0.999998

**Table 4. Comparison of radiation heat fluxes.**

Surface no.	Heat flux, Btu/hr	
	Algebraic	Numerical
1	49.33	49.33
2	64.58	64.58
3	85.71	85.71
4	112.47	112.47
5	-112.47	-112.47
6	-85.71	-85.71
7	-64.58	-64.58
8	-49.33	-49.33
9	-98.66	-98.66
10	-111.42	-111.42
11	-111.42	-111.42
12	-99.32	-99.32
13	-49.33	-49.33
14	-64.58	-64.58
15	-85.71	-85.71
16	-112.47	-112.47
17	112.47	112.47
18	85.71	85.71
19	64.58	64.58
20	49.33	49.33
21	99.32	99.32
22	111.42	111.42
23	111.42	111.42
24	99.32	99.32
Sum	0.66	0.66

## EXPERIMENTAL PROCEDURE

### Experimental apparatuses

Two 10-ft-long experimental apparatuses were constructed to simulate sections of typical rectangular utilidors. The first had an internal 1-ft  $\times$  1-ft square cross section; the second was 2 ft  $\times$  4 ft. Figure 14 is the square cross section apparatus with its lid off, with a 4-in. nominal diameter pipe installed. Heat transfer panels surrounded the sides of the enclosures and a coolant was pumped through them. The interior pipe was filled with high temperature hydraulic oil and heated by an internal, 10-ft-long, 1-kilowatt heating element. The interior of the enclosure was lined with plywood and expanded polystyrene (EPS) insulation; the conductivity of two samples of the EPS was measured according to ASTM standards using a Rapid K apparatus. The results of these tests are plotted in Figure 15. Thermocouples were placed on either side of the EPS when installed in the apparatus. The

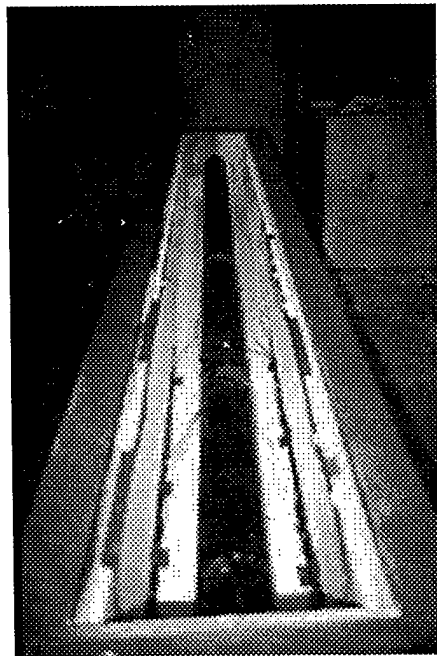


Figure 14. 1-ft  $\times$  1-ft experimental apparatus without lid.

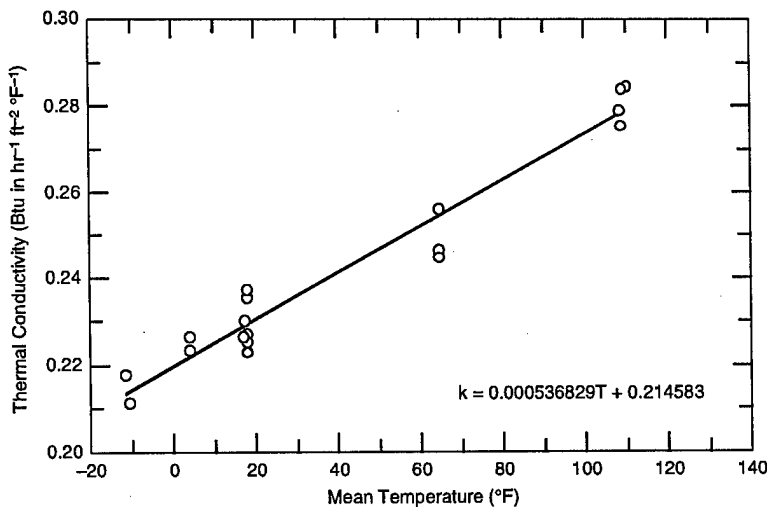


Figure 15. Thermal conductivity of expanded polystyrene.

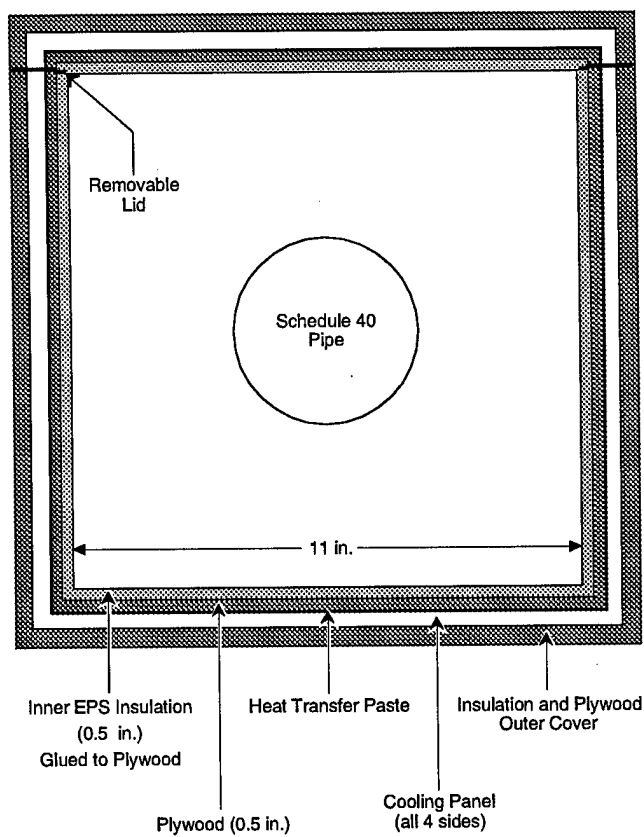


Figure 16. Schematic cross section of the 1-ft  $\times$  1-ft apparatus.

exterior of the apparatus was insulated and covered with plywood. Figure 16 is a cross section of the design.

Initial tests were done in CRREL's Frost Effects Research Facility (FERF), which supplied a glycol solution as cold as  $-22^{\circ}\text{F}$  to the apparatus. During these initial tests, it was determined that significantly colder coolant temperatures would be required to obtain temperatures typical of Alaska design conditions ( $-65^{\circ}\text{F}$  for outdoor air temperature) and to obtain near-freezing temperatures within the enclo-

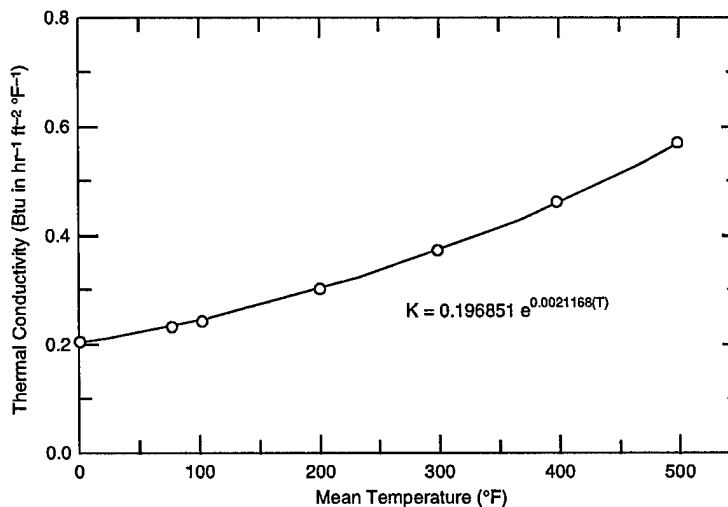


Figure 17. Thermal conductivity of fiberglass pipe insulation.

Table 5. Test apparatus configurations.

Enclosure size	Nominal pipe diam.	Pipe treatment
1 ft × 1 ft	4 in.	uninsulated, painted*, insulated
	2	uninsulated, insulated
2 ft × 4 ft	8, 4	insulated

\* The uninsulated pipe was painted with a low-emissivity paint (Rust-Oleum Aluminum No. 7715).

sure. Unfortunately, CRREL had at this time recently done away with its extreme low temperature capability for environmental reasons.

Several years after these initial experiments, CRREL regained its extreme low temperature brine capability and the apparatus was moved and replumbed to take advantage of a coolant as low as -70°F. Prior to resuming experiments, the interior surface-mounted thermocouples were replaced with 30-gage surface-mount thermocouples in order to measure the surface temperatures more accurately.

Once experiments were resumed, further experiments were conducted using the uninsulated 4-in. pipe. When these were completed, experiments continued with various pipe treatments and configurations. Figure 17 is a plot of the thermal conductivity of the fiberglass pipe insulation used. Table 5 summarizes the test apparatus configurations.

The second apparatus was constructed similarly; however, no plywood separated the cooling panels from the insulation, and a metal interior frame was used to help support the cooling panels. Figure 18 shows the 2-ft × 4-ft apparatus prior to installing the lid. Figure 19 shows a cross section with dimensions and pipe locations.

#### Data acquisition system

Two different data acquisition systems were used, one for the 1-ft × 1-ft enclosure and another for the 2-ft × 4-ft enclosure; type-T thermocouples were used to measure temperature, and a power meter was used to measure the power supplied to the pipes.

For the 1-ft × 1-ft enclosure, a personal-computer- (PC-) based data acquisition system was assembled using an 80286 processor-based computer in conjunction

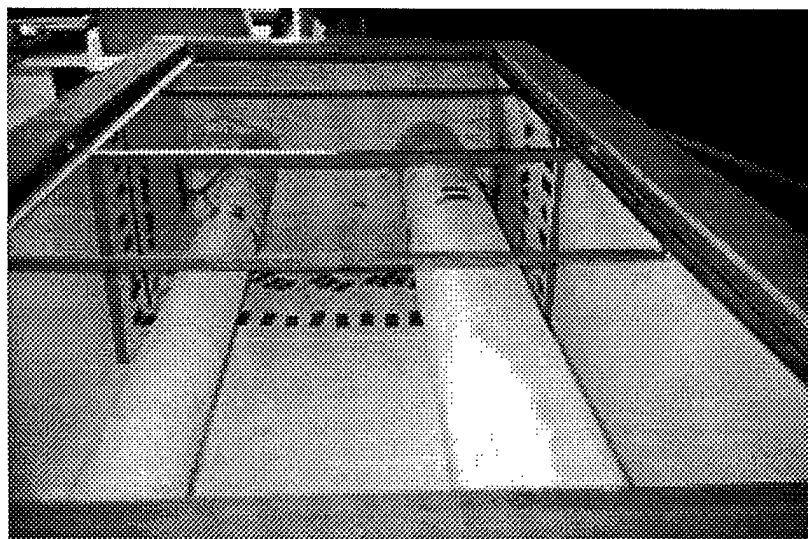


Figure 18. 2-ft  $\times$  4-ft enclosure with 4-in. and 8-in. insulated pipes.

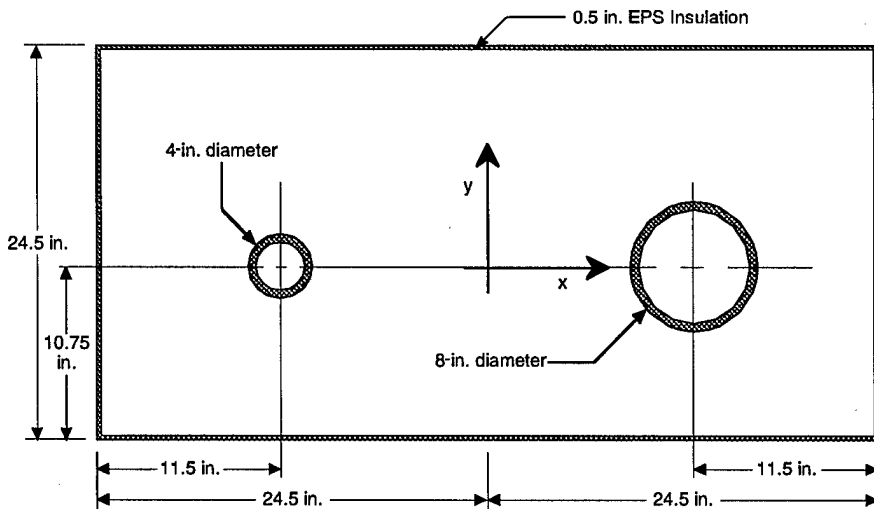


Figure 19. Schematic diagram of the 2-ft  $\times$  4-ft enclosure.

with Industrial Computer Source data acquisition boards. These boards (a total of four) were mounted in a separate enclosure and were accessed using an 8-channel multiplexor board mounted in one of the PC slots. Figure 20 is a schematic diagram of the data acquisition system; note that an electronic ice point bath was included in the thermocouple circuit for temperature compensation. The ice point bath was added because, during calibration of the system, it was found that the onboard electronic temperature compensators were not accurate. A data acquisition and display program was written to display and store the thermocouple data and measurements of the energy input to the pipe heater(s). These data were stored in ASCII format on floppy disks for later analysis. Thermocouple locations for the 1-ft  $\times$  1-ft enclosure are in Table 6.

The data acquisition system for the 2-ft  $\times$  4-ft apparatus was based on a Campbell Scientific CR-10 system with four multiplexor expansion boards. One hundred and twenty-two thermocouples were installed. Table 7 contains the thermocouples'  $x$

**Table 6. Locations of thermocouples in the 1-ft  $\times$  1-ft enclosure.**

Channel no.	x coord*	y coord*	Description of location†
0			3 o'clock on pipe
1			12 o'clock on pipe
2			6 o'clock on pipe
3			9 o'clock on pipe
4	1.5	-3.5	in air at 4.5 ft
5	6.5	-3.5	in air at 4.5 ft
6	11.5	-3.5	in air at 4.5 ft
7	1.5	3.5	in air at 4.5 ft
8	6.5	3.5	in air at 4.5 ft
9	11.5	3.5	in air at 4.5 ft
10			cold coolant inlet
11			right return
12			left return
13			lid return
14			bottom return
15			12 o'clock on pipe at 2 ft
16	-6.0	11.0	outside insulation on left side
17	-5.5	11.0	inside insulation on left side
18	6.0	2.0	outside insulation on right side
19	5.5	2.0	inside insulation on right side
20	6.0	5.0	outside insulation on right side
21	5.5	5.0	inside insulation on right side
22	6.0	8.0	outside insulation on right side
23	5.5	8.0	inside insulation on right side
24	6.0	11.0	outside insulation on right side
25	5.5	11.0	inside insulation on right side
26	6.0	6.5	outside insulation on right side at 6 ft
27**	5.5	6.5	inside insulation on right side at 6 ft
28	-6.0	6.5	outside insulation on left side at 6 ft
29**	-5.5	6.5	inside insulation on left side at 6 ft
30	0.0	0.0	outside insulation on bottom at 6 ft
31**	0.0	0.5	inside insulation on bottom at 6 ft
32	0.0	0.0	outside insulation on bottom
33	0.0	0.5	inside insulation on bottom
34	3.0	0.0	outside insulation on bottom
35	3.0	0.5	inside insulation on bottom
36	5.5	0.0	outside insulation on bottom
37	5.5	0.5	inside insulation on bottom
38	-3.0	0.0	outside insulation on bottom
39	-3.0	0.5	inside insulation on bottom
40	-5.5	0.0	outside insulation on bottom
41	-5.5	0.5	inside insulation on bottom
42	-6.0	2.0	outside insulation on left side
43	-5.5	2.0	inside insulation on left side
44	-6.0	5.0	outside insulation on left side
45	-5.5	5.0	inside insulation on left side
46	-6.0	8.0	outside insulation on left side
47	-5.5	8.0	inside insulation on left side
48	0.0	12.0	outside insulation on lid
49	0.0	11.5	inside insulation on lid
50	3.0	12.0	outside insulation on lid
51	3.0	11.5	inside insulation on lid
52	5.5	12.0	outside insulation on lid
53	5.5	11.5	inside insulation on lid
54	-3.0	12.0	outside insulation on lid
55	-3.0	11.5	inside insulation on lid
56	-5.5	12.0	outside insulation on lid
57	-5.5	11.5	inside insulation on lid
58	0.0	12.0	outside insulation on lid at 6 ft
59**	0.0	11.5	inside insulation on lid at 6 ft
60			inside insulation at tail
61			outside insulation at tail
62			inside insulation at head
63			outside insulation at head

\* The x origin is at the center of the enclosure; the y origin is at the outside of the bottom insulation panel.

† Distances are measured from the end that had inlets and outlets for the cooling panels; this end is designated the "head" and the opposite end, the "tail." Unless otherwise stated, the thermocouples were located 5 ft from the head.

\*\* These thermocouples were moved to 3, 9, 6, and 12 o'clock positions, respectively, on the pipe insulation when it was installed; they were not attached to the 2-in. bare pipe.

**Table 7. Locations of thermocouples in the 2-ft x 4-ft enclosure.**

T.C. no.	x coord. (in.)	y coord. (in.)	T.C. no.	x coord. (in.)	y coord. (in.)
<b>Inside of bottom insulation panel</b>					
1	-23.5	-10.25	61	24.5	-3
2	-21	-10.25	62	24.5	0
3	-18	-10.25	63	24.5	3
4	-15	-10.25	64	24.5	6
5	-12	-10.25	65	24.5	9
6	-9	-10.25	66	24.5	12.25
<b>Inside of upper insulation panel</b>					
7	-6	-10.25	67	22.5	13
8	-3	-10.25	68	21	13
9	0	-10.25	69	18	13
10	3	-10.25	70	15	13
11	6	-10.25	71	12	13
12	9	-10.25	72	9	13
13	12	-10.25	73	6	13
14	15	-10.25	74	3	13
15	18	-10.25	75	0	13
16	21	-10.25	76	-3	13
17	23.5	-10.25	77	-6	13
<b>Outside of bottom insulation panel</b>					
18	-23.5	-10.75	78	-9	13
19	-21	-10.75	79	-12	13
20	-18	-10.75	80	-15	13
21	-15	-10.75	81	-18	13
22	-12	-10.75	82	-21	13
23	-9	-10.75	83	-22.5	13
<b>Outside of upper insulation panel</b>					
24	-6	-10.75	84	22.5	13.5
25	-3	-10.75	85	21	13.5
26	0	-10.75	86	18	13.5
27	3	-10.75	87	15	13.5
28	6	-10.75	88	12	13.5
29	9	-10.75	89	9	13.5
30	12	-10.75	90	6	13.5
31	15	-10.75	91	3	13.5
32	18	-10.75	92	0	13.5
33	21	-10.75	93	-3	13.5
34	23.5	-10.75	94	-6	13.5
<b>Inside of left insulation panel</b>					
35	-24	-9.25	95	-9	13.5
36	-24	-6	96	-12	13.5
37	-24	-3	97	-15	13.5
38	-24	0	98	-18	13.5
39	-24	3	99	-21	13.5
40	-24	6	100	-22.5	13.5
41	-24	9	101	12 o'clock on right pipe (8 in.)	
42	-24	12.25	102	3 o'clock on right pipe (8 in.)	
<b>Outside of left insulation panel</b>					
43	-24.5	-9.25	103	6 o'clock on right pipe (8 in.)	
44	-24.5	-6	104	9 o'clock, right pipe (8 in.)	
45	-24.5	-3	105	12 o'clock, right pipe insulation	
46	-24.5	0	106	3 o'clock, right pipe insulation	
47	-24.5	3	107	6 o'clock, right pipe insulation	
48	-24.5	6	108	9 o'clock, right pipe insulation	
49	-24.5	9	109	12 o'clock on left pipe (4 in.)	
50	-24.5	12.25	110	9 o'clock on left pipe (4 in.)	
<b>Inside of right insulation panel</b>					
51	24	-9.5	111	6 o'clock on left pipe (4 in.)	
52	24	-6	112	3 o'clock on left pipe (4 in.)	
53	24	-3	113	12 o'clock, left pipe insulation	
54	24	0	114	9 o'clock, left pipe insulation	
55	24	3	115	6 o'clock, left pipe insulation	
56	24	6	116	3 o'clock, left pipe insulation	
57	24	9			
58	24	12.25	117	-18	-1
<b>Outside of right insulation panel</b>					
59	24.5	-9.5	118	-6	-1
60	24.5	-6	119	6.5	-1
			120	20	-1
			121	coolant supply	
			122	coolant return	

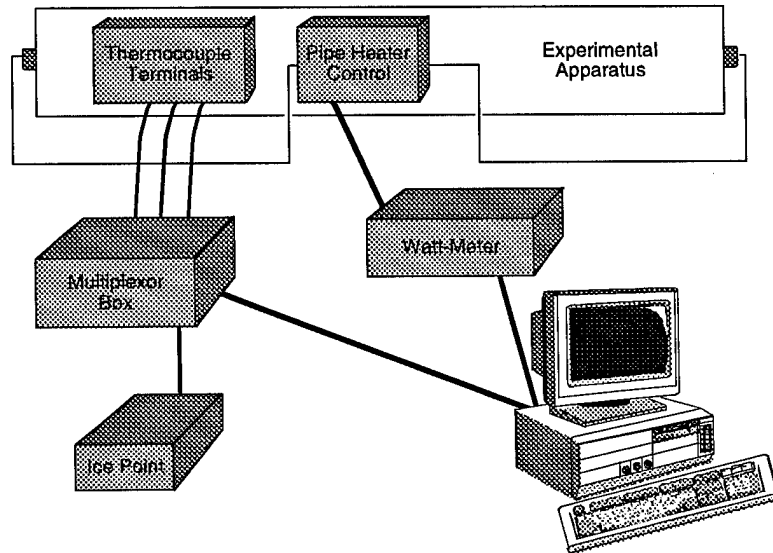


Figure 20. Data acquisition system for use with the 1-ft  $\times$  1-ft enclosure.

and  $y$  coordinates; these were placed 66 in. from the coolant supply end, except where noted. The total interior length was 106 in.

#### Procedure

Once the apparatus was connected to a coolant supply and electrical power source, several adjustments were possible. The coolant temperature could be adjusted, the coolant flow through each panel could be controlled, and the energy input to the pipe heater(s) could also be adjusted. Experiments consisted of obtaining a range of temperature conditions for both the interior walls of the apparatus and pipe(s) at steady-state conditions. Steady state was determined to be obtained once the temperatures along the top of the enclosure were changing by a small amount and in an apparently random fashion. Once a steady-state condition was reached, three sets of data from all of the thermocouples and the watt-meter were stored on an approximately hourly basis. Thus for each condition, three sets of data were collected. Temperature data from the 2-ft  $\times$  4-ft enclosure were collected continually on an hourly basis.

## RESULTS

#### General information

Data obtained from the experimental and numerical experiments are summarized in Appendixes A and B, respectively. Physical data are based on the average of three hourly readings. Temperatures, Nusselt number, Rayleigh number, heat flow through the interior wall, and the average thermal conductance at the interior enclosure surface are presented. Heat flow through each side, assuming 1 ft of enclosure length, was calculated by using the temperatures around the insulation and averaging the heat flows calculated at each thermocouple location (physical experiments) or the temperatures at each node location (numerical). These values

were averaged to obtain a heat flow value for each side (top, bottom, left, and right) and an overall average value. Nusselt and Rayleigh numbers were then calculated using the surface conductances obtained using the average interior surface temperature for material properties and the temperature difference between the average pipe and average insulation surface temperatures, for each side and for the overall average.

The following equations developed from data in Raznjevic (1976) were used for calculating material properties.

Viscosity of air (ft/s<sup>2</sup>)

$$\nu = 1.27573E - 04 + 6.1411E - 07T_{AVG}. \quad (126)$$

Density of air (lbm/ft<sup>3</sup>)

$$\rho_{air} = 8.42416E - 02 - 1.93863E - 04T_{AVG} + 4.16195E - 07T_{AVG}^2. \quad (127)$$

Volumetric specific heat of air (Btu/ft<sup>3</sup>°F)

$$C_v = 0.241\rho_{air}. \quad (128)$$

Coefficient of thermal expansion (1/°F)

$$\beta = 2.177E - 03 - 4.74865E - 06T_{AVG} + 9.42743E - 09T_{AVG}^2 - 1.04328E - 11T_{AVG}^3 \quad (129)$$

Thermal conductivities (Btu/fthr°F)

$$k_{air} = 0.01309 + 2.14766E - 05T_{AVG} \quad (130)$$

$$k_{EPS} = (0.214583 + 5.36829E - 04T_{AVG}) / 12 \quad (131)$$

$$k_{pipe\ insul} = (0.196851e^{0.00211687T_{AVG}}) / 12. \quad (132)$$

$T_{AVG}$  is the average temperature of the two pertinent surfaces, i.e., for air the average is that of the inside EPS surface and the pipe or pipe insulation surface temperatures.

The hypothetical gap width was used as the length parameter in the Nusselt and Rayleigh number calculations; these values and other enclosure dimensions are in Table 8. Table 9 shows the physical configurations and radiation emissivity values for the numerical experiments. Three sets of emissivity values were used; two different values for EPS were chosen to represent new (0.6) and old (0.9) insulation.\* For the pipe and pipe insulation the two values were for aluminized paint (0.5) and no paint (0.9).

---

\* Personal communication, Stephen N. Flanders, U.S. Army Cold Regions Research and Engineering Laboratory, 1994.

**Table 8. Enclosure dimensions and effective gap widths.**

Configuration	Pipe description	Outside radius of pipe/insulation	Effective radius of enclosure	Effective gap
1	4-in. bare	0.18750 ft	0.583568 ft <sup>a</sup>	0.396068 ft
2	4-in. insulated	0.27083	0.583568	0.312738
3	2-in. bare	0.09896	0.583568	0.484608
4	2-in. insulated	0.18229	0.583568	0.401278
5	4-in. insulated <sup>b</sup>	0.35416	0.755456 <sup>c</sup>	0.401296
6	2-in. insulated	0.18229	1.220187 <sup>d</sup>	1.037897
7	2- and 2-in. insulated	0.364583	1.220187 <sup>d</sup>	0.855605
8	4- and 8-in. insulated	0.713542 <sup>e</sup>	1.856808 <sup>f</sup>	1.143266 <sup>e</sup>

<sup>a</sup> 1-ft × 1-ft enclosure

<sup>b</sup> 2 in. of insulation

<sup>c</sup> 1.27-ft × 1.27-ft enclosure

<sup>d</sup> 2-ft × 2-ft enclosure

<sup>e</sup> 0.442708 and 1.4140, if only 8-in. pipe heated

<sup>f</sup> 2-ft × 4-ft enclosure

**Table 9. Configurations for the numerical experiments.**

Enclosure outside dimensions	Number of pipes	Pipe diameter(s)	Pipe insulation thickness	Emissivity values	
				Pipe <sup>1</sup>	Insulation
1 ft × 1 ft	1	4.5 in.	0.0 in.	0.9	0.9
	1	4.5	0.0	0.9	0.6
	1	4.5	0.0	0.5	0.9
	1	4.5	0.0	No radiation	
	1	4.5	1.0	0.9	0.9
	1	4.5	1.0	0.9	0.6
	1	4.5	1.0	0.5	0.9
	1	2.375	0.0	0.9	0.9
	1	2.375	0.0	0.9	0.6
	1	2.375	0.0	0.5	0.9
	1	2.375	1.0	0.9	0.9
	1	2.375	1.0	0.9	0.6
1.27 ft × 1.27 ft	1	2.375	1.0	0.5	0.9
	1	4.5	2.0	0.9	0.9
	2	2.375, 2.375	1.0, 1.0	0.9	0.9
	2	4.5, 8.625	1.0, 1.0	0.9	0.9

<sup>1</sup> or pipe insulation

### Experimental data

The complete set of temperature and power measurements is reported in Richmond et al. (1997). The average Nusselt and Rayleigh numbers obtained for the physical experiments conducted with the 1-ft × 1-ft enclosure are plotted in Figures 21–24. Vertical scatter is due to the radiation effect on the surface conductance; a similar effect is seen in the numerical data, shown in the next section. In Figure 21, the 1991 data result in slightly higher Nusselt numbers. Some of this difference is due to the temperature effect on the conductance, but some may also be due to the larger thermocouples used to measure surface temperatures. The effect of painting the pipe with the aluminum paint, with a subsequent lower emissivity, is clearly seen, resulting in lower Nusselt numbers compared to the unpainted pipe. Figure 22 shows similar scatter with apparently one significant outlier, which occurred in the data obtained on 28 September 1996 (see App. A). By plotting the calculated

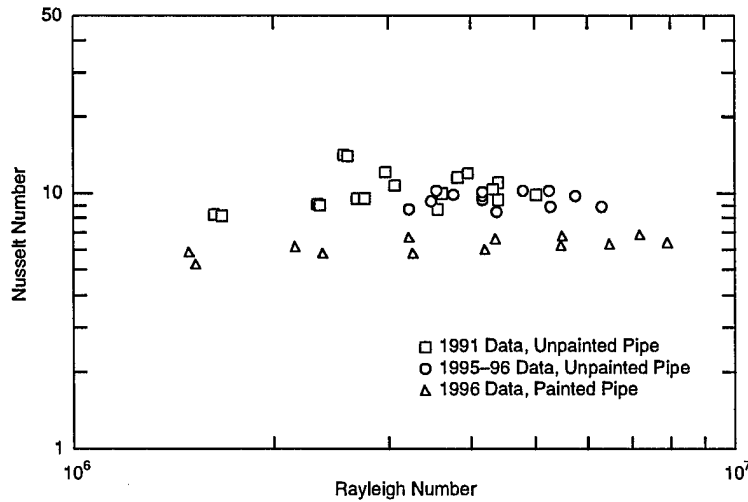


Figure 21. Nusselt and Rayleigh number plot for the 4-in. pipe in the 1-ft  $\times$  1-ft enclosure (experimental data).

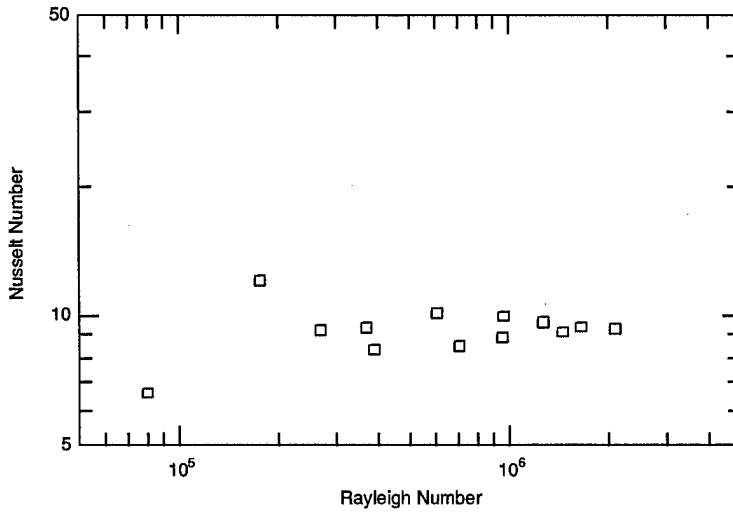


Figure 22. Nusselt and Rayleigh number plot for the insulated 4-in. pipe in the 1-ft  $\times$  1-ft enclosure (experimental data).

heat flux data versus the difference between the average interior wall temperature and the average pipe temperature, it was found that a number of data points did not agree with a general linear trend of the data. This was eventually traced to events involving the low temperature coolant supply and the fact that the low temperature chiller was being run manually. In these cases the coolant became too warm before an operator was able to get the chiller back on line. This was not observed in the thermocouple data being monitored; although it appeared that steady conditions had been reached, apparently temperatures were still changing slowly.

Figure 23 contains the data for the 2-in. uninsulated pipe; two outliers are observed. Figure 24 contains the data for the 2-in. insulated pipe; two outliers are in this plot although they cannot easily be discerned. Those data determined to be outliers are indicated in Appendix A and were not used in further analysis or comparisons.

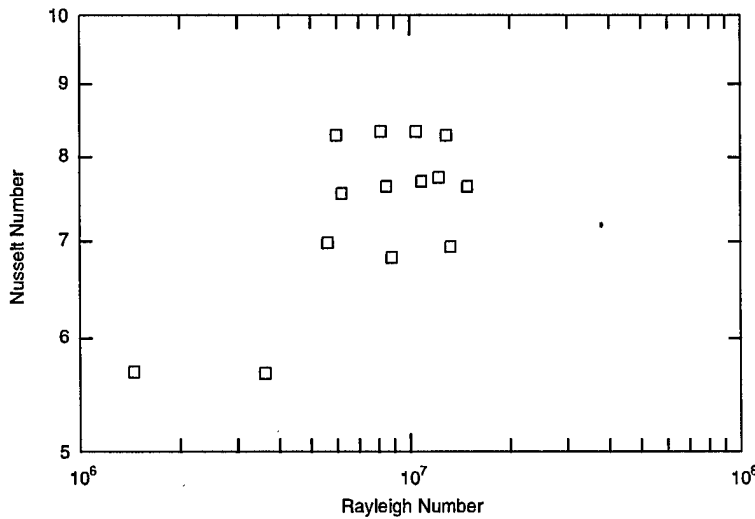


Figure 23. Nusselt and Rayleigh number plot for the 2-in. pipe in the 1-ft  $\times$  1-ft enclosure (experimental data).

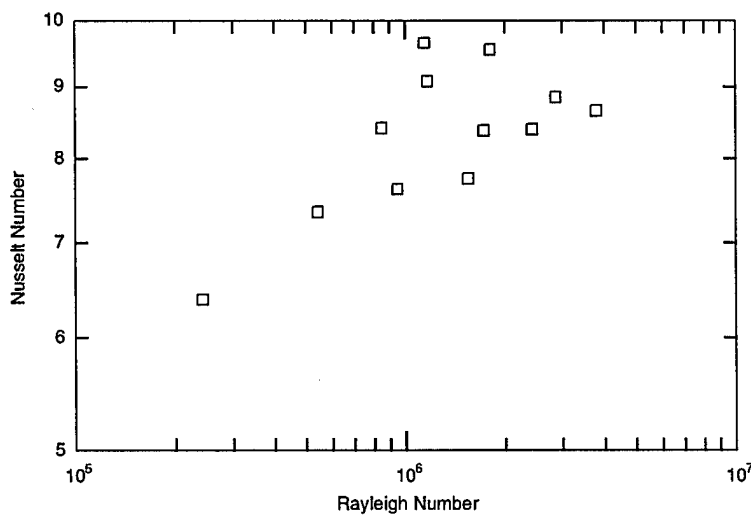


Figure 24. Nusselt and Rayleigh number plot for the 2-in. insulated pipe in the 1-ft  $\times$  1-ft enclosure (experimental data).

Experimental data obtained for the 2-ft  $\times$  4-ft enclosure are somewhat limited. Time constraints resulted in only one pipe configuration and limited temperature combinations. Steady-state temperatures took longer to achieve (compared to the 1-ft  $\times$  1-ft enclosure), and even then may have been influenced by the room temperature, which fluctuated over a  $\pm 5^{\circ}\text{F}$  temperature range. Some low temperature tests were attempted with only the 8-in. pipe heated; however, the pipe heater was not able to hold the desired temperature (at or above  $235^{\circ}\text{F}$ ) for all desired tests. Figure 25 shows the Nusselt and Rayleigh number plots. Gap width was determined by using an effective radius of the heated pipe(s); the values are in Table 8. The interior temperature range for these data is from about  $3^{\circ}\text{F}$  to  $80^{\circ}\text{F}$ . This almost spans the range of interest for most utilidor designs, even though a rather narrow range of Rayleigh numbers was obtained.

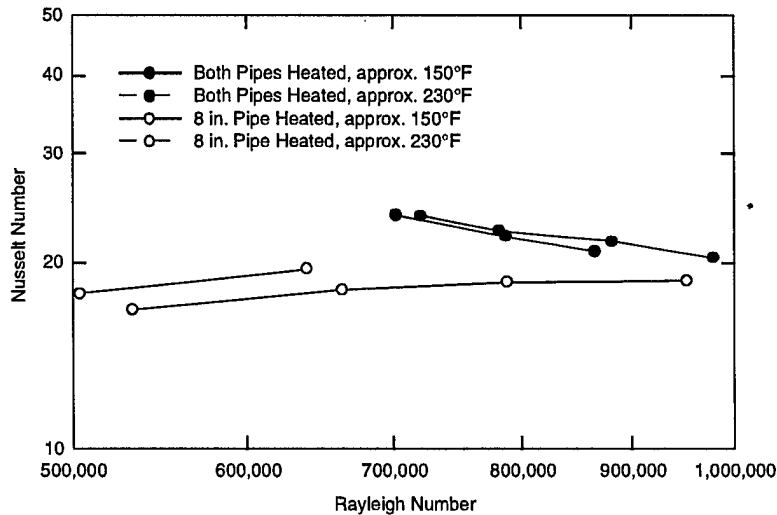


Figure 25. Nusselt and Rayleigh number plot for the 2-ft  $\times$  4-ft enclosure (experimental data).

There is significant difference in the curve shapes between the two-pipe heating conditions. This may be due to more stratification of the air in the bottom of the enclosure combined with a larger temperature difference compared to the single heated pipe configuration; this affects the heat conductance ( $h$ ) in the Nusselt number. Comparing Nusselt numbers for the bottom surfaces (App. A), it can be seen that there is a greater change for two heated pipes compared to the single heated pipe. This observation also explains the curved shape of the  $Nu$ - $Ra$  number data obtained with numerical data discussed in the next section.

#### Numerical data

The finite-element computer program FECOME, described earlier, was used to obtain additional heat transfer data from numerical experiments. The objective of the numerical experiments was to extend the database of enclosure configurations and boundary conditions, and to make comparisons with the physical experiments. The numerical experiments allowed calculations to be made without radiation boundaries and with different combinations of emissivity values.

Figure 26 shows one of the meshes used for the uninsulated 4-in. pipe in the 1-ft  $\times$  1-ft enclosure. It has the same internal dimensions as the experimental apparatus, including the 0.5-in. layer of EPS insulation enclosing the cavity of air. Temperatures around the outside of the insulation were held constant and the surface representing the outer diameter of the pipe was held at a series of temperatures. Increasing Rayleigh number values were obtained by decreasing the outside boundary temperatures in 5- or 10-degree increments until FECOME was no longer able to converge to a solution. A small temperature change in boundary conditions, and the use of a previous solution as

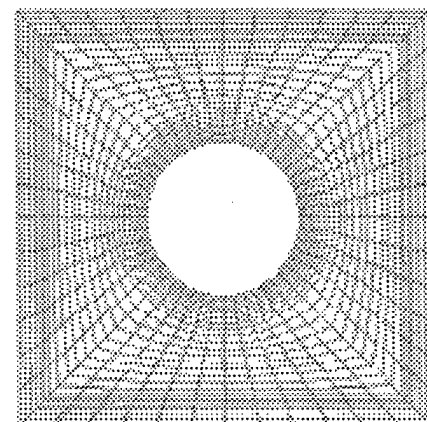


Figure 26. Mesh for the 1-ft  $\times$  1-ft enclosure with a 4-in. pipe (3,552 nodes, 1,152 elements, 10,848 d.o.f.).

an initial solution estimate, aided the model in converging to a solution. Towards the end of this study it was found that often FECOME converged to an oscillatory solution, which may actually occur in steady solutions. The temperatures were generally within or close to the convergence criteria, while the maximum velocity and pressure changes were small (2–3%). In Appendix B, the solutions that were oscillating are indicated with an asterisk in the file name.

The effect of mesh density was investigated and reported in Richmond (1997). In general, it was found that mesh density had little effect on average values, but denser meshes were required to obtain solutions at higher Rayleigh numbers. The meshes generated for all of the 1-ft square enclosure configurations are similar to Figure 26, as is the mesh for the 1.27-ft  $\times$  1.27-ft enclosure. Meshes for the other configurations are shown below (Fig. 27–29).

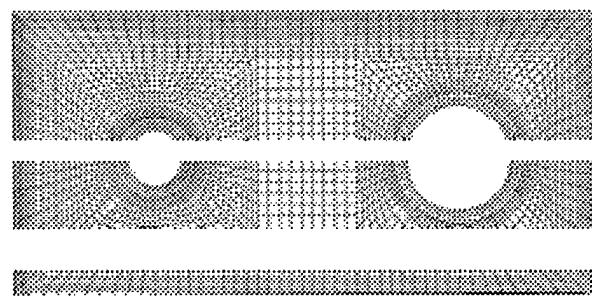


Figure 27. Mesh for the 2-ft  $\times$  2-ft enclosure with a 2-in. insulated pipe (16,704 nodes, 5,972 elements, 48,862 d.o.f.).

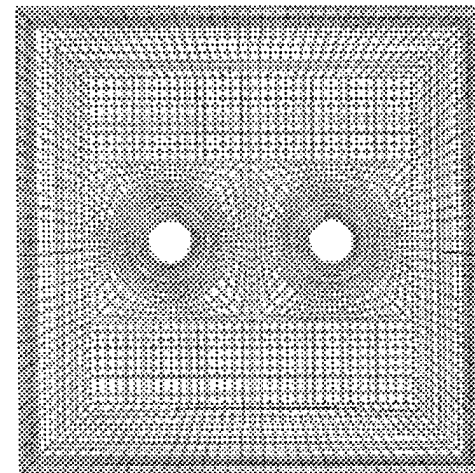


Figure 28. Mesh for the 2-ft  $\times$  4-ft enclosure, 4-in. and 8-in. insulated pipes (13,338 nodes, 4,356 elements, 38,834 d.o.f.).

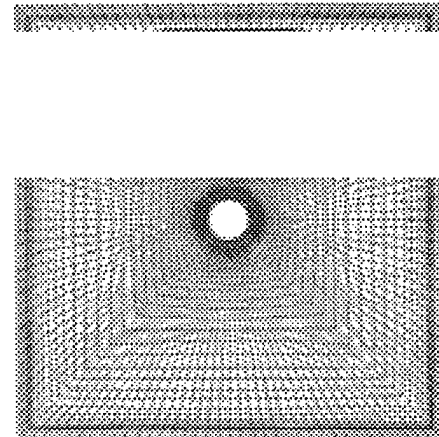


Figure 27. Mesh for the 2-ft  $\times$  2-ft enclosure with a 2-in. insulated pipe (16,704 nodes, 5,972 elements, 48,862 d.o.f.).

29). A limited number of solutions were obtained for the 2-ft  $\times$  2-ft enclosure with two pipes but none for the 2-ft  $\times$  4-ft enclosure. The reason for this is not clear, as these meshes are as dense as those used for the 1-ft  $\times$  1-ft enclosures. Attempts to solve these configurations required large quantities of memory and cpu time. It appears that the solution methods used by FECOME may not be optimal for these large-scale problems. Occasionally reports have been made in the literature regarding difficulties in obtaining solutions to high ( $10^7$ ) Rayleigh number problems, but there has been no indication of the best way to solve this problem.

Figures 30–33 display the numerical data in *Ra*-*Nu* number format; dashed lines connect data obtained with the same pipe temperatures (values of 250, 150, 100, 80, and 40°F). Data are also shown for the conditions where no radiation was modeled. The three different combinations of radiation emissivities are designated as follows:

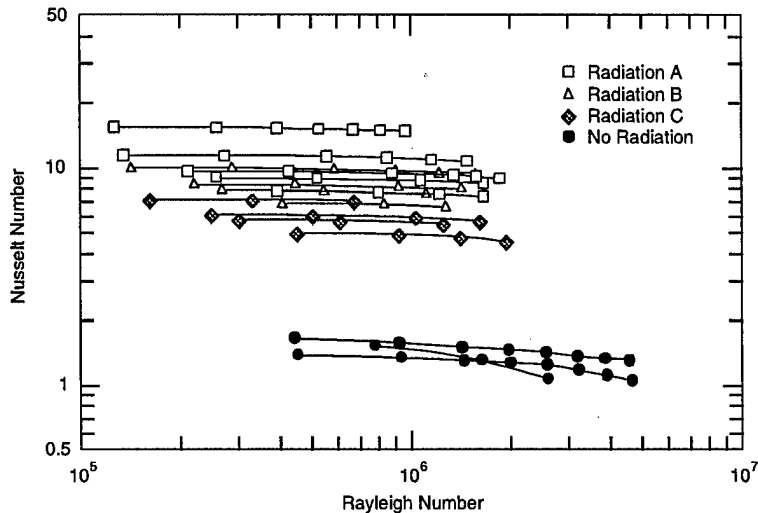


Figure 30. Nusselt and Rayleigh number plot for the 4-in. pipe in the 1-ft  $\times$  1-ft enclosure (numerical data).

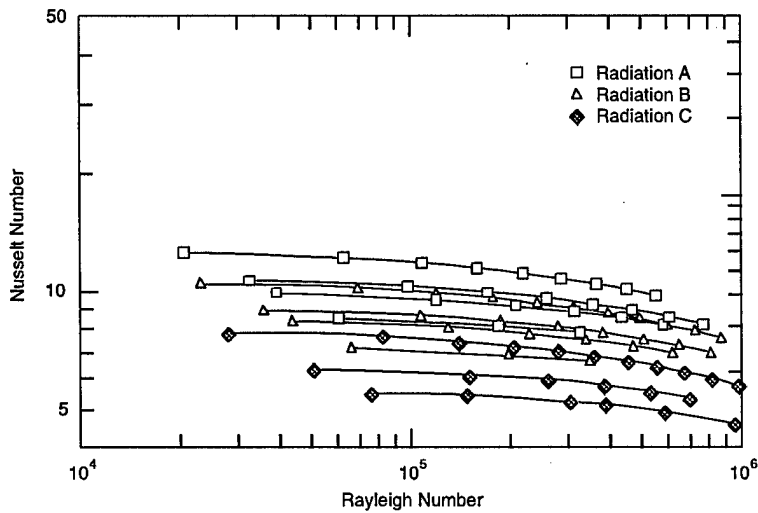


Figure 31. Nusselt and Rayleigh number plot for the insulated 4-in. pipe in the 1-ft  $\times$  1-ft enclosure (numerical data).

Radiation A, Pipe or insulation surface  $-0.9$ , inside insulation surface  $-0.9$   
 Radiation B, Pipe or insulation surface  $-0.9$ , inside insulation surface  $-0.6$   
 Radiation C, Pipe or insulation surface  $-0.5$ , inside insulation surface  $-0.9$ .

Significant differences are seen for each different radiation condition.

In Figure 30, the convection data alone (no radiation condition) do not all coincide on one line as expected. This is thought to be due to errors associated with too coarse a mesh, or for other unidentified reasons.

Figure 34 shows the data for the 1.27-ft  $\times$  1.27-ft and the 2-ft  $\times$  2-ft enclosures. The 1.27-ft  $\times$  1.27-ft enclosure had a 4-in. pipe with two inches of insulation. This resulted in nearly the same effective gap as the 2-in. insulated pipe in the 1-ft  $\times$  1-ft enclosure. The meager amount of data obtained with two pipes is also shown on the plot. The effective gap in this case was obtained using the total area of the two insulated pipes to determine an effective interior radius.

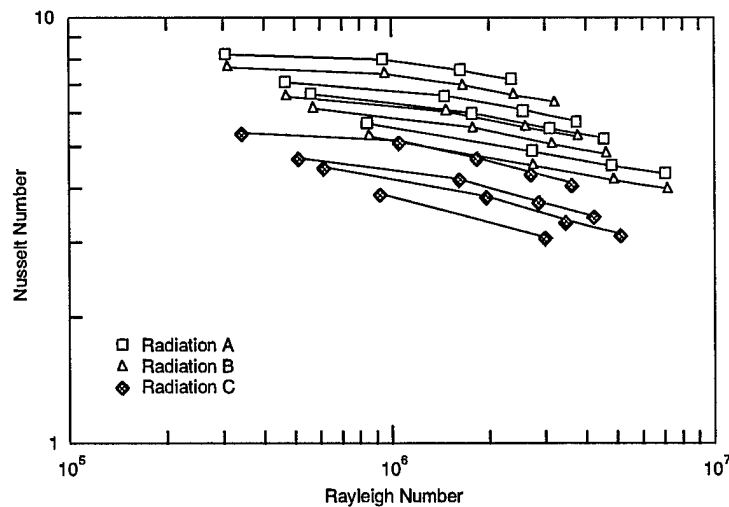


Figure 32. Nusselt and Rayleigh number plot for the 2-in. pipe in the 1-ft  $\times$  1-ft enclosure (numerical data).

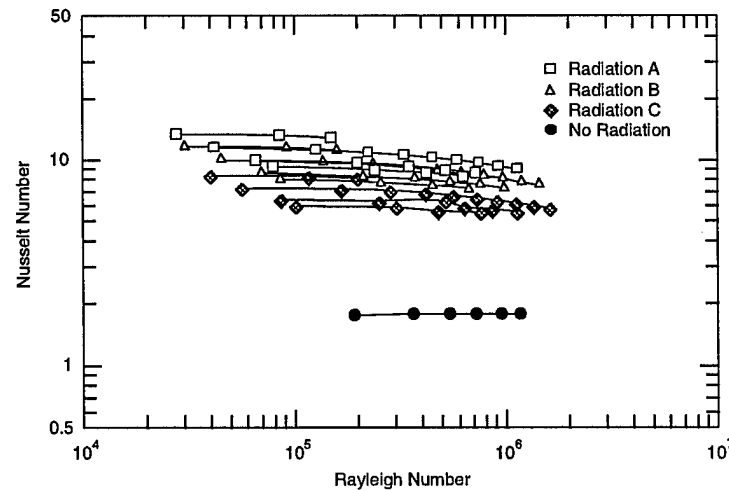


Figure 33. Nusselt and Rayleigh number plot for the insulated 2-in. pipe in the 1-ft  $\times$  1-ft enclosure (numerical data).

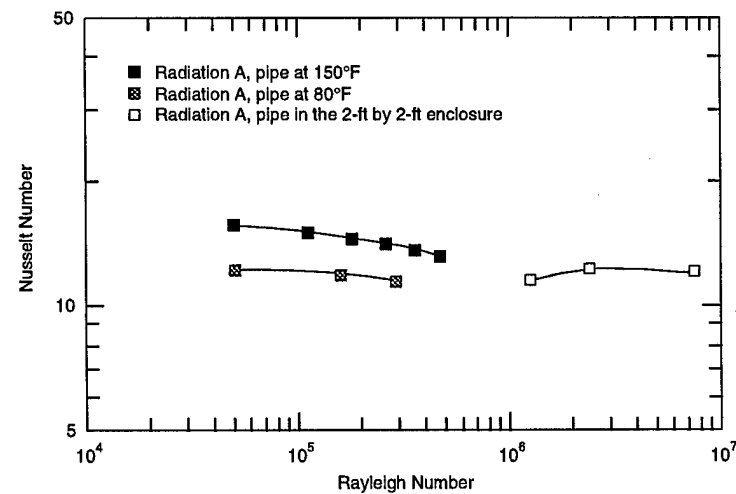
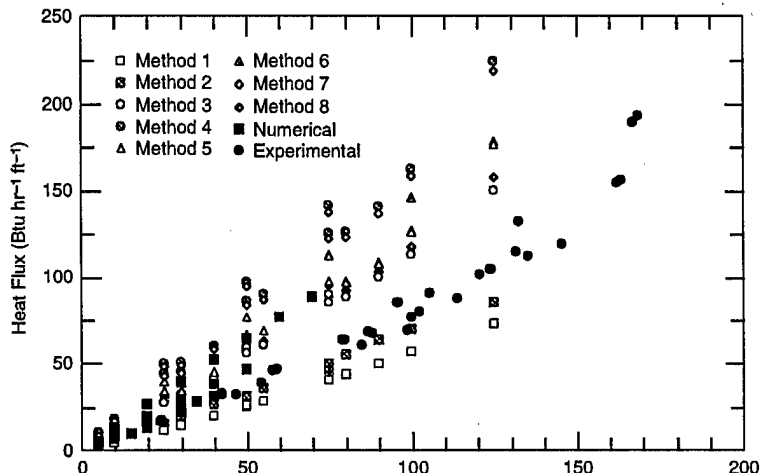
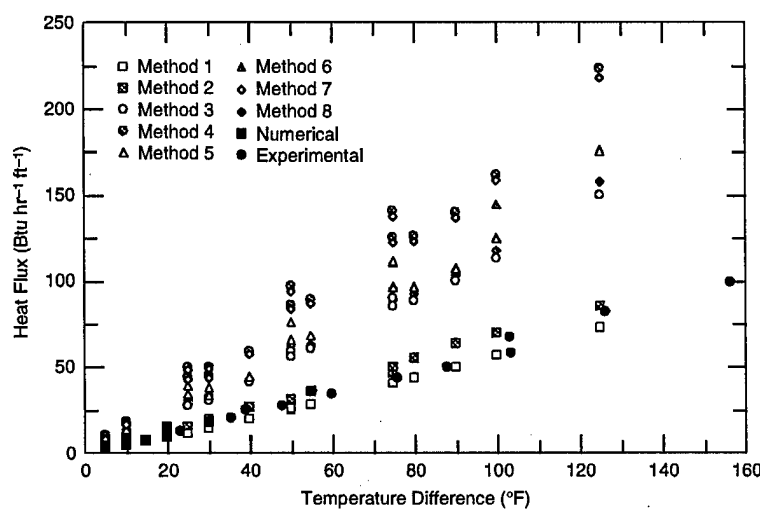


Figure 34. Nusselt and Rayleigh number plot for the 1.27-ft  $\times$  1.27-ft and 2-ft  $\times$  2-ft enclosures (numerical data).



a. Radiation A.



b. Radiation C.

Figure 35. Heat flux from the 4-in. pipe through the 1-ft  $\times$  1-ft enclosure.

## ANALYSIS

The Nusselt Number-Rayleigh Number plots in the previous section showed that no simple direct correlation between these parameters would be found. Comparisons of other parameters are made in this section and a new approximation for the effective conductivity of air is proposed. Comparisons of numerical solutions using this effective conductivity correlation are made with those obtained using FECOME and with experimental data from the 2-ft  $\times$  4-ft enclosure.

Figures 35–38 compare heat-flux-per-foot data from the numerical and experimental results with the eight methods presented in Table 1 for four configurations of the 1-ft  $\times$  1-ft enclosure. Figures 35 (a) and (b) compare the effect of emissivity values for radiation conditions A and C. In these figures, temperature difference is the total temperature difference for the system; heat flux is through the mean perimeter of the enclosure. Using the methods in Table 1 to determine the effective conductivity of the air, the heat flux was calculated using eq 51–57. Vertical scatter within a given method is related to the average interior temperatures. The

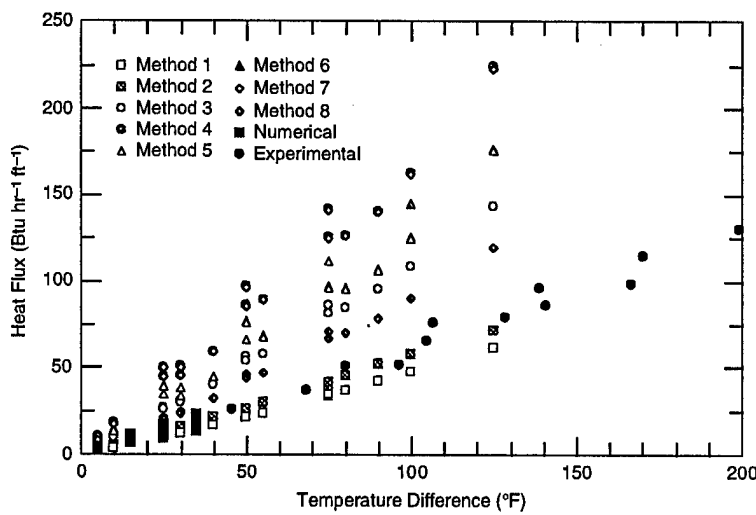


Figure 36. Heat flux from the 2-in. pipe through the 1-ft  $\times$  1-ft enclosure.

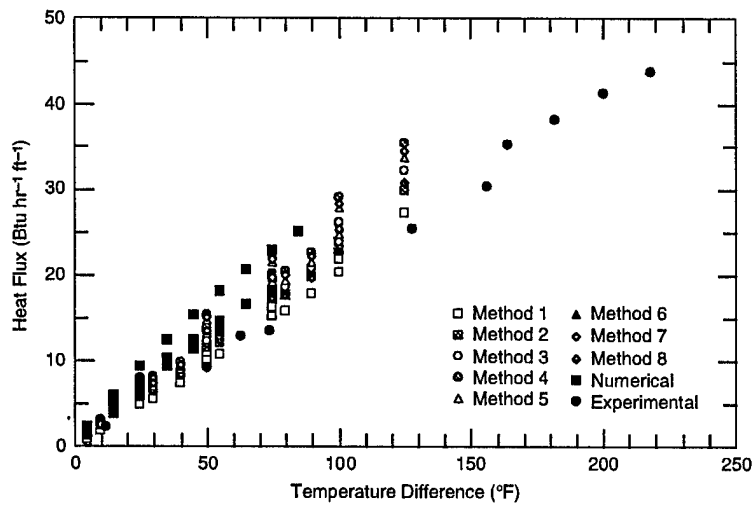


Figure 37. Heat flux from the 4-in. insulated pipe through the 1-ft  $\times$  1-ft enclosure.

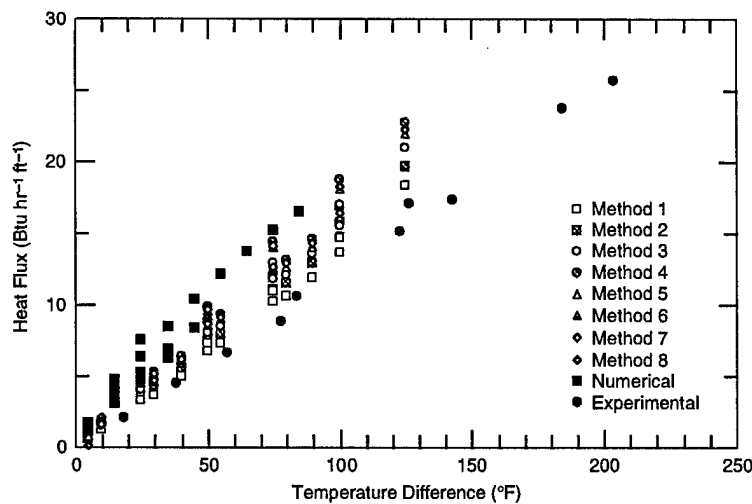


Figure 38. Heat flux from the 2-in. insulated pipe through the 1-ft  $\times$  1-ft enclosure.

numerical and experimental data compare well in all five plots. For the uninsulated pipes, the best agreement between the numerical and experimental data is with methods 1 and 2, which use eq 37 and 38 to calculate the effective conductivity. The differences caused by emissivity values can also be seen, with a slightly reduced heat flux observed for the lower emissivity (condition C). For the insulated pipes, there is general agreement between all the methods. This occurs because the thermal resistance due to the air gap becomes small relative to the resistance of the enclosure and pipe insulation.

Figures 39–42 compare the ratio of effective conductivity to the thermal conductivity of air ( $k_{\text{eff}}/k_{\text{air}}$ ) with the average temperature of the interior surfaces. The effective conductivity was calculated using eq 36 and the heat flow through the inside surface. Good agreement is seen between the numerical and experimental test data, while comparison of the Table 1 methods, in some cases, shows effects of temperature difference. Some of the methods show the same trend as the numerical and experimental data but differ in magnitude (for example, method 4 in Fig. 42).

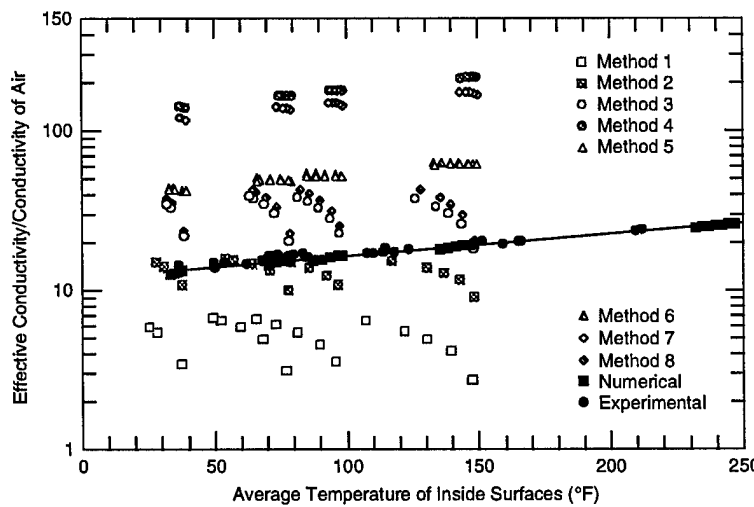


Figure 39. Ratio of effective conductivity to the conductivity of air vs. the average interior temperature (4-in. pipe).

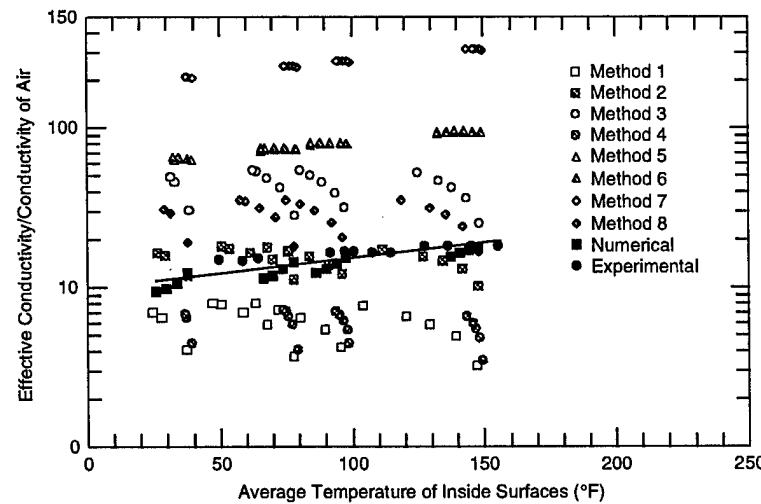


Figure 40. Ratio of effective conductivity to the conductivity of air vs. the average interior temperature (2-in. pipe).

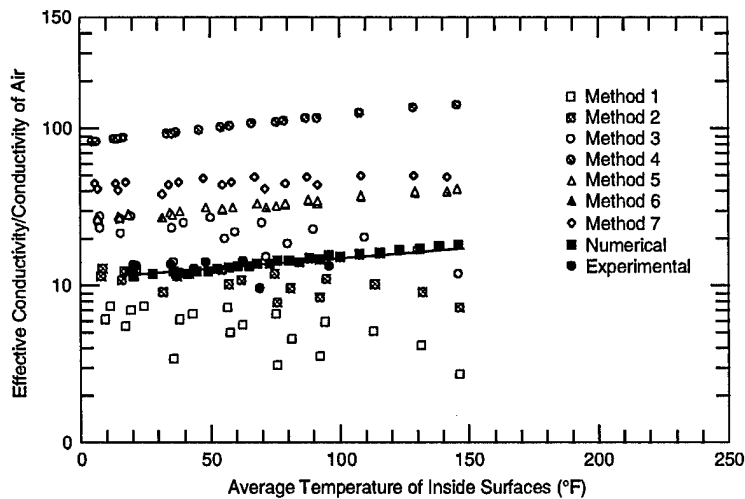


Figure 41. Ratio of effective conductivity to the conductivity of air vs. the average interior temperature (4-in. insulated pipe).

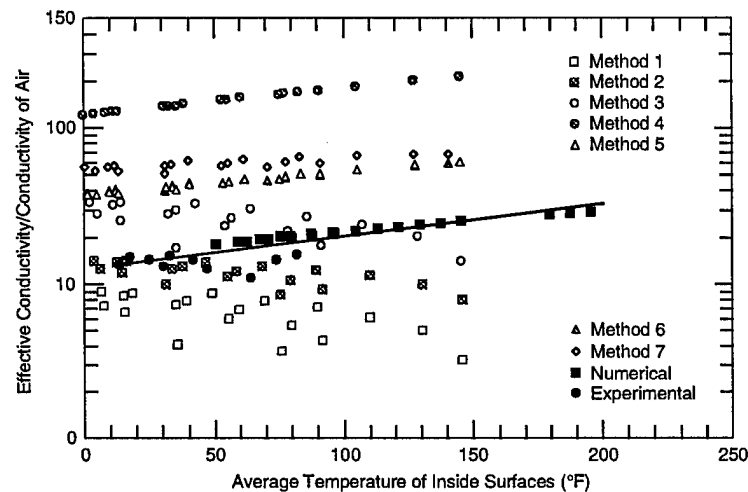


Figure 42. Ratio of effective conductivity to the conductivity of air vs. the average interior temperature (2-in. insulated pipe).

Curves of the following form were fit to the numerical and experimental data in Figures 39–42, and to the additional numerical data:

$$\frac{k_{\text{eff}}}{k_{\text{air}}} = Ae^{BT_{\text{AVG}}} \quad (133)$$

where  $T_{\text{AVG}}$  is the average of the interior surface temperatures and  $A$  and  $B$  are defined in Table 10. Equations 134–140 are plotted in Figure 43. Comparing eq 134 with eq 139 and 140 shows a reduction of 39% and 15% from radiation conditions A to B and A to C, respectively.

In an attempt to correlate the coefficients in eq 134–138 with a geometric parameter associated with the enclosure, it was found that a slight linear correlation exists between the radius ( $r$ ) of the interior pipe (or insulation) and the parameter  $A$  (the intercept). These data and the correlation are shown in Figure 44. Using an average value of the slopes ( $B$ ) results in the following equation:

Table 10. Coefficients for eq 133.

Effective gap	Pipe or insulation radius	A	B	eq	Description
0.396068	0.1875	12.026	0.003094	134	4-in. pipe in the 1-ft $\times$ 1-ft enclosure, numerical and experimental data, emissivities: pipe, 0.9; enclosure, 0.9.
0.312738	0.27083	10.9327	0.003057	135	4-in. insulated pipe in the 1-ft $\times$ 1-ft enclosure, numerical and experimental data emissivities: pipe insulation, 0.9; enclosure, 0.9.
0.484608	0.9896	9.7324	0.004123	136	2-in. pipe in the 1-ft $\times$ 1-ft enclosure, numerical and experimental data, emissivities: pipe, 0.9; enclosure, 0.9.
0.401278	0.18229	12.4199	0.001706	137	2-in. insulated pipe in the 1-ft $\times$ 1-ft enclosure, numerical and experimental data, emissivities: pipe insulation, 0.9; enclosure, 0.9.
0.401296	0.35416	13.2964	0.003680	138	4-in. pipe with 2 in. of insulation in the 1.27-ft $\times$ 1.27-ft enclosure, emissivities: pipe insulation, 0.9; enclosure, 0.9.
0.396068	0.1875	7.205	0.003387	139	4-in. pipe in the 1-ft $\times$ 1-ft enclosure, numerical and experimental data, emissivities: pipe, 0.9; enclosure, 0.6.
0.396068	0.1875	10.059	0.003424	140	4-in. pipe in the 1-ft $\times$ 1-ft enclosure, numerical and experimental data, emissivities: pipe, 0.5; enclosure, 0.9.

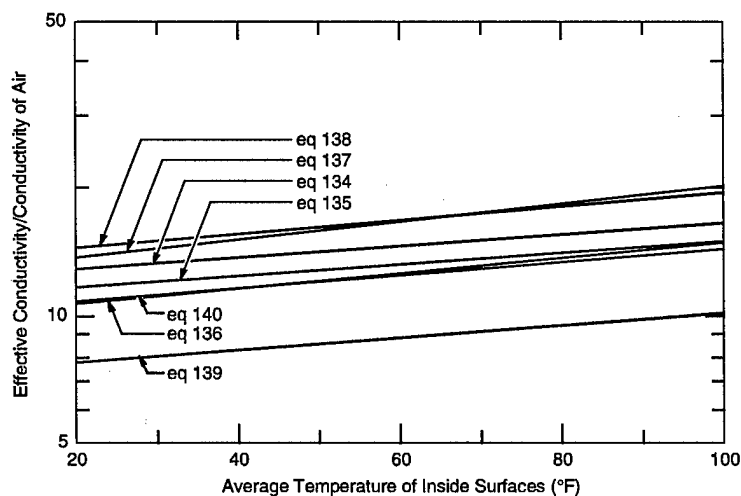


Figure 43. Effective conductivity correlations.

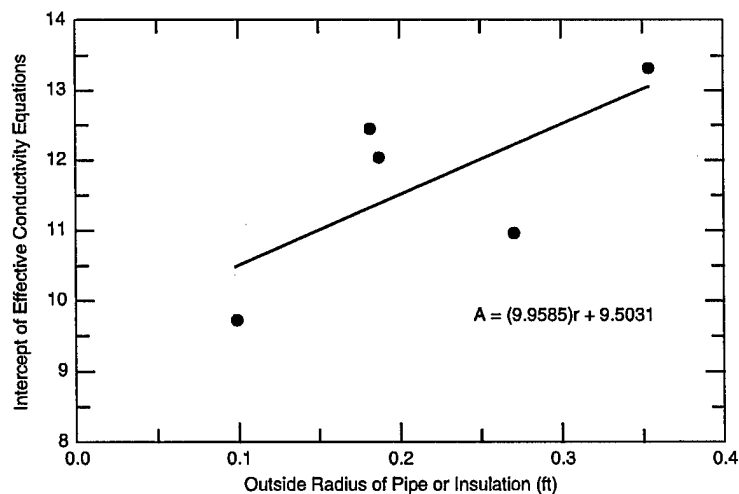


Figure 44. Correlation of pipe radius with intercepts.

$$\frac{k_{\text{eff}}}{k_{\text{air}}} = (9.5031 + 9.9585r)e^{0.00373T_{\text{AVG}}}. \quad (141)$$

Table 11 presents comparisons at three air temperatures for eq 134 through 138, and 141. The poorest comparisons are with eq 135 and 137, which have differences of -19 and 17% at an air temperature of 100°F.

The results from three numerical experiments were next compared with corresponding numerical experiments in which the conductivity of air was specified using eq 141 and treated as a solid (without radiation); the same FE meshes were used in both cases. Table 12 contains the parameters and description of each comparison. Figures 45–50 compare the inside surface temperatures and temperature contours for each comparison.

In the figures above, it can be seen that using an effective conductivity in lieu of the full convection solution will produce inaccurate temperature distributions in the air. In some cases, the predicted interior surface temperatures agree, but the quality of agreement depends on which surface (top, bottom, or side) is being considered. Better agreement is seen when a small temperature difference exists within the "air," and when the pipe is insulated. Average inside surface temperatures

**Table 11. Comparison of effective conductivity correlations.**

T <sub>AVG</sub>	Pipe radius (ft)				
	0.1875	0.27083	0.09896	0.18229	0.35416
<b>Equation 141, <math>k_{\text{eff}}/k_{\text{air}}</math></b>					
20	12.25	13.15	11.30	12.20	14.04
60	14.22	15.26	13.12	14.16	16.30
100	16.51	17.72	15.23	16.44	18.92
<b>Equations, <math>k_{\text{eff}}/k_{\text{air}}</math></b>					
	134	135	136	137	138
20	12.79	11.62	10.57	13.65	14.31
60	14.48	13.13	12.46	16.47	16.58
100	16.39	14.84	14.70	19.88	19.21
<b>Residuals</b>					
20	0.543	-1.523	-0.732	1.450	0.273
60	0.257	-2.127	-0.655	2.314	0.284
100	-0.124	-2.874	-0.531	3.448	0.291
<b>% differences</b>					
20	4.2	-13.1	-6.9	10.6	1.9
60	1.8	-16.2	-5.3	14.1	1.7
100	-0.8	-19.4	-3.6	17.3	1.5

**Table 12. Conditions for comparisons between numerical conduction and convection solutions.**

Name*	Pipe temp. (°F)	Outside temp. (°F)	Pipe radius (ft)	Estimated T <sub>AVG</sub> (°F)	k <sub>eff</sub> (Btu/hr ft <sup>2</sup> °F)
sq4ib65a	150	85	0.27083	100	0.26995
sq2d35c	80	45	0.09896	60	0.18865
sq2ic65a	150	85	0.18229	100	0.25045

\*Names correspond to file names in Appendix B.

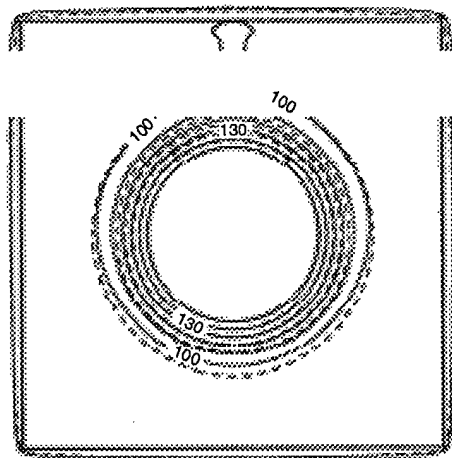


Figure 45. Temperature contours for sq4ib65a. Solid lines are from the convection and radiation solution, dashed lines are from the conduction solution.

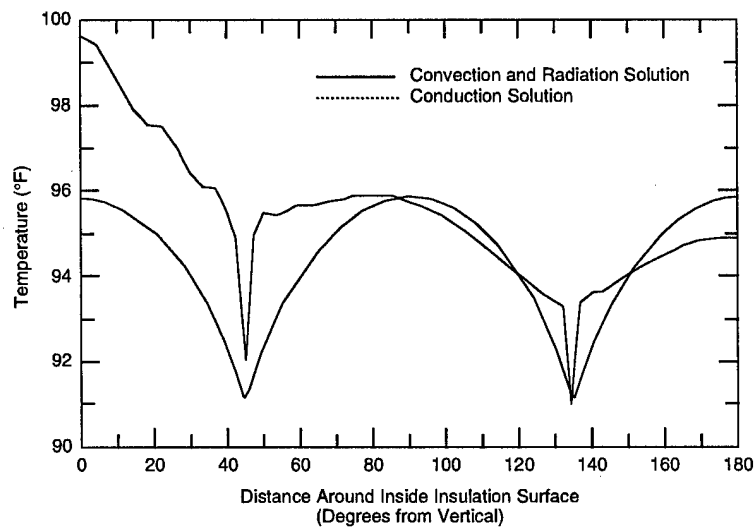


Figure 46. Inside surface temperatures for sq4ib65a.

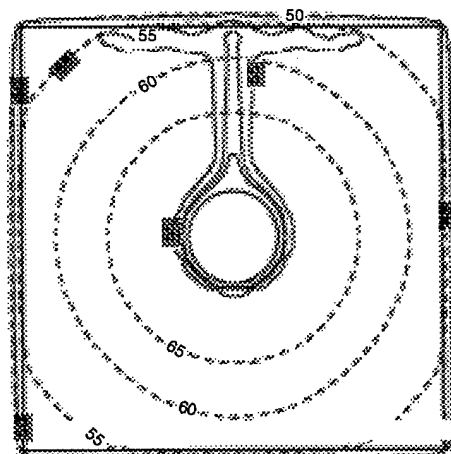


Figure 47. Temperature contours for sq2d35c. Solid lines are from the convection and radiation solution, dashed lines are from the conduction solution.

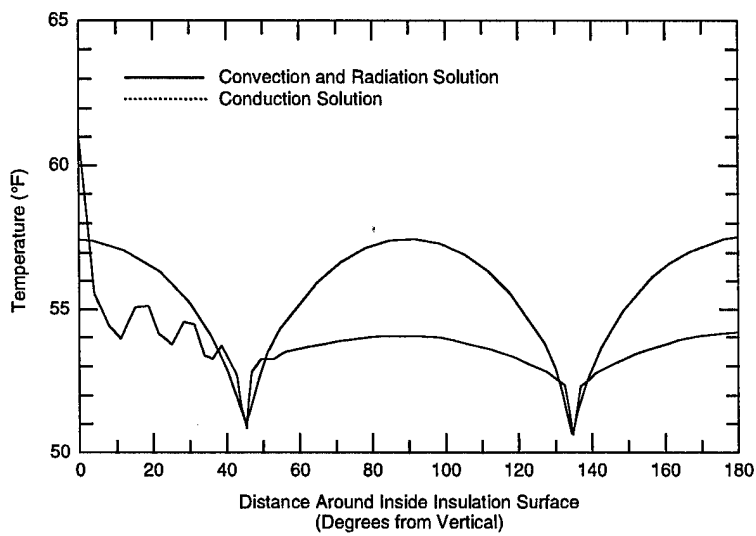


Figure 48. Inside surface temperatures for sq2d35c.

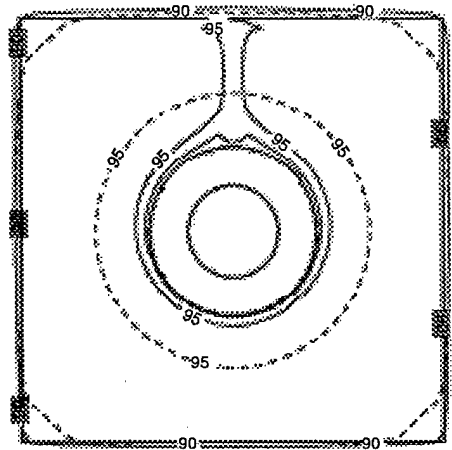


Figure 49. Temperature contours for sq2ic65a. Solid lines are from the convection and radiation solution, dashed lines are from the conduction solution.

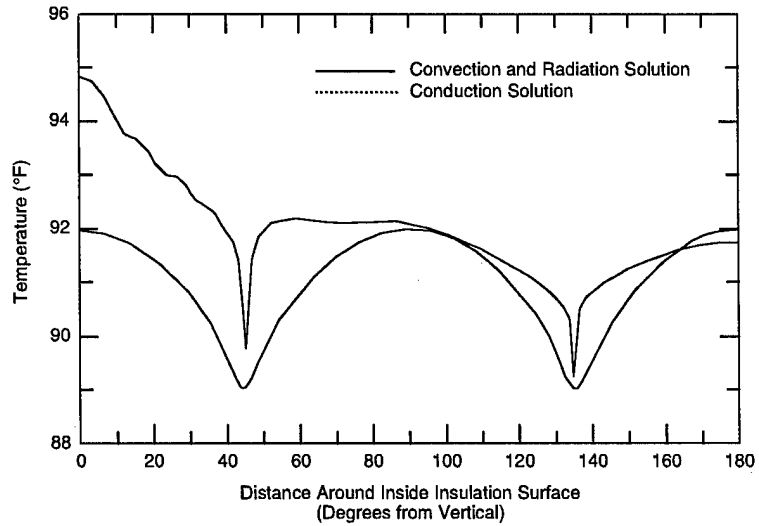


Figure 50. Inside surface temperatures for sq2ic65a.

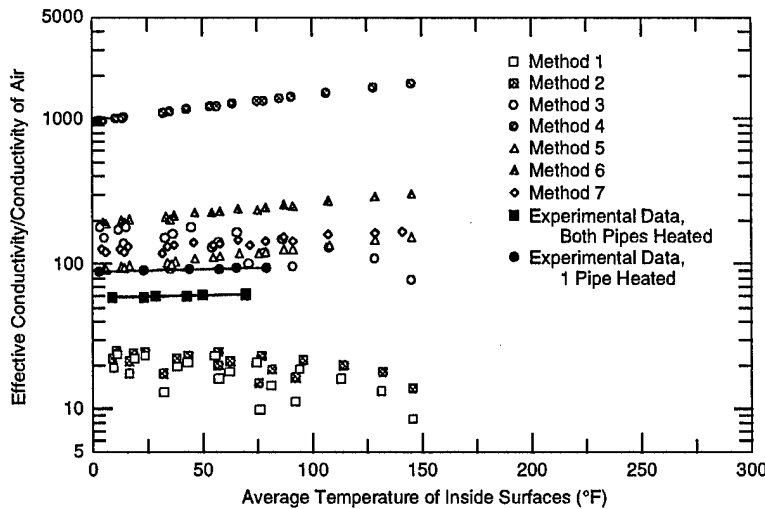


Figure 51. Ratio of effective conductivity to the conductivity of air vs. the average interior temperature (2-ft  $\times$  4-ft enclosure).

for the three cases were as follows: sq4ib65a, 95.20°F and 95.20°F; sq2d35c, 53.56°F and 55.25°F; sq2ic65a, 91.83°F and 90.82°F, for the convection versus conduction solutions, respectively. These average values agree very well, and if used in calculations of average heat loss, would give comparable values. Examining the insulation enclosure temperature contours, it can be seen that approximately midway through the insulation the temperature contours agree fairly well, but one reason for this agreement is the fixed outer boundary temperatures.

A similar approach was followed using the 2-ft  $\times$  4-ft experimental data. Figure 51 shows the comparison between the methods from Table 1 and the experimental data obtained with both pipes heated; weighted averages of the pipe insulation surface temperatures were used (note that the Table 1 methods are for two pipes heated at the same temperature, and shouldn't be compared with the experimental data for the single heated pipe). These values are much higher than those obtained from the smaller enclosure, and the intercepts do not correlate with pipe (insulation) radius as determined earlier. The slopes are near zero, and the intercepts (from curve fits) are 56.5836 and 86.6341 for the cases of both pipes heated and a single pipe heated, respectively.

Because no numerical convection and radiation solutions were obtained for this size enclosure, comparisons could be made only with the experimental data. Using the physical experimental data from 13 January 1997 and FECOME with an effective conductivity determined by two methods, comparisons were made between predicted and measured interior enclosure surface temperatures. Polynomial curve fits were made to the temperatures measured on the exterior of the 0.5-in. insulation (Fig. 52) and were applied as fixed boundary temperatures to the exterior surface nodes of the mesh shown in Figure 53. The average pipe temperatures, 142.75°F and 146.20°F, were used for the 4- and 8-in. pipes, respectively. Two values for the effective conductivity of air were used. One value was determined by using the effective radius of the two pipes (0.71354 ft) and eq 141, which yields a  $k_{eff}$  of 0.22863. The other value was 0.752115, determined from  $k_{eff}/k_{air} = 56.584$  (the curve fit to the test data in Fig. 51), which resulted in a  $k_{eff}$  of 0.1773. The air temperature (9.39°F) from the experimental test data was used to determine  $k_{air}$ .

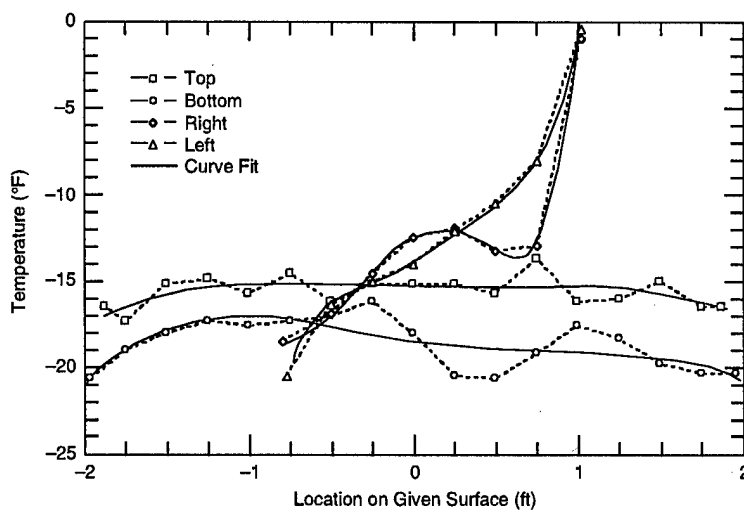


Figure 52. Polynomial curve fits to experimental boundary data.

Figure 53. Finite element mesh used for conduction solution of the 2-ft  $\times$  4-ft enclosure.

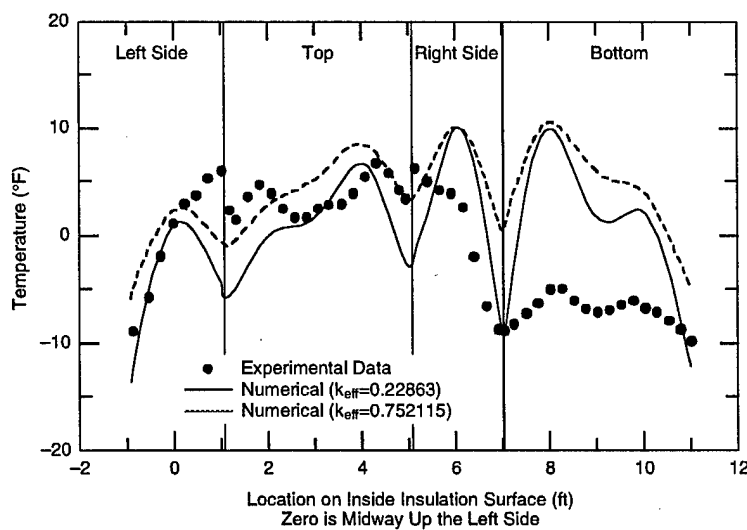


Figure 54. Comparison of experimental and numerical inside insulation surface temperatures (data from 13 January 1997).

Figure 54 compares the measured and calculated interior insulation surface temperatures. Fair agreement is obtained for all surfaces except the bottom, where temperatures are much warmer than measured. It can also be observed that the temperatures are not very sensitive to changes in the effective conductivity. The case chosen was that which had the greatest temperature difference across the air gap, and this should be considered when comparing the temperatures. It could also be noted that closeness of the outside boundary conditions to the compared temperatures are ensuring reasonable results. In defense of this, in an actual utilidor design the wall thickness would be much greater, but with well-known thermal properties. Because conduction solutions can be obtained with a high degree of confidence, then temperatures in similar locations will in most cases be known fairly well.

## SUMMARY

Three approaches to the thermal analysis of utilidors were investigated: the traditional or currently accepted practice of one-dimensional analysis, numerical analysis with modeling of convection and radiation, and numerical conduction analysis using an effective conductivity to account for convection and radiation effects. Each method has limitations and advantages.

The one-dimensional analysis did not produce good results when uninsulated pipes were modeled; only some correlations can account for multiple pipes, off-center locations, or other two-dimensional design possibilities. However, the method is easy to use, and good agreement with overall heat losses was observed with insulated pipes.

Numerical modeling with convection and radiation was demonstrated, producing good comparisons of heat loss with the experimental data; however, large geometries and/or large temperature differences across the air gap were difficult to model. The inclusion of radiation is required, and effects of surface emissivity values can be observed. Numerical data were obtained only for relatively small utilidors, the primary limitation being related to computational memory requirements and the matrix solution methods. Future improvements in computational methods and storage hardware may make this analysis method practical.

Numerical conduction analysis using an effective conductivity produced reasonable approximations to temperature distributions on inside surfaces; the method was easy to use, and the solutions were all obtained on a personal computer. Two-dimensional effects can be differentiated, but the information regarding temperature distribution within the air gap is inaccurate. The method seems to be most accurate for small temperature differences across the air gap and is relatively insensitive to minor changes in the effective conductivity value.

## CONCLUSIONS AND RECOMMENDATIONS

Average heat losses can be calculated reliably for insulated pipes using one-dimensional analysis, and these results will compare well with full (convection and radiation) numerical solutions (of average heat loss).

A full numerical solution will provide the best two-dimensional analysis. However, the current model may not be able to converge to a solution given reasonable computer resources. Ignoring radiation in a numerical convection model of

utilidors will have a significant effect on the temperature distribution and will result in lower predicted heat transfer rates.

The use of an effective conductivity for air in a numerical conduction analysis will produce reasonably good temperature distributions on interior surfaces. However, the air temperature distribution will be in error. The procedure is relatively insensitive to the effective conductivity, the pipe, and enclosure insulation dominating the heat loss, at least for the cases investigated in this work.

A more efficient and robust numerical modeling approach is required. Two possible improvements are to (1) convert the solution procedure to a "segregated method" where each of the governing equations are solved individually and a Poisson equation is substituted for the continuity equation, or to (2) incorporate an upwinding scheme such as the Petrov-Galerkin method into the element quadrature procedure.

Some temperature data from actual utilidors are available; comparisons with these data and numerical modeling of the entire soil mass should be done. Additionally, comparisons with an effective conductivity correlation in a transient conduction model, including the soil mass, and compared with field data, may also produce some interesting results.

#### LITERATURE CITED

Arpaci, V.S., and Y. Bayazitoglu (Ed.) (1990) Fundamentals of natural convection. *American Society of Mechanical Engineers, HTD, 140*.

Babus'Haq, R.F., S.D. Probert, and M.J. Shilston (1986) Improved pipeline configurations for DHC distribution systems. *ASHRAE Transactions, 92(2)*: 234-245.

Boyd, R.D. (1981) A new correlation theory for steady natural convective heat-transport data for horizontal annuli. In *Proceedings of the ASME/AICHE 20th National Heat Transfer Conference*, Milwaukee, Wisconsin.

de Vahl Davis, G., and I.P. Jones (1983) Natural convection in a square cavity: A comparison exercise. *International Journal for Numerical Methods in Fluids, 3*: 227-248.

Dropkin, D., and E. Somerscales (1965) Heat transfer by natural convection in liquids confined by two parallel plates which are inclined at various angles with respect to the horizon. *Journal of Heat Transfer, 87*: 77.

Eckert, E.R.G., and W.O. Carlson (1961) Natural convection in an air layer enclosed between two vertical plates with different temperatures. *International Journal of Heat and Mass Transfer, 2*: 23.

Elder, J.W. (1965) Turbulent-free convection in a vertical slot. *Journal of Fluid Mechanics, 23*: 99.

Emery, A.F., O. Johansson, M. Lobo, and A. Abrous (1991) A comparative study of methods for computing the diffuse radiation viewfactors for complex structures. *Transactions of the ASME, Journal of Heat Transfer, 113*: 413-422.

Ergatoudis, I., B.M. Irons, and O.C. Zienkiewicz (1968) Curved isoparametric, "quadrilateral" elements for finite element analysis. *International Journal of Solids, Structures, 4*: 31-42.

Federal Guide Specification (1981) National Federal Guide Specification (NFGS)-1570S, p. 15.

Gartling, D.K. (1977) Convective heat transfer analysis by the finite element method. *Computer Methods in Applied Mechanics and Engineering, 12*: 365-382.

Gartling, D.K. (1987) NACHOS II: A finite element computer program for incom-

pressible flow problems. Part I: Theoretical background. Sandia National Laboratories, Albuquerque, New Mexico, SAND86-1816.

**Gebhart, B., Y. Jaluria, R.L. Mahajan, and B. Sammakia** (1988) *Buoyancy Induced Flows and Transport*. New York: Hemisphere Publishing Corporation.

**Ghaddar, N.K.** (1992) Natural convection heat transfer between a uniformly heated cylindrical element and its rectangular enclosure. *International Journal of Heat and Mass Transfer*, 35(10): 2327–2334.

**Grigull, U., and W. Hauf** (1966) Natural convection in horizontal cylindrical annuli. In *Proceedings of the Third International Heat Transfer Conference*, August 7–12, Vol. 2.

**Grober, H.S., S. Erk, and U. Grigull** (1961) *Fundamentals of Heat Transfer*. New York: McGraw-Hill Book Company.

**Han, J.T.** (1967) Numerical solution for an isolated vortex in a slot and free convection across a square cavity. M.S. Thesis, Department of Mechanical Engineering, University of Toronto (unpublished).

**Holman, J.P.** (1976) *Heat Transfer*. Fourth Edition. New York: McGraw-Hill Book Company.

**Hornbeck, R.W.** (1975) *Numerical Methods*. New York: Quantum Publishers, Inc.

**Huebner, K.H., and E.A. Thornton** (1982) *The Finite Element Method for Engineers*. Second Edition. New York: John Wiley and Sons.

**Jakob, M.** (1949) *Heat Transfer*. New York: John Wiley and Sons.

**Jaluria, Y., and K.E. Torrance** (1986) *Computational Heat Transfer*. New York: Hemisphere Publishing Corporation.

**Kennedy, F.E., G. Phetteplace, N. Hamilton, and V. Prabhakar** (1988) Thermal performance of a shallow utilidor. In *Proceedings of the Fifth International Conference on Permafrost, Trondheim, Norway*.

**Kraichnan, R.H.** (1962) Turbulent thermal convection at arbitrary Prandtl number. *Physics of Fluids*, 5: 1374.

**Kuehn, T.H., and R.J. Goldstein** (1978) An experimental study of natural convection heat transfer in concentric and eccentric horizontal cylindrical annuli. *Transactions of the ASME, Journal of Heat Transfer*, 100: 635–640.

**Lunardini, V.J.** (1990) Measurement of heat losses from a conduit-type heat distribution system. In *Proceedings of the 1990 Army Science Conference*, Durham, South Carolina.

**MacGregor, R.K., and A.F. Emery** (1969) Free convection through vertical plane layers: Moderate and high Prandtl number fluids. *Journal of Heat Transfer*, 92: 391.

**Newell, M.E., and F.W. Schmidt** (1969) Heat transfer by laminar natural convection within rectangular enclosures. ASME Paper 69-HT-42.

**Ostrach, S.** (1972) Natural convection in enclosures. *Advances in Heat Transfer*, 8: 161.

**Özisik, M.N.** (1980) *Heat Conduction*. New York: John Wiley and Sons, p. 58–60.

**Phetteplace, G.L., W. Willey, and M.A. Novick** (1981) Losses from the Fort Wainwright heat distribution system. USA Cold Regions Research and Engineering Laboratory, Special Report 81-14.

**Phetteplace, G., P. Richmond, and N. Humiston** (1986) Thermal analysis of a shallow utilidor. 77th Conference of the International District Heating and Cooling Association, Asheville, North Carolina, June 8–12.

**Powe, R.E., and R.O. Warrington, Jr.** (1983) Natural convection heat transfer between bodies and their spherical enclosure. *Transactions of the ASME*, 105: 440–446.

**Raznjevic, K.** (1976) *Handbook of Thermodynamic Tables and Charts*. New York: Hemisphere Publishing Corporation.

**Richmond, P.W.** (1995) A finite element computer code for the heat transfer analysis of enclosures, description and source code. USA Cold Regions Research and Engineering Laboratory, Internal Report 1156.

**Richmond, P.W.** (1997) Natural convection and radiation heat transfer from a heated pipe to a square enclosure. Unpublished report.

**Richmond, P.W., H.J. Bunker, and A.K. Notman** (1997) Temperature data for heated pipes in rectangular enclosures. USA Cold Regions Research and Engineering Laboratory, Internal Report 1173.

**Siegel, R., and J.R. Howell** (1992) *Thermal Radiation Heat Transfer*. Third Edition. New York: Hemisphere Publishing Corporation.

**Silveston, P.L.** (1958) *Forsch. Geb. Ingenieurwes.*, **24**: 59. (See Gebhart et al. 1988, p. 754.)

**Smith, D.W., S. Reed, J.J. Cameron, G.W. Heinke, F. James, B. Reis, W.L. Ryan, and J. Schibner** (1979) Cold climate utilities delivery design manual. U.S. Environmental Protection Agency, Report EPA-600/8-79-027.

**Stewart, W.E., Jr., and J.L. Verhulst** (1985) Experimental free convection from piping in district heating utilidors. American Society of Mechanical Engineers 85-WA/HT-55.

**U.S. Army** (1987) Arctic and subarctic construction: Utilities. Headquarters, Department of the Army and the Air Force, Washington, D.C.

**Warrington, R.O., Jr., and R.E. Powe** (1985) The transfer of heat by natural convection between bodies and their enclosures. *International Journal of Heat and Mass Transfer*, **28**(2): 319–330.

**Zarling, J.P., and W.A. Braley** (1984) Heat loss factors for insulated building foundations. Institute of Water Resources/Engineering Experiment Station, University of Alaska, Fairbanks, Alaska.

**Zirjacks, W.L., and C.T. Hwang** (1983) Underground utilidors at Barrow, Alaska: A two-year history. In *Proceedings of the 4th International Conference on Permafrost, 17–22 July, Fairbanks, Alaska*. Washington, D.C.: National Academy Press, p. 1513–1517.

## APPENDIX A: EXPERIMENTAL RESULTS

Date	Temperature (°F)		1-ft x 1-ft enclosure, 4.5 inch pipe, unpainted						Average heat Conductance								
	Pipe	Inside	Outside	EPS	EPS	Dtemp <sup>1</sup>	T <sub>Avg</sub> <sup>2</sup>	Bottom	Right Side	Left Side	Nu	Ra	Nu	Ra	Nu	Ra	Flux (Btu/hr ft)
<b>1-ft x 1-ft enclosure, 4.5 inch pipe, unpainted</b>																	
28-Jun-91	57.25	42.68	33.59	14.57	49.95	6.08	1.86E+06	7.31	1.58E+06	8.34	1.62E+06	10.44	1.42E+06	8.20	1.62E+06	15.709	0.294
1-Jul-91	58.23	43.14	33.91	15.09	50.68	6.03	1.89E+06	7.11	1.64E+06	8.17	1.66E+06	10.15	1.48E+06	8.03	1.67E+06	15.953	0.288
2-Jul-91	81.32	56.07	38.72	25.25	68.36	6.96	2.65E+06	7.74	2.32E+06	9.01	2.35E+06	11.23	2.09E+06	8.97	2.35E+06	30.602	0.331
3-Jul-91	80.96	55.90	38.47	25.06	68.45	7.01	2.65E+06	7.93	2.29E+06	8.98	2.35E+06	11.42	2.07E+06	9.08	2.34E+06	30.722	0.334
5-Jul-91	80.91	56.08	38.71	24.83	68.51	7.03	2.63E+06	8.06	2.25E+06	9.10	2.32E+06	11.37	2.06E+06	9.14	2.32E+06	30.658	0.337
8-Jul-91	102.66	69.06	44.81	33.61	85.86	6.96	3.09E+06	8.14	2.62E+06	9.62	2.66E+06	11.94	2.36E+06	9.38	2.69E+06	43.752	0.355
11-Jul-91	102.13	67.92	43.06	34.21	85.01	6.93	3.18E+06	8.15	2.68E+06	9.59	2.73E+06	12.18	2.41E+06	9.43	2.76E+06	44.681	0.356
15-Jul-91 A	150.32	98.13	54.83	52.18	124.25	7.91	3.54E+06	9.05	2.95E+06	10.83	3.01E+06	13.68	2.68E+06	10.66	3.05E+06	81.452	0.426
15-Jul-91 B	150.25	97.77	54.35	52.47	123.99	7.88	3.56E+06	9.01	2.97E+06	10.79	3.04E+06	13.67	2.70E+06	10.63	3.07E+06	81.603	0.424
17-Jul-91 A	200.67	132.26	68.10	68.40	166.44	9.10	3.40E+06	10.11	2.82E+06	12.00	2.91E+06	14.96	2.61E+06	11.97	2.94E+06	126.810	0.506
17-Jul-91 B	199.90	131.49	67.20	68.41	165.48	9.10	3.43E+06	10.13	2.83E+06	12.02	2.92E+06	15.00	2.62E+06	11.98	2.96E+06	126.858	0.506
22-Jul-91	232.45	172.59	83.81	79.86	212.41	10.38	3.01E+06	11.50	2.47E+06	13.38	2.58E+06	19.88	2.10E+06	14.14	2.54E+06	184.986	0.632
23-Jul-91	249.65	170.00	82.74	79.65	209.74	10.24	3.05E+06	11.31	2.52E+06	13.28	2.61E+06	19.68	2.13E+06	13.93	2.58E+06	180.722	0.619
8-Aug-91	50.63	22.64	3.81	27.99	36.66	5.94	4.16E+06	7.20	3.46E+06	8.66	3.49E+06	11.85	3.07E+06	8.32	3.55E+06	30.635	0.299
9-Aug-91	104.34	60.26	25.44	44.03	84.03	6.88	3.43E+06	8.83	3.39E+06	9.84	3.64E+06	13.11	3.18E+06	9.90	3.65E+06	60.639	0.375
13-Aug-91	101.56	131.51	50.48	57.60	6.75	5.11E+06	7.27	4.82E+06	9.99	4.22E+06	13.09	3.74E+06	9.28	4.39E+06	63.854	0.345	
14-Aug-91	80.20	24.15	67.76	114.04	7.72	4.95E+06	8.00	4.35E+06	10.88	4.14E+06	13.98	3.71E+06	10.23	4.29E+06	99.744	0.401	
15-Aug-91	80.67	24.59	68.00	114.62	7.72	4.94E+06	7.98	4.35E+06	10.84	4.14E+06	13.90	3.71E+06	10.20	4.29E+06	99.886	0.401	
16-Aug-91	201.56	117.55	39.23	84.00	159.53	8.89	4.33E+06	9.17	3.82E+06	12.15	3.65E+06	14.92	3.33E+06	11.48	3.79E+06	147.720	0.480
7-Oct-91	150.29	80.27	18.54	70.02	115.27	7.66	5.23E+06	9.08	4.25E+06	11.39	4.29E+06	14.96	3.75E+06	10.82	4.39E+06	109.427	0.426
9-Oct-91	193.32	110.13	29.66	83.19	151.71	8.63	4.69E+06	9.67	3.86E+06	12.48	3.87E+06	15.98	3.41E+06	11.82	3.97E+06	149.191	0.489
10-Oct-91	100.25	44.43	0.30	55.82	72.33	6.57	6.04E+06	8.18	4.92E+06	10.30	4.90E+06	14.00	4.22E+06	9.69	5.03E+06	73.456	0.359
27-Oct-95	102.95	58.14	23.36	44.81	80.55	7.18	4.41E+06	8.06	3.95E+06	10.18	3.71E+06	13.08	3.27E+06	9.81	3.76E+06	60.305	0.367
28-Oct-95	102.66	53.73	15.78	48.93	78.20	6.83	4.97E+06	8.03	3.99E+06	10.18	4.13E+06	13.23	3.61E+06	9.70	4.19E+06	64.923	0.362
2-Nov-95	102.71	45.95	0.18	56.75	74.33	6.67	6.07E+06	8.20	4.77E+06	10.57	4.90E+06	13.69	4.29E+06	9.87	5.03E+06	76.186	0.366
3-Nov-95	102.51	39.47	-11.53	63.03	70.99	6.60	6.97E+06	8.02	5.45E+06	10.30	5.66E+06	13.78	4.85E+06	9.74	5.75E+06	83.067	0.357
28-Nov-95 *	103.18	61.16	30.93	42.02	82.17	5.89	4.19E+06	8.05	3.28E+06	9.95	3.36E+06	12.67	2.99E+06	9.18	3.47E+06	53.066	0.344
29-Nov-95	147.98	89.45	42.54	58.53	118.71	6.53	4.35E+06	8.84	3.37E+06	10.92	3.46E+06	14.04	3.05E+06	10.15	3.57E+06	85.994	0.401
30-Nov-95	147.83	81.39	27.11	66.44	114.61	6.40	5.16E+06	8.78	3.94E+06	10.98	4.05E+06	14.32	3.54E+06	10.14	4.19E+06	97.010	0.398
1-Dec-95	147.63	73.75	12.43	73.87	110.69	6.30	5.97E+06	8.70	4.49E+06	11.03	4.64E+06	14.47	4.03E+06	10.11	4.81E+06	106.912	0.395
2-Dec-95	147.52	68.43	1.84	79.09	107.97	6.24	6.58E+06	8.64	4.90E+06	11.05	5.07E+06	14.68	4.38E+06	10.10	5.26E+06	113.996	0.393
3-Dec-95 *	80.30	37.47	8.86	42.82	58.88	5.11	5.32E+06	7.54	4.13E+06	9.05	4.23E+06	11.85	3.73E+06	8.37	4.37E+06	47.634	0.303
4-Dec-95	78.62	29.07	-6.33	49.56	53.84	5.20	6.60E+06	7.78	4.97E+06	9.50	5.13E+06	12.88	4.43E+06	8.76	5.31E+06	57.285	0.315
5-Dec-95	78.43	21.36	-20.29	57.08	49.89	5.03	8.02E+06	7.59	5.92E+06	9.72	6.10E+06	13.35	5.22E+06	8.77	6.35E+06	63.629	0.314

Date	Pipe	Temperature (°F)			Bottom			Right Side			Left Side			Top			Average			Average heat	
		Pipe	Inside	Outside	EPS	EPS	Dtemp <sup>1</sup>	T <sub>Avg</sub> <sup>2</sup>	Nu	Ra	Nu	Ra	Nu	Ra	Nu	Ra	Nu	Ra	Flux	Conductance	
<b>1-ft x 1-ft enclosure, 4.5 inch pipe, painted aluminum</b>																					
6-Dec-95	78.93	46.42	24.75	32.52	62.68	5.31	3.86E+06	7.75	3.04E+06	9.02	3.12E+06	12.01	2.74E+06	8.54	3.20E+06	37.130	0.311				
29-Aug-96	79.14	62.49	56.01	16.65	70.81	3.03	1.76E+06	5.27	1.44E+06	5.47	1.49E+06	7.09	1.38E+06	5.20	1.52E+06	11.711	0.192				
30-Aug-96	79.15	54.25	43.46	24.90	66.70	3.28	2.79E+06	5.45	2.25E+06	6.05	2.31E+06	8.19	2.08E+06	5.69	2.36E+06	19.049	0.209				
31-Aug-96	79.45	46.26	31.42	33.19	62.86	3.22	3.90E+06	5.46	3.12E+06	6.09	3.20E+06	8.67	2.80E+06	5.77	3.26E+06	25.619	0.211				
1-Sep-96	79.30	38.35	19.21	40.95	58.82	3.26	5.05E+06	5.58	3.98E+06	6.34	4.08E+06	8.99	3.56E+06	5.93	4.18E+06	32.281	0.215				
5-Sep-96	79.20	28.24	3.19	50.95	53.72	3.25	6.72E+06	5.66	5.17E+06	6.60	5.32E+06	9.53	4.56E+06	6.10	5.46E+06	40.974	0.219				
6-Sep-96	79.16	20.92	-8.74	58.24	50.04	3.22	8.06E+06	5.71	6.11E+06	6.75	6.28E+06	9.97	5.32E+06	6.21	6.47E+06	47.389	0.222				
7-Sep-96	79.21	11.46	-24.29	67.75	45.35	3.23	9.96E+06	5.75	7.43E+06	6.82	7.64E+06	10.30	6.37E+06	6.28	7.88E+06	55.351	0.223				
9-Sep-96	147.54	48.11	-8.92	99.42	97.82	3.57	9.03E+06	6.11	6.78E+06	7.44	6.94E+06	10.78	5.87E+06	6.73	7.19E+06	94.143	0.238				
10-Sep-96	147.64	65.86	21.15	81.79	106.75	3.73	6.73E+06	6.29	5.21E+06	7.12	5.36E+06	10.22	4.58E+06	6.70	5.49E+06	78.004	0.260				
11-Sep-96	147.78	79.77	44.63	68.00	113.77	3.75	5.21E+06	6.22	4.14E+06	6.89	4.22E+06	9.66	3.65E+06	6.54	4.32E+06	63.915	0.256				
12-Sep-96 *	147.90	94.35	67.26	53.55	121.12	4.40	3.81E+06	6.11	3.08E+06	6.66	3.14E+06	9.19	2.76E+06	6.59	3.21E+06	51.230	0.261				
13-Sep-96	147.92	109.88	92.59	38.04	128.90	3.78	2.51E+06	5.89	2.06E+06	6.31	2.11E+06	8.48	1.89E+06	6.10	2.15E+06	34.090	0.244				
14-Sep-96	147.95	120.55	108.88	27.40	134.25	3.69	1.71E+06	5.72	1.41E+06	6.02	1.47E+06	7.89	1.33E+06	5.84	1.49E+06	23.645	0.235				
<b>1-ft x 1-ft enclosure, 4.5 inch pipe, insulated</b>																					
19-Sep-96 *	148.30	89.19	79.83	71.66	9.37	84.51	6.73	4.43E+05	8.39	3.35E+05	9.53	3.69E+05	11.50	3.38E+05	9.34	3.73E+05	15.292	0.445			
20-Sep-96 *	148.71	68.38	55.86	43.81	12.53	62.12	7.62	7.17E+05	8.34	5.68E+05	10.42	5.98E+05	12.42	5.49E+05	10.07	6.11E+05	21.318	0.464			
22-Sep-96	149.27	52.28	35.65	21.28	16.63	43.97	5.93	1.18E+06	7.70	8.89E+05	9.12	9.50E+05	12.04	8.27E+05	8.85	9.66E+05	24.222	0.397			
23-Sep-96	149.70	31.74	11.74	-6.54	20.01	21.74	5.68	1.85E+06	7.77	1.34E+06	9.67	1.42E+06	13.11	1.21E+06	9.10	1.46E+06	28.942	0.395			
24-Sep-96	148.81	99.95	92.43	86.06	7.52	96.19	6.65	3.22E+05	8.28	2.42E+05	9.27	2.70E+05	11.32	2.46E+05	9.18	2.71E+05	12.264	0.445			
27-Sep-96	79.32	70.22	68.45	67.37	1.77	69.34	4.44	9.75E+04	8.50	5.02E+04	6.87	8.09E+04	6.2953	8.86E+04	6.58	8.08E+04	1.993	0.307			
28-Sep-96 *	79.58	55.84	52.45	48.62	3.39	54.14	5.50	2.58E+05	14.14	1.11E+05	13.05	1.70E+05	15.517	1.59E+05	11.99	1.78E+05	6.791	0.546			
29-Sep-96	80.11	41.73	35.30	30.19	6.43	38.52	5.59	4.71E+05	7.72	3.47E+05	8.59	3.88E+05	10.245	3.62E+05	8.29	3.93E+05	8.703	0.369			
30-Sep-96	80.40	23.93	14.37	6.47	9.55	19.15	5.48	8.77E+05	7.55	6.51E+05	8.96	6.99E+05	11.174	6.31E+05	8.45	7.18794.4	12.771	0.365			
1-Oct-96	197.52	59.95	37.06	15.34	22.90	48.51	6.23	1.59E+06	8.15	1.17E+06	10.029	1.25E+06	13.514	1.06E+06	9.60	1.271964	36.410	0.434			
2-Oct-96	197.88	48.00	-2.40	25.97	35.02	5.87	2.09E+06	7.92	1.51E+06	9.92	1.61E+06	13.52	1.35E+06	9.35	1.63E+06	39.400	0.414				
3-Oct-96	197.94	35.08	6.66	-20.34	28.42	20.87	5.54	2.72E+06	7.69	1.91E+06	9.9887	2.04E+06	14.072	1.68E+06	9.26	20.98894	41.755	0.401			
4-Oct-96	197.68	73.06	53.01	33.68	20.05	6.51	1.20E+06	8.50	9.02E+05	10.353	9.46E+05	13.741	8.10E+05	9.93	9.69424.1	33.720	0.459				
<b>1-ft x 1-ft enclosure, 2.375 inch pipe, unpainted</b>																					
17-Oct-96 *	80.30	71.28	68.19	9.03	75.79	4.30	1.58E+06	5.66	1.34E+06	5.84	1.43E+06	6.58	1.41E+06	5.67	1.44E+06	5.704	0.172				
18-Oct-96 *	82.31	60.37	52.73	21.94	4.30	4.02E+06	5.21	3.53E+06	5.62	3.62E+06	7.22	3.41E+06	5.65	3.63E+06	13.732	0.171					
19-Oct-96	80.80	48.95	34.99	31.84	64.87	4.94	6.33E+06	6.37	5.42E+06	7.25	5.53E+06	8.93	5.16E+06	6.96	5.63E+06	24.280	0.208				
20-Oct-96	82.47	35.22	14.41	47.25	58.85	4.81	9.96E+06	5.97	8.64E+06	6.93	8.78E+06	9.23	7.91E+06	6.78	8.84E+06	34.787	0.201				
21-Oct-96	83.13	17.38	-13.39	65.75	50.26	4.71	1.53E+07	5.93	1.31E+07	7.11	1.33E+07	9.86	1.17E+07	6.91	1.34E+07	48.662	0.202				
25-Oct-96	162.32	87.98	62.18	54.34	115.15	5.68	6.91E+06	6.74	6.14E+06	7.61	6.22E+06	9.63	5.70E+06	7.53	6.25E+06	48.215	0.242				

Date	Pipe	Temperature (F)						Average heat											
		Pipe			Inside	Outside	EPS	EPS	EPS	Dtemp <sup>1</sup>	T <sub>avg</sub> <sup>2</sup>	Bottom	Right Side	Left Side					
		Insul.	EPS	EPS	Ra	Nu	Ra	Nu	Ra	Nu	Ra	Nu	Ra	Flux					
26-Oct-96	143.27		73.28	38.66	70.00	108.28	5.66	9.30E+06	6.66	8.37E+06	7.67	8.48E+06	10.05	8.51E+06	62.106	0.242			
27-Oct-96	143.60		58.65	14.85	84.95	101.13	5.64	1.23E+07	6.58	1.08E+07	7.76	1.09E+07	10.40	9.72E+06	7.67	1.09E+07	75.270	0.242	
30-Oct-96	143.87		51.61	2.85	92.26	97.74	5.57	1.39E+07	6.63	1.20E+07	7.81	1.22E+07	10.68	1.07E+07	7.73	1.22E+07	81.952	0.242	
31-Oct-96	146.23		37.88	-20.55	108.34	92.05	5.33	1.73E+07	6.43	1.48E+07	7.75	1.50E+07	10.86	1.31E+07	7.61	1.51E+07	93.938	0.236	
<b>1-ft x 1-ft enclosure, 2.375 inch pipe, insulated</b>																			
1-Nov-96	191.00		65.44	-8.27	125.56	128.22	6.10	1.48E+07	6.94	1.28E+07	8.39	1.30E+07	11.30	1.14E+07	8.26	1.30E+07	124.294	0.270	
2-Nov-96	191.32		82.66	21.04	108.66	136.99	6.24	1.19E+07	7.18	1.04E+07	8.35	1.05E+07	11.03	9.40E+06	8.31	1.06E+07	109.540	0.275	
3-Nov-96	190.85		101.02	52.13	89.83	145.93	6.38	9.08E+06	7.27	8.08E+06	8.29	8.16E+06	10.74	7.39E+06	8.31	8.18E+06	91.663	0.278	
4-Nov-96	190.72		120.44	83.95	70.28	155.58	6.44	6.56E+06	7.32	5.88E+06	8.21	5.96E+06	10.39	5.47E+06	8.25	5.97E+06	72.102	0.280	
6-Nov-96	192.99		88.75	75.46	66.67	13.29	82.11	6.36	1.33E+06	8.10	1.08E+06	9.17	1.13E+06	11.79	1.01E+06	9.03	1.14E+06	16.291	0.334
7-Nov-96 *	193.50		66.10	49.68	38.00	16.42	57.89	6.06	2.13E+06	8.21	1.67E+06	9.67	1.74E+06	13.60	1.48E+06	9.48	1.76E+06	20.391	0.339
8-Nov-96	193.82		43.64	23.15	9.28	20.50	33.40	5.61	3.37E+06	7.71	2.69E+06	9.01	2.76E+06	12.67	2.25E+06	8.78	2.80E+06	22.710	0.302
9-Nov-96	194.61		29.64	6.51	-9.11	23.12	18.07	5.26	4.54E+06	7.54	3.58E+06	8.86	3.66E+06	12.92	3.05E+06	8.61	3.72E+06	24.509	0.289
10-Nov-96	150.12		33.31	17.36	7.14	15.95	25.33	5.29	2.84E+06	7.48	2.27E+06	8.52	2.34E+06	11.89	2.01E+06	8.34	2.37E+06	16.568	0.283
11-Nov-96	149.89		48.93	35.40	26.50	13.53	42.17	5.56	1.99E+06	7.49	1.61E+06	8.53	1.67E+06	11.36	1.47E+06	8.33	1.69E+06	14.419	0.291
12-Nov-96 *	149.55		64.50	53.92	46.42	10.58	59.21	6.67	1.32E+06	8.45	1.06E+06	9.80	1.12E+06	12.74	9.75E+05	9.57	1.12E+06	13.291	0.343
13-Nov-96	148.55		79.04	70.07	64.58	8.97	74.56	5.91	9.58E+05	7.78	7.60E+05	8.47	8.23E+05	10.71	7.45E+05	8.39	8.24E+05	10.099	0.307
14-Nov-96	80.59		65.42	63.09	62.02	2.32	64.26	4.23	2.84E+05	7.89	1.68E+05	6.05	2.41E+05	7.18	2.33E+05	6.38	2.35E+05	1.960	0.230
15-Nov-96	80.96		49.70	45.24	42.83	4.46	47.47	4.90	6.19E+05	7.71	4.48E+05	7.32	5.29E+05	8.82	5.01E+05	7.33	5.28E+05	4.214	0.258
16-Nov-96	81.54		34.24	27.65	23.89	6.59	30.94	4.97	1.08E+06	7.47	8.35E+05	7.75	9.10E+05	9.69	8.48E+05	7.60	9.24E+05	6.294	0.260
17-Nov-96	82.00		18.47	9.31	4.23	8.96	13.99	4.92	1.78E+06	7.29	1.40E+06	7.96	1.48E+06	10.32	1.34E+06	7.71	1.51E+06	8.456	0.257

<sup>1</sup> Dtemp is the temperature difference between the average pipe or pipe insulation surface temperature and the inside EPS temperature.

<sup>2</sup> T<sub>avg</sub> is the average of the two temperatures used to calculate Dtemp.

\* These data were found to be faulty and were not included in the analysis.

Date	Temperature (°F)								Bottom Ra	Right Side Nu Ra	Left side Nu Ra	Top Nu	Average Ra	Average Ra	Average Ra	Flux (Btu/hr ft)	Conductance (Btu/hr ft <sup>2</sup> °F)	Average heat flux			
	left (4 in.)	right (8 in.)	left	right	avg.	Inside	Outside	Diemp <sup>1</sup>													
<b>Data from the 2-ft x 4-ft apparatus, both pipes heated</b>																					
10-Jan-97	147.9	147.1	75.4	76.0	75.8	65.1	55.8	9.2	70.4	19.48	5.90E+05	24.57	7.48E+05	21.39	6.50E+05	29.97	9.13E+05	23.59	7.17E+05	54.69	0.425
11-Jan-97	147.4	145.7	57.3	57.7	57.5	43.4	31.8	11.6	50.5	17.32	6.00E+05	23.47	8.20E+05	19.87	6.94E+05	30.79	1.08E+06	22.44	7.82E+05	65.15	0.384
12-Jan-97	146.8	144.2	38.0	38.0	38.0	20.8	7.2	13.5	29.4	15.38	6.22E+05	22.31	9.13E+05	19.00	7.78E+05	32.09	1.31E+06	21.54	8.78E+05	72.13	0.349
13-Jan-97	146.6	143.1	19.8	19.3	19.5	-0.7	-15.7	15.0	9.4	13.14	6.23E+05	20.91	1.01E+06	17.86	8.63E+05	33.61	1.62E+06	20.37	9.78E+05	75.65	0.312
25-Jan-97	226.9	226.4	38.0	38.4	38.3	9.0	-13.1	22.1	23.7	12.67	5.17E+05	22.07	9.27E+05	18.40	7.73E+05	36.63	1.55E+06	20.79	8.66E+05	113.46	0.324
27-Jan-97	227.8	228.4	56.1	57.0	56.7	30.6	9.8	20.9	43.7	14.71	5.18E+05	23.53	8.46E+05	19.88	7.15E+05	35.32	1.28E+06	22.01	7.87E+05	112.94	0.362
29-Jan-97	230.1	234.7	80.9	82.3	81.7	59.1	39.6	19.5	70.4	17.77	5.21E+05	25.29	7.53E+05	21.83	6.49E+05	33.43	1.00E+06	23.69	7.02E+05	112.97	0.416

**Data from the 2-ft x 4-ft apparatus, left pipe unheated**

15-Jan-97	10.0	142.6	-3.0	13.7	13.7	-6.7	-18.0	11.2	3.5	13.19	6.65E+05	20.75	1.06E+06	13.94	7.10E+05	28.01	1.43E+06	18.61	9.46E+05	55.94	0.228
16-Jan-97	21.2	143.7	16.9	32.7	32.7	15.0	5.3	9.7	23.9	14.33	6.10E+05	21.59	9.29E+05	13.85	5.93E+05	25.76	1.11E+06	18.61	7.97E+05	51.21	0.241
17-Jan-97	37.9	144.8	38.1	52.2	52.2	37.2	29.2	8.0	44.7	14.97	5.44E+05	21.57	7.90E+05	13.41	4.89E+05	22.95	8.40E+05	18.03	6.58E+05	44.50	0.247
18-Jan-97	56.5	147.1	60.3	72.2	72.2	60.4	54.6	5.8	66.3	14.70	4.60E+05	20.30	6.36E+05	12.82	4.01E+05	20.30	6.23E+05	16.86	5.29E+05	34.40	0.244
20-Jan-97	66.5	236.8	69.0	90.6	90.6	68.3	36.5	11.8	79.5	14.94	4.18E+05	21.81	6.17E+05	14.06	3.95E+05	22.50	6.36E+05	17.98	5.08E+05	70.40	0.263
21-Jan-97	52.3	233.5	48.0	70.7	70.7	46.0	31.9	14.1	58.4	15.38	4.94E+05	23.17	7.55E+05	14.85	4.81E+05	26.00	8.47E+05	19.45	6.30E+05	79.78	0.270

<sup>1</sup> Diemp is the temperature difference between the weighted average pipe insulation surface temperature and the inside Diemp.

<sup>2</sup>  $T_{Ave}$  is the average of the two temperatures used to calculate Diemp.

## APPENDIX B: NUMERICAL RESULTS

File Name	Pipe	Insul.	Temperature (°F)			Bottom	Side	Top	Average	Conductance					
			Pipe	EPS	Dtemp	$T_{AVG}^2$	Nu	Ra	Nu	Ra	Flux	(Btu/hr ft <sup>2</sup> °F)			
<b>1-ft x 1-ft enclosure, 4.5-inch pipe, no radiation</b>															
sq4d10m	300	290.45	290	9.55	295.22	0.0074	1.98E+05	0.43	1.92E+05	1.98	1.75E+05	0.70	1.89E+05	1.21	0.035
sq4d50m	300	252.70	250	47.30	276.35	0.0002	1.10E+06	0.37	1.07E+06	2.76	9.22E+05	0.83	1.04E+06	6.92	0.040
sp4d90m	300	214.71	210	85.29	257.36	0.0000	2.20E+06	0.31	2.15E+06	2.65	1.85E+06	0.77	2.08E+06	11.35	0.036
sq4d110m	300	195.26	190	104.74	247.63	0.0000	2.84E+06	0.26	2.78E+06	2.38	2.42E+06	0.69	2.70E+06	12.26	0.032
<b>1-ft x 1-ft enclosure, 4.5-inch pipe, no radiation</b>															
sq4h10c	80	71.01	70	8.99	75.51	0.0005	8.76E+05	0.87	8.24E+05	5.13	6.36E+05	1.53	7.88E+05	1.87	0.057
sq4h20c	80	61.77	60	18.23	70.89	0.0000	1.83E+06	0.62	1.75E+06	4.63	1.36E+06	1.30	1.67E+06	3.21	0.048
sq4h30c	80	52.26	50	27.74	66.13	0.0000	2.86E+06	0.42	2.77E+06	3.94	2.21E+06	1.08	2.65E+06	4.01	0.039
sq4y10	150	141.04	140	8.96	145.52	0.0039	4.99E+05	1.10	4.63E+05	5.20	3.65E+05	1.65	4.47E+05	2.22	0.068
sq4y20	150	132.02	130	17.98	141.01	0.0005	1.03E+06	0.92	9.67E+05	5.34	7.47E+05	1.57	9.27E+05	4.21	0.064
sq4y30	150	122.94	120	27.06	136.47	0.0001	1.60E+06	0.80	1.51E+06	5.34	1.16E+06	1.50	1.44E+06	6.03	0.061
sq4y40	150	113.82	110	36.18	131.91	3.03E-05	2.21E+06	0.72	2.10E+06	5.30	1.59E+06	1.44	2.00E+06	7.70	0.058
sq4y50	150	104.68	100	45.32	127.33	9.5E-06	2.86E+06	0.65	2.72E+06	5.25	2.06E+06	1.39	2.59E+06	9.26	0.056
sq4y60	150	95.53	90	54.47	122.75	3.38E-06	3.51E+06	0.59	3.40E+06	5.21	2.56E+06	1.35	3.22E+06	10.72	0.054
sq4y70	150	86.36	80	63.64	118.17	1.34E-06	4.29E+06	0.54	4.12E+06	5.18	3.09E+06	1.31	3.90E+06	12.10	0.052
sq4y80	150	77.20	70	72.80	113.59	5.44E-07	5.09E+06	0.50	4.90E+06	5.16	3.65E+06	1.28	4.63E+06	13.41	0.050
<b>1-ft x 1-ft enclosure, 4.5-inch pipe, emissivity of pipe: 0.9, emissivity of EPS: 0.9</b>															
sq4g05p	150	147.22	145	2.78	148.61	10.42	1.41E+05	10.89	1.38E+05	12.36	1.31E+05	11.38	1.36E+05	4.77	0.468
sq4g10p	150	144.44	140	5.56	147.22	10.34	2.85E+05	10.80	2.80E+05	12.42	2.63E+05	11.33	2.74E+05	9.48	0.465
sq4g20p	150	138.88	130	11.12	144.44	10.21	5.82E+05	10.62	5.72E+05	12.38	5.34E+05	11.20	5.59E+05	18.67	0.458
sq4g30p	150	133.29	120	16.71	141.65	10.09	8.91E+05	10.44	8.78E+05	12.22	8.19E+05	11.04	8.57E+05	27.54	0.449
sq4g40p	150	127.67	110	22.33	138.83	9.96	1.21E+06	10.26	1.20E+06	12.00	1.12E+06	10.85	1.17E+06	36.07	0.440
sq4g50p	150	122.03	100	27.97	136.01	9.83	1.55E+06	10.09	1.53E+06	11.77	1.43E+06	10.68	1.50E+06	44.29	0.432
sq4g05r	100	97.05	95	2.95	98.53	8.68	2.21E+05	9.16	2.16E+05	10.81	2.02E+05	9.65	2.12E+05	4.01	0.371
sq4g10r	100	94.10	90	5.90	97.05	8.59	4.48E+05	9.06	4.39E+05	10.85	4.07E+05	9.58	4.29E+05	7.94	0.367
sq4g20r	100	88.17	80	11.83	94.08	8.46	9.20E+05	8.84	9.04E+05	10.70	8.35E+05	9.40	8.82E+05	15.56	0.359
sq4g30r	100	82.16	70	17.84	91.08	8.32	1.42E+06	8.61	1.40E+06	10.37	1.30E+06	9.17	1.36E+06	22.78	0.348

Filename	Pipe	Temperature (°F)				Side				Bottom				Top				Average			
		Inside	Outside	EPS	EPS	Dtemp	$T_{avg}^2$	Nu	Ra	Nu	Ra	Nu	Ra	Nu	Ra	Nu	Ra	Flux	Conductance		
																			(Btu/hr ft)	(Btu/hr ft <sup>2</sup> F)	
sq4gr35r	100	79.13	65	20.87	89.57	8.24	1.68E+06	8.50	1.66E+06	10.18	1.54E+06	9.05	1.62E+06	26.25		0.343					
sq4gr40r	100	76.08	60	23.92	88.04	8.17	1.94E+06	8.38	1.92E+06	9.98	1.79E+06	8.92	1.88E+06	29.60		0.337					
sq4gr05v	80	76.98	75	3.02	78.49	8.02	2.69E+05	8.52	2.63E+05	10.24	2.44E+05	9.00	2.57E+05	3.71		0.336					
sq4gr10v	80	73.96	70	6.04	76.98	7.94	5.46E+05	8.40	5.35E+05	10.26	4.93E+05	8.93	5.22E+05	7.36		0.332					
sq4gr20v	80	67.86	60	12.14	73.93	7.80	1.12E+06	8.15	1.11E+06	10.01	1.02E+06	8.70	1.08E+06	14.35		0.322					
sq4gr30v	80	61.67	50	18.33	70.83	7.65	1.74E+06	7.91	1.72E+06	9.58	1.59E+06	8.44	1.68E+06	20.92		0.311					
sq4gr05v	40	36.84	35	3.16	38.42	6.79	4.13E+05	7.29	4.03E+05	9.17	3.69E+05	7.77	3.94E+05	3.16		0.273					
sq4gr10v	40	33.67	30	6.33	36.84	6.71	8.41E+05	7.14	8.23E+05	9.11	7.51E+05	7.66	8.02E+05	6.23		0.269					
sq4gr15v	40	30.45	25	9.55	35.23	6.62	1.28E+06	6.97	1.26E+06	8.87	1.15E+06	7.50	1.23E+06	9.17		0.262					
sq4gr20v	40	27.20	20	12.80	33.60	6.53	1.75E+06	6.82	1.72E+06	8.56	1.58E+06	7.33	1.68E+06	12.00		0.256					
sq4gr10z	250	245.08	240	4.92	247.54	14.30	1.31E+05	14.71	1.30E+05	16.06	1.24E+05	15.30	1.27E+05	12.84		0.711					
sq4gr20z	250	240.16	230	9.84	245.08	14.17	2.67E+05	14.57	2.63E+05	16.06	2.50E+05	15.20	2.57E+05	25.40		0.704					
sq4gr30z	250	235.26	220	14.74	242.63	14.05	4.06E+05	14.44	4.00E+05	16.00	3.80E+05	15.08	3.92E+05	37.68		0.697					
sq4gr40z	250	230.35	210	19.65	240.18	13.94	5.48E+05	14.30	5.41E+05	15.91	5.13E+05	14.96	5.29E+05	49.67		0.689					
sq4gr50z	250	225.45	200	24.55	237.73	13.82	6.95E+05	14.16	6.87E+05	15.79	6.50E+05	14.84	6.71E+05	61.36		0.682					
sq4gr60z	250	220.55	190	29.45	235.27	13.71	8.46E+05	14.02	8.36E+05	15.66	7.91E+05	14.71	8.17E+05	72.75		0.674					
sq4gr70z	250	215.65	180	34.35	232.82	13.59	1.00E+06	13.89	9.90E+05	15.53	9.36E+05	14.57	9.67E+05	83.85		0.666					
1-ft x 1-ft enclosure, 4.5-inch pipe, emissivity of pipe: 0.9, emissivity of EPS: 0.6																					
sq4gr05q	150	147.07	145	2.93	148.54	9.02	1.49E+05	9.55	1.46E+05	11.38	1.36E+05	10.07	1.43E+05	4.45		0.414					
sq4gr10q	150	144.14	140	5.86	147.07	8.95	3.02E+05	9.45	2.96E+05	11.47	2.73E+05	10.02	2.89E+05	8.83		0.411					
sq4gr20q	150	138.27	130	11.73	144.13	8.83	6.18E+05	9.26	6.07E+05	11.44	5.55E+05	9.88	5.91E+05	17.38		0.404					
sq4dr30q	150	132.36	120	17.64	141.18	8.72	9.48E+05	9.08	9.34E+05	11.25	8.53E+05	9.71	9.08E+05	25.58		0.395					
sq4dr40q	150	126.39	110	23.61	138.20	8.60	1.29E+06	8.89	1.28E+06	10.97	1.17E+06	9.52	1.24E+06	33.42		0.386					
sq4dr50q	150	120.39	100	29.61	135.20	8.48	1.65E+06	8.72	1.64E+06	10.66	1.51E+06	9.34	1.59E+06	40.93		0.377					
sq4gr05s	100	96.91	95	3.09	98.46	7.50	2.33E+05	8.04	2.28E+05	10.05	2.08E+05	8.56	2.22E+05	3.73		0.329					
sq4gr10s	100	93.81	-90	6.19	96.91	7.43	4.73E+05	7.92	4.63E+05	10.12	4.20E+05	8.49	4.51E+05	7.38		0.325					
sq4gr20s	100	87.58	80	12.42	93.79	7.31	9.73E+05	7.69	9.55E+05	9.95	8.64E+05	8.30	9.29E+05	14.42		0.317					
sq4gr30s	100	81.25	70	18.75	90.62	7.18	1.50E+06	7.47	1.48E+06	9.54	1.35E+06	8.06	1.44E+06	21.04		0.306					

Filename	Pipe	Temperature (°F)				Nu	Ra	Nu	Ra	Nu	Ra	Average heat Flux (Btu/hr ft <sup>2</sup> °F)		
		Inside	Outside	EPS	EPS	Dtemp	$T_{A\sigma^2}$	Bottom	Side	Top				
<b>1-ft x 1-ft enclosure, 4.5-inch pipe, emissivity of pipe: 0.5, emissivity of EPS: 0.9</b>														
sq4gr05u	80	76.84	75	3.16	78.42	6.93	2.83E+05	7.47	2.76E+05	9.56	2.51E+05	8.00	2.70E+05	
sq4gr10u	80	73.68	70	6.32	76.84	6.86	5.76E+05	7.34	5.63E+05	9.60	5.08E+05	7.91	5.48E+05	
sq4gr20u	80	67.28	60	12.72	73.64	6.73	1.19E+06	7.08	1.17E+06	9.32	1.05E+06	7.68	1.13E+06	
sq4gr05w	40	36.71	35	3.29	38.36	5.85	4.33E+05	6.39	4.22E+05	8.64	3.78E+05	6.92	4.11E+05	
sq4gr10w	40	33.40	30	6.60	36.70	5.78	8.83E+05	6.23	8.63E+05	8.57	7.70E+05	6.80	8.38E+05	
sq4gr15w	40	30.04	25	9.96	35.02	5.71	1.35E+06	6.06	1.32E+06	8.32	1.19E+06	6.64	1.29E+06	
<b>1-ft x 1-ft enclosure, 4.5-inch pipe, emissivity of pipe: 0.5, emissivity of EPS: 0.9</b>														
sq4gr05x	150	146.66	145	3.34	148.33	6.24	1.70E+05	6.74	1.66E+05	8.09	1.56E+05	7.08	1.63E+05	
sq4gr10x	150	143.32	140	6.68	146.66	6.19	3.44E+05	6.68	3.36E+05	8.19	3.13E+05	7.06	3.30E+05	
sq4gr20x	150	136.63	130	13.37	143.32	6.08	7.07E+05	6.53	6.91E+05	8.19	6.40E+05	6.95	6.78E+05	
sq4gr05y	100	96.53	95	3.47	98.26	5.23	2.61E+05	5.75	2.55E+05	7.28	2.36E+05	6.10	2.50E+05	
sq4gr10y	100	93.05	90	6.95	96.53	5.17	5.31E+05	5.66	5.18E+05	7.36	4.76E+05	6.06	5.08E+05	
sq4gr20y	100	86.05	80	13.95	93.02	5.05	1.10E+06	5.47	1.07E+06	7.24	9.33E+05	5.90	1.05E+06	
sq4gr30y	100	78.89	70	21.11	89.45	4.91	1.70E+06	5.24	1.67E+06	6.89	1.54E+06	5.66	1.64E+06	
sq4gr05z	80	76.48	75	3.52	78.24	4.84	3.16E+05	5.37	3.07E+05	6.99	2.83E+05	5.73	3.01E+05	
sq4gr10z	80	72.94	70	7.06	76.47	4.78	6.43E+05	5.27	6.26E+05	7.04	5.72E+05	5.67	6.13E+05	
sq4gr20z	80	65.80	60	14.20	72.90	4.65	1.33E+06	5.05	1.30E+06	6.83	1.19E+06	5.48	1.27E+06	
sq4ib05a	40	36.37	35	3.63	38.19	4.11	4.78E+05	4.65	4.63E+05	6.44	4.21E+05	5.03	4.54E+05	
sq4ib10a	40	32.72	30	7.28	36.36	4.04	9.75E+05	4.51	9.50E+05	6.40	8.58E+05	4.93	9.28E+05	
sq4ib15a	40	29.01	25	10.99	34.50	3.96	1.50E+06	4.36	1.46E+06	6.20	1.32E+06	4.78	1.43E+06	
sq4ib20a	40	25.24	20	14.76	32.62	3.88	2.04E+06	4.21	2.00E+06	5.90	1.82E+06	4.62	1.95E+06	
<b>1-ft x 1-ft enclosure, 4.5-inch pipe with 1 inch of insulation, emissivity of pipe insulation: 0.9, emissivity of EPS: 0.9</b>														
sq4ib05a	150	146.81	145.95	145	0.86	146.38	10.67	2.26E+04	11.88	2.15E+04	14.54	1.92E+04	12.51	2.09E+04
sq4ib15a	150	140.13	137.67	135	2.46	138.90	10.13	6.94E+04	11.44	6.54E+04	14.82	5.69E+04	12.18	6.33E+04
sq4ib25a	150	133.31	129.28	125	4.03	131.30	9.71	1.21E+05	11.02	1.14E+05	14.68	9.78E+04	11.80	1.10E+05
sq4ib35a	150	126.44	120.82	115	5.62	123.63	9.33	1.79E+05	10.64	1.69E+05	14.55	1.43E+05	11.44	1.63E+05
sq4ib45a	150	119.55	112.32	105	7.23	115.94	8.95	2.46E+05	10.27	2.31E+05	14.41	1.93E+05	11.10	2.22E+05
sq4ib55a	150	112.65	103.78	95	8.87	108.22	8.57	3.22E+05	9.91	3.02E+05	14.24	2.50E+05	10.76	2.90E+05
sq4ib65a	150	105.76	95.20	85	10.56	100.48	8.19	4.10E+05	9.57	3.83E+05	14.06	3.14E+05	10.42	3.68E+05
sq4ib75a	150	98.88	86.58	75	12.30	92.73	7.81	5.12E+05	9.23	4.76E+05	13.86	3.87E+05	10.08	4.57E+05

Filename	Pipe	Temperature (°F)				Bottom				Side				Top				Average			
		Inside	Outside	EPS	EPS	Dtemp	$T_{avg}^2$	Nu	Ra	Nu	Ra	Nu	Ra	Nu	Ra	Nu	Ra	Flux	Conductance	(Btu/hr ft <sup>2</sup> °F)	(Btu/hr ft)
		150	92.00	77.92	65	14.08	84.96	7.44	6.30E+05	8.90	5.83E+05	13.62	4.70E+05	9.73	5.59E+05	23.96	0.464				
sq4ib05b	100	96.79	95.88	95	0.91	96.34	8.73	3.60E+04	9.98	3.38E+04	12.97	2.96E+04	10.60	3.29E+04	1.72	0.514					
sq4ib15b	100	90.03	87.43	85	2.59	88.73	8.25	1.10E+03	9.51	1.03E+03	13.11	8.76E+04	10.23	9.95E+04	4.66	0.490					
sq4ib25b	100	83.11	78.88	75	4.24	81.00	7.83	1.93E+03	9.11	1.81E+03	13.05	1.51E+05	9.87	1.74E+05	7.27	0.468					
sq4ib35b	100	76.15	70.26	65	5.90	73.21	7.48	2.89E+03	8.73	2.70E+03	12.97	2.22E+05	9.54	2.60E+05	9.67	0.447					
sq4ib45b	100	69.17	61.58	55	7.59	65.38	7.11	4.01E+03	8.38	3.74E+03	12.84	3.03E+05	9.21	3.59E+05	11.87	0.427					
sq4ib55b	100	62.19	52.87	45	9.32	57.59	6.74	5.33E+03	8.05	4.95E+03	12.66	3.97E+05	8.88	4.74E+05	13.90	0.407					
sq4ib65b	100	55.20	44.10	35	11.10	49.65	6.38	6.88E+03	7.73	6.37E+03	12.43	5.06E+05	8.54	6.10E+05	15.73	0.386					
sq4ib75b	100	48.17	35.24	25	12.93	41.71	6.02	8.69E+03	7.40	8.02E+03	12.08	6.35E+05	8.17	7.68E+05	17.33	0.365					
sq4ib05c	80	76.79	75.85	75	0.93	76.32	8.05	4.39E+04	9.25	4.13E+04	12.38	3.57E+04	9.88	4.00E+04	1.59	0.466					
sq4ib15c	80	69.98	67.34	65	2.64	68.66	7.57	1.34E+05	8.77	1.26E+05	12.48	1.06E+05	9.50	1.21E+05	4.29	0.442					
sq4ib25c	80	63.03	58.71	55	4.32	60.87	7.16	2.37E+05	8.38	2.22E+05	12.47	1.82E+05	9.15	2.13E+05	6.67	0.421					
sq4ib35c	80	56.03	50.02	45	6.01	53.02	6.79	3.56E+05	8.02	3.33E+05	12.39	2.70E+05	8.83	3.19E+05	8.84	0.402					
sq4ib45c	80	49.01	41.28	35	7.73	45.15	6.43	4.98E+05	7.68	4.64E+05	12.24	3.71E+05	8.50	4.44E+05	10.83	0.382					
sq4ib55c	80	41.99	32.49	25	9.50	37.24	6.06	6.65E+05	7.36	6.17E+05	12.04	4.89E+05	8.17	5.90E+05	12.63	0.363					
sq4ib05d	40	36.76	35.79	35	0.98	36.28	6.69	6.77E+04	7.89	6.33E+04	11.23	5.36E+04	8.51	6.12E+04	1.35	0.378					
sq4ib15d	40	29.87	27.13	25	2.74	28.50	6.23	2.07E+05	7.40	1.94E+05	11.37	1.59E+05	8.13	1.86E+05	3.57	0.356					
sq4ib25d	40	22.84	18.37	15	4.47	20.61	5.86	3.70E+05	7.01	3.46E+05	11.39	2.76E+05	7.80	3.31E+05	5.53	0.338					
<b>1 ft x 1-ft enclosure, 4.5-inch pipe with 1 inch of insulation, emissivity of pipe insulation: 0.9, emissivity of EPS: 0.6</b>																					
sq4ib05e	150	146.86	145.90	145	0.96	146.38	8.76	2.56E+04	9.90	2.42E+04	12.80	2.13E+04	10.52	2.35E+04	1.93	0.546					
sq4ib15e	150	140.25	137.51	135	2.74	138.88	8.31	7.76E+04	9.51	7.31E+04	13.16	6.22E+04	10.25	7.06E+04	5.29	0.527					
sq4ib25e	150	133.47	129.00	125	4.47	131.23	7.97	1.35E+05	9.14	1.27E+05	13.11	1.06E+05	9.93	1.22E+05	8.28	0.505					
sq4ib35e	150	126.62	120.42	115	6.20	123.52	7.66	1.98E+05	8.80	1.87E+05	13.06	1.54E+05	9.64	1.80E+05	11.03	0.485					
sq4ib45e	150	119.72	111.78	105	7.94	115.75	7.36	2.71E+05	8.48	2.55E+05	12.99	2.07E+05	9.36	2.44E+05	13.57	0.466					
sq4ib55e	150	112.80	103.10	95	9.70	107.95	7.06	3.53E+05	8.17	3.33E+05	12.87	2.67E+05	9.08	3.18E+05	15.90	0.447					
sq4ib65e	150	105.87	94.37	85	11.49	100.12	6.77	4.47E+05	7.89	4.21E+05	12.72	3.35E+05	8.79	4.01E+05	18.06	0.429					
sq4ib75e	150	98.94	85.61	75	13.32	92.27	6.47	5.56E+05	7.61	5.21E+05	12.54	4.11E+05	8.52	4.97E+05	20.05	0.410					
sq4ibb5e	150	91.99	76.80	65	15.20	84.40	6.17	6.80E+05	7.34	6.36E+05	12.32	4.99E+05	8.23	6.06E+05	21.86	0.392					
sq4ibb5e	150	85.01	67.91	55	17.11	76.46	5.88	8.22E+05	7.07	7.67E+05	12.02	6.00E+05	7.93	7.32E+05	23.44	0.374					
sqib105e	150	77.98	58.94	45	19.05	68.46	5.60	9.85E+05	6.80	9.17E+05	11.64	7.17E+05	7.62	8.76E+05	24.78	0.355					

Filename	Pipe	Insul.	EPS	EPS	Diemp	$T_{AIG}^2$	Temperature (°F)						Top	Side	Bottom	Nu	Ra	Nu	Ra	Nu	Ra	Average	Flux	Conductance
							Inside	Outside	Bottom	Side	Bottom	Side			Bottom	Side	Bottom	Side	Bottom	Side	Bottom	Side	Bottom	Side
sq4ib05f	100	96.84	95.83	95	1.02	96.34	7.17	4.02E+04	8.33	3.78E+04	11.57	3.23E+04	8.96	3.66E+04	1.62	0.434								
sq4ib15f	100	90.12	87.27	85	2.85	88.70	6.77	1.21E+05	7.91	1.14E+05	11.79	9.45E+04	8.65	1.10E+05	4.34	0.415								
sq4ib25f	100	83.23	78.59	75	4.64	80.91	6.45	2.12E+05	7.54	1.99E+05	11.83	1.61E+05	8.36	1.91E+05	6.74	0.396								
sq4ib35f	100	76.26	69.85	65	6.41	73.05	6.16	3.15E+05	7.22	2.96E+05	11.83	2.36E+05	8.08	2.83E+05	8.91	0.379								
sq4ib45f	100	69.25	61.04	55	8.21	65.14	5.87	4.34E+05	6.92	4.08E+05	11.72	3.21E+05	7.81	3.89E+05	10.88	0.362								
sq4ib55f	100	62.21	52.19	45	10.03	57.20	5.59	5.74E+05	6.65	5.38E+05	11.56	4.19E+05	7.54	5.12E+05	12.69	0.345								
sq4ib65f	100	55.16	43.28	35	11.88	49.22	5.30	7.36E+05	6.39	6.89E+05	11.33	5.33E+05	7.26	6.55E+05	14.30	0.328								
sq4ib75f	100	48.04	34.28	25	13.76	41.16	5.03	9.25E+05	6.13	8.63E+05	10.99	6.67E+05	6.96	8.22E+05	15.69	0.311								
sq4ib05g	80	76.83	75.80	75	1.03	76.32	6.59	4.88E+04	7.74	4.58E+04	11.10	3.88E+04	8.37	4.43E+04	1.49	0.394								
sq4ib15g	80	70.06	67.17	65	2.89	68.62	6.20	1.47E+05	7.30	1.38E+05	11.30	1.13E+05	8.05	1.33E+05	3.98	0.375								
sq4ib25g	80	63.12	58.43	55	4.70	60.78	5.89	2.58E+05	6.94	2.43E+05	11.39	1.94E+05	7.77	2.32E+05	6.16	0.358								
sq4ib35g	80	56.10	49.61	45	6.49	52.86	5.60	3.86E+05	6.63	3.63E+05	11.35	2.85E+05	7.50	3.45E+05	8.12	0.341								
sq4ib45g	80	49.04	40.74	35	8.30	44.89	5.32	5.35E+05	6.35	5.03E+05	11.22	3.90E+05	7.23	4.78E+05	9.89	0.325								
sq4ib55g	80	41.96	31.81	25	10.15	36.89	5.04	7.11E+05	6.09	6.66E+05	11.01	5.13E+05	6.95	6.33E+05	11.48	0.309								
sq4ib05h	40	36.80	35.73	35	1.07	36.27	5.49	7.44E+04	6.61	6.95E+04	10.19	5.75E+04	7.25	6.70E+04	1.26	0.321								
sq4ib15h	40	29.93	26.97	25	2.96	28.45	5.12	2.25E+05	6.15	2.11E+05	10.45	1.68E+05	6.93	2.02E+05	3.30	0.304								
sq4ib25h	40	22.89	18.09	15	4.80	20.49	4.84	3.98E+05	5.81	3.74E+05	10.53	2.90E+05	6.66	3.56E+05	5.07	0.288								
<b>1 ft x 1 ft enclosure, 4.5-inch pipe with 1 inch of insulation, emissivity of pipe insulation: 0.5, emissivity of EPS: 0.9</b>																								
sq4ib05i	150	146.98	145.81	145	1.17	146.39	6.35	3.08E+04	7.37	2.91E+04	9.71	2.59E+04	7.81	2.85E+04	1.73	0.405								
sq4ib15i	150	140.48	137.23	135	3.26	138.86	6.01	9.20E+04	7.12	8.67E+04	10.08	7.44E+04	7.65	8.40E+04	4.70	0.393								
sq4ib25i	150	133.78	128.52	125	5.26	131.15	5.75	1.58E+05	6.86	1.48E+05	10.14	1.25E+05	7.44	1.44E+05	7.30	0.379								
sq4ib35i	150	126.98	119.75	115	7.23	123.37	5.51	2.31E+05	6.62	2.17E+05	10.18	1.81E+05	7.25	2.10E+05	9.67	0.365								
sq4ib45i	150	120.11	110.92	105	9.19	115.52	5.29	3.14E+05	6.39	2.94E+05	10.19	2.41E+05	7.06	2.83E+05	11.84	0.351								
sq4ib55i	150	113.17	102.03	95	11.14	107.61	5.08	4.07E+05	6.17	3.81E+05	10.13	3.09E+05	6.86	3.66E+05	13.80	0.338								
sq4ib65i	150	106.20	93.09	85	13.10	99.64	4.86	5.12E+05	5.95	4.79E+05	10.03	3.85E+05	6.66	4.59E+05	15.57	0.324								
sq4ib75i	150	99.19	84.10	75	15.08	91.65	4.65	6.31E+05	5.74	5.90E+05	9.89	4.71E+05	6.45	5.65E+05	17.18	0.311								
sq4ib85i	150	92.14	75.05	65	17.09	83.59	4.44	7.67E+05	5.53	7.16E+05	9.70	5.70E+05	6.23	6.86E+05	18.58	0.297								
sq4ib95i	150	85.02	65.91	55	19.10	75.47	4.23	9.23E+05	5.31	8.60E+05	9.46	6.83E+05	6.00	8.24E+05	19.77	0.282								
s4ib105i	150	77.79	56.68	45	21.11	67.23	4.03	1.10E+06	5.09	1.02E+06	9.15	8.13E+05	5.76	9.81E+05	20.71	0.268								

Filename	Pipe	Temperature (°F)				Nu	Ra	Nu	Ra	Nu	Ra	Nu	Ra	Average heat Flux (Btu/hr ft <sup>2</sup> °F)		
		Pipe	Inside	Outside	EPS	EPS	Dtemp	$T_{Avg}^2$								
sq4ib05j	80	76.92	75.71	75	1.21	76.32	4.80	5.70E+04	5.86	5.34E+04	8.61	4.58E+04	6.33	5.19E+04	1.33	0.298
sq4ib15j	80	70.23	66.90	65	3.33	68.57	4.49	1.69E+05	5.56	1.58E+05	8.93	1.31E+05	6.13	1.53E+05	3.48	0.285
sq4ib25j	80	63.33	57.99	55	5.35	60.66	4.25	2.94E+05	5.30	2.75E+05	9.09	2.22E+05	5.94	2.64E+05	5.36	0.274
sq4ib35j	80	56.31	48.99	45	7.32	52.65	4.04	4.36E+05	5.07	4.07E+05	9.12	3.24E+05	5.76	3.90E+05	7.02	0.262
sq4ib45j	80	49.21	39.93	35	9.28	44.57	3.84	5.99E+05	4.85	5.60E+05	9.03	4.40E+05	5.56	5.35E+05	8.49	0.250
sq4ib55j	80	42.04	30.80	25	11.24	36.26	3.64	7.91E+05	4.64	7.38E+05	8.85	5.77E+05	5.34	7.05E+05	9.77	0.237

1-ft x 1-ft enclosure, 2.375-inch pipe, emissivity of pipe insulation: 0.9, emissivity of EPS: 0.9															
sq2d05a	150	1146.60	145	3.40	148.30	7.44	3.14E+05	7.85	3.09E+05	9.30	2.92E+05	8.20	3.04E+05	3.44	0.276
sq2d15a	150	139.73	135	10.27	144.87	7.23	9.70E+05	7.54	9.58E+05	9.06	9.03E+05	7.93	9.43E+05	9.99	0.265
sq2d25a	150	132.64	125	17.36	141.32	6.95	1.67E+06	7.16	1.66E+06	8.39	1.58E+06	7.50	1.64E+06	15.89	0.250
sq2d35a	150	125.41	115	24.59	137.71	6.70	2.42E+06	6.85	2.41E+06	7.81	2.31E+06	7.13	2.38E+06	21.30	0.236

sq2d05b	100	96.47	95	3.53	98.24	6.25	4.82E+05	6.66	4.74E+05	8.31	4.43E+05	7.05	4.66E+05	2.86	0.221
sq2d15b	100	89.21	85	10.79	94.61	5.92	1.51E+06	6.18	1.49E+06	7.55	1.41E+06	6.53	1.47E+06	8.06	0.204
sq2d25b	100	81.69	75	18.31	90.85	5.62	2.62E+06	5.77	2.60E+06	6.72	2.50E+06	6.04	2.57E+06	12.59	0.187
sq2d35b	100	74.09	65	25.91	87.05	5.42	3.81E+06	5.50	3.80E+06	6.22	3.68E+06	5.72	3.76E+06	16.79	0.177

sq2d05c	80	76.41	75	3.59	78.21	5.79	5.82E+05	6.20	5.72E+05	7.91	5.32E+05	6.60	5.62E+05	2.64	0.201
sq2d15c	80	68.98	65	11.02	74.49	5.41	1.83E+06	5.64	1.81E+06	6.90	1.71E+06	5.97	1.78E+06	7.31	0.181
sq2d25c	80	61.30	55	18.70	70.65	5.13	3.19E+06	5.25	3.17E+06	6.08	3.05E+06	5.49	3.14E+06	11.35	0.165
sq2d35c	80	53.57	45	26.43	66.79	4.95	4.65E+06	5.01	4.63E+06	5.66	4.50E+06	5.22	4.59E+06	15.15	0.156
sq2d05d	40	36.29	-35	3.71	38.15	4.89	8.81E+05	5.28	8.65E+05	7.03	8.00E+05	5.68	8.49E+05	2.22	0.163
sq2d15d	40	28.49	25	11.51	34.25	4.45	2.80E+06	4.62	2.78E+06	5.58	2.65E+06	4.87	2.74E+06	5.87	0.139
sq2d25d	40	20.54	15	19.46	30.27	4.23	4.90E+06	4.30	4.88E+06	4.95	4.73E+06	4.50	4.84E+06	9.10	0.127
sq2d35d	40	12.58	5	27.42	26.30	4.10	7.18E+06	4.12	7.17E+06	4.67	6.97E+06	4.30	7.10E+06	12.19	0.121

Filename	Pipe	Insul.	EPS	Dtemp	$T_{\mu G}^2$	Temperature (°F)						Average heat Flux (Btu/hr ft <sup>2</sup> °F)				
						Bottom	Side	Top	Average	Nu	Ra	Nu	Ra			
<b>1-ft x 1-ft enclosure, 2.375-inch pipe, emissivity of pipe: 0.9, emissivity of EPS: 0.6</b>																
sq2d05e	150		146.53	145	3.47	148.26	6.74	3.23E+05	7.25	3.16E+05	9.11	2.94E+05	7.67	3.11E+05	3.28	0.257
sq2d15e	150		139.49	135	10.51	144.75	6.55	9.99E+05	6.92	9.83E+05	8.82	9.12E+05	7.38	9.65E+05	9.50	0.247
sq2d25e	150		132.24	125	17.76	141.13	6.31	1.72E+06	6.57	1.70E+06	8.08	1.60E+06	6.96	1.67E+06	15.07	0.231
sq2d35e	150		124.86	115	25.14	137.44	6.11	2.49E+06	6.29	2.47E+06	7.45	2.35E+06	6.61	2.44E+06	20.16	0.219
sq2d45e	150		117.41	105	32.59	133.72	5.95	3.30E+06	6.07	3.29E+06	7.00	3.16E+06	6.34	3.25E+06	24.96	0.209
sq2d05f	100		96.40	95	3.60	98.20	5.63	4.95E+05	6.14	4.84E+05	8.19	4.45E+05	6.59	4.75E+05	2.73	0.207
sq2d15f	100		88.99	85	11.01	94.50	5.36	1.55E+06	5.67	1.53E+06	7.34	1.42E+06	6.07	1.50E+06	7.65	0.189
sq2d25f	100		81.33	75	18.67	90.67	5.12	2.68E+06	5.30	2.66E+06	6.44	2.53E+06	5.60	2.63E+06	11.90	0.174
sq2d35f	100		73.58	65	26.42	86.80	4.95	3.90E+06	5.06	3.88E+06	5.91	3.74E+06	5.30	3.84E+06	15.85	0.164
sq2d05g	80		76.35	75	3.65	78.17	5.21	5.98E+05	5.71	5.84E+05	7.81	5.34E+05	6.16	5.73E+05	2.52	0.188
sq2d15g	80		68.77	65	11.23	74.39	4.91	1.87E+06	5.18	1.85E+06	6.70	1.73E+06	5.55	1.82E+06	6.93	0.168
sq2d25g	80		60.95	55	19.05	70.48	4.68	3.26E+06	4.83	3.24E+06	5.81	3.10E+06	5.09	3.20E+06	10.72	0.154
sq2d35g	80		53.09	45	26.91	66.55	4.53	4.75E+06	4.62	4.73E+06	5.37	4.57E+06	4.84	4.68E+06	14.30	0.145
sq2d05h	40		36.23	35	3.77	38.11	4.39	9.03E+05	4.85	8.83E+05	6.96	8.03E+05	5.31	8.64E+05	2.11	0.152
sq2d15h	40		28.30	25	11.70	34.15	4.05	2.86E+06	4.25	2.83E+06	5.39	2.68E+06	4.53	2.79E+06	5.55	0.129
sq2d25h	40		20.22	15	19.78	30.12	3.87	5.00E+06	3.97	4.97E+06	4.71	4.79E+06	4.18	4.92E+06	8.58	0.118
sq2d35h	40		12.15	5	27.85	26.08	3.76	7.32E+06	3.80	7.30E+06	4.43	7.08E+06	3.99	7.23E+06	11.49	0.113
<b>1-ft x 1-ft enclosure, 2.375-inch pipe, emissivity of pipe: 0.5, emissivity of EPS: 0.9</b>																
sq2d05i	150		146.17	145	3.83	148.09	4.65	3.54E+05	5.05	3.48E+05	6.39	3.28E+05	5.34	3.43E+05	2.52	0.179
sq2d15i	150		138.42	135	11.58	144.21	4.46	1.10E+06	4.77	1.08E+06	6.13	1.02E+06	5.09	1.07E+06	7.22	0.170
sq2d25i	150		130.36	125	19.64	140.18	4.17	1.91E+06	4.40	1.89E+06	5.44	1.80E+06	4.66	1.87E+06	11.14	0.155
sq2d35i	150		122.12	115	27.88	136.06	3.94	2.78E+06	4.10	2.76E+06	4.87	2.66E+06	4.30	2.73E+06	14.53	0.142
sq2d45i	150		113.83	105	36.17	131.92	3.77	3.71E+06	3.89	3.68E+06	4.50	3.58E+06	4.06	3.66E+06	17.69	0.133
sq2d05j	100		96.08	95	3.92	98.04	3.94	5.36E+05	4.36	5.26E+05	5.89	4.90E+05	4.69	5.18E+05	2.11	0.147
sq2d15j	100		87.99	85	12.01	94.00	3.62	1.69E+06	3.89	1.66E+06	5.09	1.57E+06	4.17	1.64E+06	5.73	0.130
sq2d25j	100		79.56	75	20.44	89.78	3.32	2.95E+06	3.49	2.92E+06	4.27	2.82E+06	3.69	2.90E+06	8.57	0.114
sq2d35j	100		71.06	65	28.94	85.53	3.15	4.31E+06	3.26	4.29E+06	3.83	4.17E+06	3.41	4.25E+06	11.16	0.105

### Temperature (°F)

Filename	Pipe	Temperature (°F)			Bottom			Side			Top			Average			Conductance (Btu/hr ft <sup>2</sup> °F)
		Inside	Outside	EPS	EPS	Dtemp	$T_{avg}^2$	Nu	Ra	Nu	Ra	Nu	Ra	Nu	Ra	Nu	
sq2d05k	80	76.04	75	3.96	78.02	3.67	6.44E+05	4.08	6.31E+05	5.67	5.86E+05	4.42	6.21E+05	1.95	0.135		
sq2d15k	80	67.80	65	12.20	73.90	3.29	2.04E+06	3.54	2.01E+06	4.62	1.91E+06	3.79	1.99E+06	5.14	0.115		
sq2d25k	80	59.24	55	20.76	69.62	3.01	3.57E+06	3.16	3.54E+06	3.83	3.43E+06	3.33	3.51E+06	7.63	0.100		
sq2d35k	80	50.67	45	29.33	65.34	2.87	5.23E+06	2.97	5.20E+06	3.49	5.06E+06	3.11	5.16E+06	10.00	0.093		
sq2d05l	40	35.96	35	4.04	37.98	3.10	9.64E+05	3.50	9.44E+05	5.13	8.73E+05	3.85	9.28E+05	1.64	0.110		
sq2d15l	40	27.39	25	12.61	33.70	2.66	3.08E+06	2.85	3.05E+06	3.66	2.93E+06	3.04	3.02E+06	4.01	0.087		

### Average heat

sq2ix10a	150	144.05	140.44	140	3.61	142.24	2.00E+02	2.15E+05	1.29	1.97E+05	5.06	1.59E+05	1.74	1.92E+05	0.93	0.070	
sq2ix20a	150	137.32	130.81	130	6.51	134.06	5.40E+03	4.13E+05	1.21	3.81E+05	5.55	2.98E+05	1.77	3.68E+05	1.68	0.071	
sq2ix30a	150	130.29	121.14	120	9.14	125.72	2.16E+03	6.19E+05	1.13	5.73E+05	5.86	4.38E+05	1.78	5.50E+05	2.34	0.070	
sq2ix40a	150	123.06	111.46	110	11.59	117.26	1.04E+03	8.38E+05	1.07	7.80E+05	6.10	5.86E+05	1.78	7.45E+05	2.94	0.069	
sq2ix50a	150	115.66	101.76	100	13.90	108.71	1.08E+06	1.08E+06	1.01	1.00E+06	6.31	7.43E+05	1.77	9.55E+05	3.47	0.068	
sq2ix60a	150	108.13	92.05	90	16.08	100.09	3.14E+04	3.34E+06	0.96	1.25E+06	6.49	9.12E+05	1.77	1.19E+06	3.96	0.067	
<b>1-ft x 1-ft enclosure, 2.375-inch pipe with 1 inch of insulation, no radiation</b>																	
sq2ie05a	150	146.45	145.64	145	0.81	146.04	10.06	4.41E+04	10.92	4.26E+04	12.90	3.95E+04	11.37	4.19E+04	1.77	0.595	
sq2ie15a*	150	139.16	136.81	135	2.35	137.99	9.69	1.36E+05	10.62	1.31E+05	12.96	1.20E+05	11.10	1.29E+05	4.95	0.575	
sq2ie25a	150	131.78	127.92	125	3.86	129.85	9.38	2.38E+05	10.28	2.30E+05	12.84	2.08E+05	10.79	2.25E+05	7.82	0.553	
sq2ie35a*	150	124.34	118.96	115	5.38	121.66	9.04	3.54E+05	9.92	3.41E+05	12.70	3.06E+05	10.45	3.34E+05	10.44	0.530	
sq2ie45a*	150	116.86	109.96	105	6.90	113.42	8.71	4.85E+05	9.58	4.67E+05	12.53	4.15E+05	10.13	4.57E+05	12.83	0.507	
sq2ie55a	150	109.35	100.92	95	8.43	105.15	8.38	6.35E+05	9.25	6.11E+05	12.36	5.39E+05	9.81	5.96E+05	15.01	0.486	
sq2ie65a*	150	101.81	91.83	85	9.98	96.84	8.05	8.06E+05	8.91	7.76E+05	12.17	6.79E+05	9.50	7.56E+05	17.00	0.465	
sq2ie75a*	150	94.26	82.71	75	11.56	88.50	7.71	1.00E+06	8.58	9.65E+05	11.99	8.38E+05	9.17	9.40E+05	18.80	0.444	
sq2ie85a*	150	86.68	73.53	65	13.15	80.13	7.38	1.23E+06	8.24	1.18E+06	11.80	1.02E+06	8.85	1.15E+06	20.40	0.423	
sq2ic05d	100	96.46	95.59	95	0.86	96.03	8.36	6.98E+04	9.26	6.71E+04	11.44	6.13E+04	9.70	6.58E+04	1.50	0.474	
sq2ic15d	100	89.13	86.66	85	2.47	87.90	8.02	2.15E+05	8.92	2.06E+05	11.50	1.83E+05	9.41	2.02E+05	4.12	0.454	
sq2ic25d*	100	81.68	77.64	75	4.04	79.67	7.68	3.77E+05	8.56	3.63E+05	11.44	3.21E+05	9.08	3.54E+05	6.41	0.433	
sq2ic35d*	100	74.15	68.56	65	5.59	71.36	7.36	5.63E+05	8.22	5.41E+05	11.33	4.74E+05	8.76	5.28E+05	8.47	0.413	
sq2ic45d*	100	66.56	59.43	-55	7.14	63.01	7.03	7.79E+05	7.89	7.48E+05	11.19	6.49E+05	8.45	7.29E+05	10.31	0.394	
sq2ic05h	80	76.46	75.58	75	0.88	76.02	7.72	8.51E+04	8.64	8.17E+04	10.89	7.43E+04	9.07	8.02E+04	1.40	0.431	
sq2ic15h	80	69.11	66.60	65	2.52	67.86	7.38	2.62E+05	8.28	2.51E+05	10.97	2.24E+05	8.76	2.46E+05	3.79	0.411	

Filename	Pipe	Temperature (°F)						Bottom						Side						Top						Average heat	
		Inside	Outside	Insul.	EPS	EPS	Diemp	$T_{41G}$ <sup>2</sup>	Nu	Ra	Nu	Ra	Nu	Ra	Nu	Ra	Nu	Ra	Nu	Ra	Nu	Ra	Flux	Conductance	(Btu/hr ft)	(Btu/hr ft <sup>2</sup> )	
																									(Btu/hr ft)	(Btu/hr ft <sup>2</sup> )	
sq2ic25h	80	61.62	57.53	55	4.10	59.58	7.04	4.61E+05	7.92	4.42E+05	10.93	3.88E+05	8.44	4.32E+05	5.87	4.32E+05	0.391	0.391	0.391	0.391	0.391	0.391	0.391	0.391	0.391		
sq2ic15k*	80	54.05	48.39	45	5.66	51.23	6.72	6.91E+05	7.58	6.63E+05	10.83	5.75E+05	8.13	6.46E+05	7.72	6.46E+05	0.372	0.372	0.372	0.372	0.372	0.372	0.372	0.372	0.372		
1-ft x 1-ft enclosure, 2.375-inch pipe with 1 inch of insulation, emissivity of pipe insulation: 0.9, emissivity of EPS: 0.6																											
sq2ic05b	150	146.49	145.61	145	0.88	146.05	8.69	4.82E+04	9.60	4.64E+04	11.88	4.24E+04	10.05	4.55E+04	1.70	4.55E+04	0.526	0.526	0.526	0.526	0.526	0.526	0.526	0.526	0.526		
sq2ic15b	150	139.27	136.73	135	2.53	138.00	8.39	1.48E+05	9.32	1.42E+05	12.02	1.27E+05	9.82	1.39E+05	4.73	1.39E+05	0.509	0.509	0.509	0.509	0.509	0.509	0.509	0.509	0.509		
sq2ic25b	150	131.92	127.77	125	4.15	129.85	8.10	2.57E+05	8.99	2.48E+05	11.98	2.19E+05	9.53	2.42E+05	7.43	2.42E+05	0.488	0.488	0.488	0.488	0.488	0.488	0.488	0.488	0.488		
sq2ic35b	150	124.51	118.75	115	5.76	121.64	7.81	3.81E+05	8.66	3.66E+05	11.90	3.21E+05	9.23	3.58E+05	9.88	3.58E+05	0.468	0.468	0.468	0.468	0.468	0.468	0.468	0.468	0.468		
sq2ic45b	150	117.05	109.68	105	7.37	113.38	7.52	5.20E+05	8.35	5.01E+05	11.79	4.34E+05	8.94	4.88E+05	12.10	4.88E+05	0.448	0.448	0.448	0.448	0.448	0.448	0.448	0.448	0.448		
sq2ic55b	150	109.55	100.57	95	8.98	105.08	7.24	6.78E+05	8.05	6.54E+05	11.65	5.62E+05	8.66	6.36E+05	14.12	6.36E+05	0.429	0.429	0.429	0.429	0.429	0.429	0.429	0.429	0.429		
sq2ic65b	150	102.01	91.41	85	10.60	96.74	6.96	8.59E+05	7.75	8.28E+05	11.50	7.06E+05	8.38	8.04E+05	15.94	8.04E+05	0.410	0.410	0.410	0.410	0.410	0.410	0.410	0.410	0.410		
sq2ic75b	150	94.45	82.21	75	12.24	88.36	6.68	1.07E+06	7.45	1.03E+06	11.34	8.69E+05	8.10	9.97E+05	17.57	9.97E+05	0.392	0.392	0.392	0.392	0.392	0.392	0.392	0.392	0.392		
sq2ic85b	150	86.85	72.96	65	13.89	79.95	6.40	1.30E+06	7.15	1.26E+06	11.17	1.05E+06	7.82	1.22E+06	19.01	1.22E+06	0.373	0.373	0.373	0.373	0.373	0.373	0.373	0.373	0.373		
sq2ic95b	150	79.21	63.66	55	15.55	71.48	6.13	1.57E+06	6.85	1.52E+06	10.99	1.26E+06	7.53	1.47E+06	20.26	1.47E+06	0.355	0.355	0.355	0.355	0.355	0.355	0.355	0.355	0.355		
sq2ic05e	100	96.50	95.57	95	0.93	96.03	7.21	7.56E+04	8.16	7.24E+04	10.64	6.51E+04	8.60	7.10E+04	1.43	7.10E+04	0.420	0.420	0.420	0.420	0.420	0.420	0.420	0.420	0.420		
sq2ic15e	100	89.22	86.58	85	2.64	87.90	6.91	2.31E+05	7.83	2.21E+05	10.80	1.95E+05	8.33	2.16E+05	3.90	2.16E+05	0.403	0.403	0.403	0.403	0.403	0.403	0.403	0.403	0.403		
sq2ic25e	100	81.79	77.50	75	4.30	79.65	6.62	4.04E+05	7.49	3.87E+05	10.82	3.35E+05	8.04	3.78E+05	6.05	3.78E+05	0.384	0.384	0.384	0.384	0.384	0.384	0.384	0.384	0.384		
sq2ic35e	100	74.28	68.35	65	5.93	71.33	6.35	6.00E+05	7.17	5.77E+05	10.76	4.93E+05	7.76	5.61E+05	7.96	5.61E+05	0.366	0.366	0.366	0.366	0.366	0.366	0.366	0.366	0.366		
sq2ic45e	100	66.70	59.15	55	7.55	62.94	6.08	8.27E+05	6.87	7.95E+05	10.66	6.71E+05	7.48	7.72E+05	9.65	7.72E+05	0.349	0.349	0.349	0.349	0.349	0.349	0.349	0.349	0.349		
sq2ic55e	100	59.06	49.89	45	9.17	54.50	5.81	1.09E+06	6.57	1.05E+06	10.53	8.75E+05	7.21	1.01E+06	11.15	1.01E+06	0.332	0.332	0.332	0.332	0.332	0.332	0.332	0.332	0.332		
sq2ic65e	80	76.50	75.53	75	0.95	76.03	6.65	9.20E+04	7.61	8.79E+04	10.18	7.85E+04	8.05	8.61E+04	1.33	8.61E+04	0.383	0.383	0.383	0.383	0.383	0.383	0.383	0.383	0.383		
sq2ic75e	80	69.19	66.51	65	2.68	67.86	6.35	2.80E+05	7.26	2.68E+05	10.37	2.34E+05	7.77	2.62E+05	3.59	2.62E+05	0.365	0.365	0.365	0.365	0.365	0.365	0.365	0.365	0.365		
sq2ic85e	80	61.72	57.38	55	4.35	59.56	6.07	4.91E+05	6.92	4.71E+05	10.40	4.03E+05	7.48	4.58E+05	5.53	4.58E+05	0.347	0.347	0.347	0.347	0.347	0.347	0.347	0.347	0.347		
sq2ic95e	80	54.16	48.18	45	5.98	51.18	5.80	7.33E+05	6.61	7.04E+05	10.34	5.94E+05	7.20	6.83E+05	7.23	6.83E+05	0.330	0.330	0.330	0.330	0.330	0.330	0.330	0.330	0.330		
sq2ic05i	200	196.48	195.65	195	0.83	196.07	10.30	3.22E+04	11.17	3.11E+04	13.23	2.88E+04	11.62	3.06E+04	1.98	3.06E+04	0.648	0.648	0.648	0.648	0.648	0.648	0.648	0.648	0.648		
sq2ic15i	200	189.29	186.87	185	2.41	188.08	10.00	9.87E+04	10.93	9.52E+04	13.43	8.67E+04	11.43	9.33E+04	5.59	9.33E+04	0.632	0.632	0.632	0.632	0.632	0.632	0.632	0.632	0.632		
sq2ic25i	200	182.01	178.03	175	3.98	180.02	9.70	1.72E+05	10.60	1.66E+05	13.33	1.50E+05	11.14	1.62E+05	8.89	1.62E+05	0.609	0.609	0.609	0.609	0.609	0.609	0.609	0.609	0.609		

Filename	Pipe	Temperature (°F)				Bottom	Side	Top	Average	Nu	Ra	Nu	Ra	Average	Nu	Ra	Nu	Ra	Conductance (Btu/hr ft <sup>2</sup> °F)		
		Pipe	Inside	Outside	EPS																
<b>1-ft x 1-ft enclosure, 2.375-inch pipe with 1 inch of insulation, emissivity of pipe insulation: 0.5, emissivity of EPS: 0.9</b>																					
sq2ic05c	150	146.64	145.55	145	1.10	146.10	6.09	5.98E+04	6.86	5.76E+04	8.59	5.33E+04	7.17	5.68E+04	1.51		0.376				
sq2ic15c*	150	139.63	136.53	135	3.10	138.08	5.90	1.80E+05	6.73	1.73E+05	8.84	1.57E+05	7.08	1.70E+05	4.17		0.367				
sq2ic25c	150	132.44	127.43	125	5.01	129.94	5.71	3.09E+05	6.53	2.97E+05	8.94	2.66E+05	6.93	2.92E+05	6.52		0.355				
sq2ic35c*	150	125.14	118.27	115	6.87	121.72	5.52	4.53E+05	6.33	4.35E+05	8.98	3.85E+05	6.75	4.26E+05	8.61		0.342				
sq2ic45c*	150	117.76	109.07	105	8.69	113.43	5.32	6.13E+05	6.13	5.88E+05	8.98	5.16E+05	6.58	5.76E+05	10.50		0.329				
sq2ic55c*	150	110.31	99.81	95	10.49	105.08	5.13	7.92E+05	5.93	7.61E+05	8.96	6.60E+05	6.40	7.43E+05	12.20		0.317				
sq2ic65c*	150	102.80	90.52	85	12.28	96.68	4.94	9.95E+05	5.73	9.53E+05	8.93	8.21E+05	6.23	9.32E+05	13.71		0.305				
sq2ic75c*	150	95.22	81.18	75	14.04	88.23	4.75	1.22E+06	5.53	1.18E+06	8.88	1.00E+06	6.04	1.14E+06	15.05		0.292				
sq2ic85c*	150	87.59	71.79	65	15.80	79.73	4.56	1.49E+06	5.32	1.43E+06	8.81	1.21E+06	5.86	1.39E+06	16.20		0.280				
sq2ic95c*	150	79.88	62.35	55	17.53	71.17	4.37	1.78E+06	5.11	1.71E+06	8.72	1.43E+06	5.67	1.66E+06	17.18		0.267				
sq2ic05f	100	96.63	95.50	95	1.13	96.07	5.11	9.15E+04	5.93	8.78E+04	7.86	8.00E+04	6.25	8.64E+04	1.27		0.305				
sq2ic15f	100	89.53	86.38	85	3.15	87.96	4.91	2.74E+05	5.75	2.62E+05	8.16	2.33E+05	6.13	2.57E+05	3.42		0.296				
sq2ic25f*	100	82.21	77.17	75	5.04	59.58	4.86	5.67E+05	5.70	5.43E+05	8.56	4.76E+05	6.14	5.32E+05	5.26		0.285				
sq2ic35f	100	74.77	67.90	65	6.87	71.35	4.52	6.95E+05	5.34	6.66E+05	8.37	5.74E+05	5.80	6.50E+05	6.89		0.273				
sq2ic45f	100	67.23	58.57	55	8.65	62.99	4.34	9.47E+05	5.14	9.07E+05	8.40	7.73E+05	5.63	8.84E+05	8.32		0.262				
sq2ic55f*	100	59.60	49.20	45	10.40	54.43	4.16	1.24E+06	4.94	1.18E+06	8.39	9.98E+05	5.45	1.15E+06	9.57		0.251				
sq2ic05j	80	76.63	75.48	75	1.14	76.06	4.74	1.10E+05	5.57	1.05E+05	7.60	9.54E+04	5.90	1.04E+05	1.17		0.280				
sq2ic15j	80	69.47	66.32	65	3.15	67.90	4.53	3.29E+05	5.37	3.14E+05	7.94	2.77E+05	5.77	3.08E+05	3.13		0.271				
sq2ic25j	80	62.10	57.06	55	5.04	67.90	4.29	5.26E+05	5.10	5.03E+05	7.99	4.35E+05	5.53	4.92E+05	4.80		0.260				
sq2ic35j	80	54.59	47.75	45	6.85	51.19	4.15	8.39E+05	4.96	8.02E+05	8.17	6.84E+05	5.44	7.82E+05	6.25		0.249				
sq2ic05m	200	196.65	195.59	195	1.06	190.12	7.21	4.24E+04	7.93	4.11E+04	9.49	3.85E+04	8.24	4.05E+04	1.78		0.456				
sq2ic15m*	200	189.69	186.67	185	3.02	188.18	7.01	1.23E+05	7.77	1.19E+05	9.67	1.10E+05	8.13	1.17E+05	4.98		0.449				
sq2ic25m	200	182.60	177.68	175	4.92	180.14	6.79	2.12E+05	7.59	2.04E+05	9.71	1.86E+05	7.97	2.01E+05	7.87		0.436				
<b>1.27-ft x 1.27-ft enclosure, 4.5-inch pipe with 2 inches of insulation, emissivity of pipe insulation: 0.9, emissivity of EPS: 0.9</b>																					
sq1-410b*	150	142.03	141.06	140	0.97	141.56	14.51	5.42E+04	15.01	5.33E+04	17.56	4.90E+04	15.78	5.19E+04	2.93		0.634				
sq1-420b	150	134.04	132.08	130	1.96	133.06	13.76	1.17E+05	14.50	1.14E+05	17.16	1.05E+05	15.21	1.11E+05	5.62		0.605				
sq1-430b*	150	126.09	123.10	120	2.99	124.60	13.27	1.91E+05	14.02	1.86E+05	16.84	1.69E+05	14.75	1.81E+05	8.22		0.579				

Filename	Pipe	Temperature (°F)				Nu	Ra	Nu	Ra	Nu	Ra	Nu	Ra	Average	Average heat	
		Pipe	Inside	Outside	EPS	$T_{Avg}^2$	Bottom	Side	Top	Flux	Conductance					
sc1-440b*	150	118.19	114.12	110	4.07	116.17	12.84	2.78E+05	13.52	2.71E+05	16.57	2.44E+05	14.31	2.64E+05	10.74	0.556
sc1-450b*	150	110.35	105.13	100	5.22	107.76	12.30	3.82E+05	13.00	3.72E+05	16.26	3.32E+05	13.81	3.61E+05	13.13	0.530
sc1-460b*	150	102.55	96.12	90	6.42	99.36	11.72	5.06E+05	12.46	4.92E+05	15.91	4.35E+05	13.29	4.77E+05	15.37	0.504
sc1-405c	80	76.05	75.50	75	0.56	75.78	10.94	5.36E+04	11.82	5.17E+04	14.37	4.71E+04	12.40	5.06E+04	1.20	0.455
sc1-415c	80	68.06	66.43	65	1.64	67.25	10.59	1.70E+05	11.33	1.63E+05	14.17	1.48E+05	12.00	1.61E+05	3.38	0.435
sc1-425c	80	60.11	57.34	55	2.77	58.73	10.03	3.13E+05	10.84	3.03E+05	13.97	2.69E+05	11.54	2.95E+05	5.43	0.413
<b>2-ft x 2-ft enclosure, two, 2-inch insulated pipes, emissivity of pipe insulation: 0.9, emissivity of EPS: 0.9</b>																
2s2ii1	150	146.91	145.46	145	1.45	148.42	11.18	1.29E+06	11.45	1.28E+06	13.07	1.24E+06	11.83	1.27E+06	2.06	0.0018
2s2ii2*	150	143.47	140.88	140	2.59	142.28	11.90	2.42E+06	12.19	2.40E+06	14.22	2.31E+06	12.67	2.38E+06	3.91	0.0036
2s2ii3	150	129.54	122.41	120	7.13	126.37	11.51	7.52E+06	11.79	7.48E+06	14.32	7.11E+06	12.39	7.39E+06	10.32	0.0107

<sup>1</sup> Dtemp is the temperature difference between the average pipe or pipe insulation surface temperature and the inside EPS temperature.

<sup>2</sup>  $T_{Avg}$  is the average of the two temperatures used to calculate Dtemp.

\* These data were from oscillating solutions.